DEVELOPMENT AND APPLICATION OF IDMS BASED PROCEDURE FOR TOTAL SULPHUR IN COPPER METALS AND ITS ALLOYS

Dissertation

zur Erlangung des akademischen Grades

doctor rerum naturalium

(Dr. rer. nat.)

im Fach Chemie

Mathematisch-Naturwissenschaftlichen Fakultät

der Humboldt-Universität zu Berlin

von

M.Sc. Pranee, Phukphatthanachai

Präsidentin der Humboldt-Universität zu Berlin

Prof. Dr.-Ing. Dr. Sabine Kunst

Dekan der Mathematisch-Naturwissenschaftlichen Fakultät

Prof. Dr. Elmar Kulke

Gutavhter/innen:
1. Prof. Ulrich Panne
2. Prof. Wolfgang Frenzel
3. Prof. Thomas Meisel

Tag der mündlichen Prüfung: 29. March 2019

For…

Paul De Bièvre

(1933-2016)

Paul De Bièvre was very active in the international activities of chemistry and he was a charter member of many international chemistry organizations, including the BIPM Consultative Committee on the Amount of Substance (CCQM), EURACHEM, and CITAC; and he was a nearly permanent member of IUPAC. He had a penchant for philosophy of science and he believed that great measurements start with great thinking. His writings on metrology in chemistry appeared frequently in *Accreditation and Quality Assurance* (Springer). He often said some phrases such as "back to basic", "lifting the fog" which pulled me out of the confusions in analytical chemistry and made it clearer when consider in chemical metrology way. He was the one who was very engaged in the *International Vocabulary of Metrology - Basic and general concepts and associated terms* (VIM 2008), and *Measurement Uncertainty and Metrological Traceability of Measurement Results in Chemistry: Concepts and Implementation* (IUPAC Technical Report). For the author of this work he was a legend in chemical metrology.

Acknowledgements

Prof. Ulrich Panne

Thank you for the opportunity to do research at BAM and becoming my academic supervisor.

Dr. Jochen Vogl

I have no word to thank you. Ultimately, I made a good decision to follow you to study in Germany and do research with you. I have learned from you, like how to be a good analytical chemist /metrologist, culture and work style. And thank you for being my advisor. "khob khun na ka"

Dr. Norbert Jakubowski

Thank you for sharing and passing your experiences and for being my scientific advisor.

Dr. Heike Traub

Thank you for sharing and giving me the experience /knowledge about LA-ICP-MS. I had a good time while we were measuring with a loud noise.

Maren Koenig

Thank you for training, providing information on ICP-MS, cleanroom, equipment and others.

Dorit Becker

Thank you for the general information and patience with my questions not only about laboratory chemicals, lab-stuff but also about how to survive in Berlin.

Jens Pfeifer

Thanks for working hard on GDMS. All GDMS results were measured by you.

Dr. Sutthinun Taebunpakul

Thanks P'Book (ka) for advisory support while I study in Berlin ka.

Dr. Charun Yafa

Thanks P'Charun for general support (na ka).

"I would like to keep these people as a record because my memory will fade out one day, but this record will stay longer."

Pranee Phukphatthanachai, Berlin, 2018

Zusammenfassung

Bei der Schwefelquantifizierung in Kupfer und anderen reinen Metallen zeigte sich in der Vergangenheit eine mangelnde SI-Rückführung und zusätzlich inkonsistente Ergebnisse, wenn verschiedene Methoden verglichen wurden. Um diesen Mangel zu beheben ist ein Referenzverfahren erforderlich, welches SI-rückführbare Werte mit einem zuverlässigen Unsicherheitsbudget ermöglicht. In dieser Studie wurde ein entsprechendes Referenzverfahren zur Quantifizierung von Gesamtschwefel in Kupfer basierend auf der induktiv gekoppelten Plasma-Massenspektrometrie und der Isotopenverdünnungsanalyse (ICP-IDMS) entwickelt.

Aus dieser Studie ging somit ein Referenzverfahren zur Quantifizierung des Gesamtschwefels in Kupfer mittels induktiv gekoppelter Plasma-Isotopenverdünnungsmassenspektrometrie (ICP-IDMS) hervor, das erfolgreich für die Kalibrierung von Routineverfahren verwendet wurde. Darüber hinaus wurde ein Verfahren basierend auf der LA-ICP-IDMS entwickelt, um die Probenvorbereitung deutlich zu verkürzen. Zugleich konnte erstmals die SI-Rückführungskette und das Messunsicherheitsbudget für LA-ICP-IDMS realisiert werden.

Schwefel (S) ist eine wesentliche Verunreinigung in Kupfer, welche die chemischen, physikalischen und mechanischen Eigenschaften wie Farbe, Härte, und Zugfestigkeit von Kupfer direkt beeinflusst. Die generellen Schwierigkeiten bei der Quantifizierung von Schwefel in Kupfer mittels ICP-MS sind ein typischerweise niedriger Schwefelgehalt (sub-$\mu g \cdot g^{-1}$-Gehalt), ein hoher Blindwert und somit hohe Nachweis- und Bestimmungsgrenzen. Zusätzlich wirkt sich die Kupfermatrix selbst direkt auf die Messung durch das ICP-MS aus, indem sie die Empfindlichkeit deutlich verringert (30-70%), zu einer Messabweichung des Isotopenverhältnisses führt (1% bei w(Kupfer) > 75 $\mu g \cdot g^{-1}$) und eine umfangreiche Reinigung der Probenzuführung und der Ionenquelle erforderlich macht.

Um diese Probleme zu lösen wurde mit Hilfe der Ionenaustauschchromatographie ein Schwefel-Matrix-Trennverfahren entwickelt, bei dem Kupfer zu über 99,99 % entfernt werden konnte, aber gleichzeitig der Schwefel aufkonzentriert wurde. Dieses Trennverfahren wurde mit ICP-IDMS kombiniert, um Schwierigkeiten mit der Kalibrierung zu lösen und fehlende metrologische Konzepte

einzuführen. Das entwickelt Verfahren wurde mit Hilfe von ZRMs, schrittweiser Validierung und laborübergreifenden Vergleichsmessungen validiert, um zuverlässige Messwerte zu erhalten.

Ein bedeutender Vorzug der IDMS sind die konkurrenzlos niedrigen Messunsicherheiten, die es ermöglichen andere Analysenverfahren zu kalibrieren. So wurden die in diesem Projekt erzielten IDMS-Messwerte für die Kalibrierung von GDMS und LA-ICP-MS verwendet, beides Verfahren die im industriellen Einsatz üblich sind. Dadurch konnten mit beiden Routineverfahren zuverlässige Ergebnisse erzeilt warden, die zudem auf SI rückführbar sind.

Darüber hinaus wurde ein auf der LA-ICP-IDMS basierendes Verfahren entwickelt, um den Probenvorbereitungsschritt von ICP-IDMS mit Schwefel-Matrix-Trennung zu reduzieren. Die Vorteile dieser Methode sind ein geringerer Arbeits- und Zeitaufwand, die SI- Rückführung der Messergebnisse und eine für LA-ICP-MS vergleichsweise hohe Genauigkeit. Die Schlüsselrolle hierbei spielte der innovative Einsatz von Polyethylenfritten als Trägermaterial der aufgelösten Probe. Dadurch war die Quantifizierung von Schwefel in Kupferproben mittels LA-ICP-IDMS möglich. Die wesentlichen Parameter wie Absorptionseffizienz der Fritten und Matrixeffekt wurden untersucht. Das entwickelte Verfahren konnte mit Hilfe der ICP-IDMS vollständig validiert werden.

Abstract

Sulphur quantification in copper and other pure metals in the past revealed a lack of SI-traceability and also showed inconsistent results, when different methods are compared. Therefore, a reference procedure is required to enable SI-traceable measurement results accompanied by a sound uncertainty budget. In this study, such a procedure was developed for the quantification of total sulphur in copper using inductively coupled plasma-isotope dilution mass spectrometry (ICP-IDMS).

This study resulted in a reference procedure for the quantification of total sulphur in copper using ICP-IDMS, which was successfully applied the calibration of routine analytical procedures. Furthermore, a LA-ICP-IDMS procedure was developed, which for the first time clearly demonstrated the complete SI-traceability chain and a complete measurement uncertainty budget.

Sulphur (S) is a major impurity in copper, which directly influences chemical, physical, and mechanical properties such as colour, hardness, and tensile strength of copper. The major obstacles to the sulphur quantification in copper by ICP-MS involve low sulphur content (sub-$\mu g \cdot g^{-1}$ level), high sulphur background, high LOD, and high LOQ. Additionally, the copper matrix directly affects the ICP-MS measurement by significantly decreasing the sensitivity (30-70 %), leading to a bias in isotope ratio measurements (sulphur isotope ratio deviate 1 % when copper > 75 $\mu g \cdot g^{-1}$) and requiring an extensive cleaning of the sample introduction system and the ion source.

For solving these problems ion exchange chromatography was applied, and a sulphur-matrix separation procedure was developed. The procedure made it possible to removed copper more than 99.99 % and preconcentrate sulphur. This procedure was combined with ICP-IDMS to solve difficulties with the calibration and to realize metrological concepts. The developed analytical procedure was validated by using certified reference materials (CRMs), stepwise validation and an inter-laboratory comparison to enable reliable measurement results.

One of major benefits of IDMS is unrivalled small measurement uncertainties, which enable the calibration of other analytical procedures. Such an application of the IDMS procedure was realized by using the measurement results

of specific copper samples values for calibrating glow discharge mass spectrometry (GDMS) and laser ablation ICP-MS (LA-ICP-MS). Both techniques are considered routine techniques. Thus, they could provide reliable results which are traceable to the SI.

Additionally, a procedure based on LA-ICP-IDMS was developed to significantly reduce the sample preparation step of ICP-IDMS with sulphur-matrix separation. This procedure is less laborious and the measurement results are still SI traceable and offer a comparatively high accuracy for LA-ICP-MS. Key for this development was the innovative application of polyethylene frits as support material for the dissolved sample. Thus, the quantification of sulphur in copper samples by LA-ICP-IDMS could be realized. The essential parameters are investigated such as the absorption efficiency of the frit and matrix effects. The developed procedure was fully validated by means of the ICP-IDMS results.

Contents

List of Abbreviations

AER	Anion Exchange Resin
amu	Atomic Mass Unit
Ar	Argon
BAM	Bundesanstalt für Materialforschung und -prüfung
BIPM	International Bureau of Weights and Measures
CCQM	Consultative committee of amount of substance (Comite Consultatif pour la Quantite de Matiere)
CER	Cation Exchange Resin
CHGE	Carrier Hot Gas Extraction
CITAC	Cooperation of International Traceability in Analytical Chemistry
cps	Count per second
CRM	Certified Reference Material
CV	Certified Value
DC	Direct current
DoE	Degree of Equivalence
E_n	Normalized Error
ERM	European Reference Materials®
ESA	Electrostatic Sector
EURACHEM	A network of organisations in Europe, having the objective of establishing a system for the international traceability of chemical measurements and the promotion of good quality practices.
GDMS	Glow Discharge Mass Spectrometry
GUM	Guide to the expression of uncertainty in measurement
HPA	High Pressure Asher
HR-MS-ICP-MS	High Resolution Inductively Coupled Plasma Mass Spectrometers
IAWG	Inorganic Analysis Working Group
IBR	Ion Beam Ratios
ICP-IDMS	Inductively Coupled Plasma Isotope Dilution Mass Spectrometry
ICP-MS	Inductively Coupled Plasma Mass Spectrometry
ICP-OES	Inductively Coupled Plasma Optical Emission Spectrometry
ICP-QMS	Inductively Coupled Plasma Quadrupole Mass Spectrometry
IDMS	Isotope Dilution Mass Spectrometry
IEC	International Electrotechnical Commission
ISO	International Organization for Standardization
ISO/IEC 17025	General Requirements for the Competence of Testing and Calibration Laboratories
IUPAC	International Union of Pure and Applied Chemistry
IV	Information Value
JCGM	Joint Committee for Guides in Metrology
k	Coverage Factor

List of abbreviations

LA-ICP-IDMS	Isotope Dilution Laser Ablation Inductively Coupled Plasma Mass Spectrometry
LA-ICP-MS	Laser Ablation Inductively Coupled Plasma Mass Spectrometry
LOD	Limit of Detection
LOQ	Limit of Quantification
MC-ICP-MS	Multi-collector Inductively Coupled Plasma Mass Spectrometry
MU	Measurement Uncertainty
NIMT	National Institute of Metrology (Thailand)
NIST	National Institute of Standards and Technology
NMIJ	National Metrology Institute of Japan
PE	Polyethylene
PFA	Perfluoroalkoxy polymer, Fluoro-Plastic
PT	Proficiency Testing
RF	Radio Frequency
RM	Reference material
RSD	Relative Standard Deviation
RSF	Relative Sensitivity Factor
RV	Reference Value
SD	Standard Deviation
SEM	Secondary Electron Multiplier
SI	International System of Units
SRM	Standard Reference Material®
TIMS	Thermal Ionization Mass Spectrometer
UKAS	United Kingdom Accreditation Service
U_{rel}	Relative Expanded Measurement Uncertainty
USA	United States
VIM	International Vocabulary of Metrology

Preface

What. This thesis summarizes the research for development of the analytical procedure for the sulphur quantification in copper metals and its alloys by isotope dilution ICP-MS and LA-ICP-MS. The required sulphur-matrix separation procedure and the sulphur measurements are described, as well as the application of the developed IDMS procedure to the calibration of measurement techniques such as GD-MS and LA-ICP-MS. An overview of this thesis is shown in the figure below.

Why. This research had two main drivers being economic impact and metrological issues. The copper industry has been one of the most important metal industry for the past decades. Keeping up the quality of copper and its alloys in technology requires special reference materials. Sulphur plays a crucial role in this technology because it is a major impurity of copper and strongly affects the metal properties. In the view of analytical chemistry, the sulfur mass fraction in metals is still a big challenge due to inaccurate/unreliable techniques and a lack of SI-traceability which is reflected by inconsistent results, when different methods are compared. Additionally, the sulphur mass fraction is an important parameter in purity assessment of high-purity metals being used as primary assays in the realization and dissemination of SI traceability.

What for. This research provides reliable measurement procedures which enable sufficiently low measurement uncertainties and SI traceability of the results. Therefore, these procedures are well suited for the certification of reference materials, the assignment of reference values, and the calibration of other analytical procedures. Applying such reference procedures to the quantification of sulphur in copper metals and its alloys, the results will be accepted worldwide in every technical and scientific section.

DEVELOPMENT AND APPLICATION OF IDMS BASED PROCEDURES FOR TOTAL SULPHUR DETERMINATION IN COPPER METALS AND ITS ALLOYS

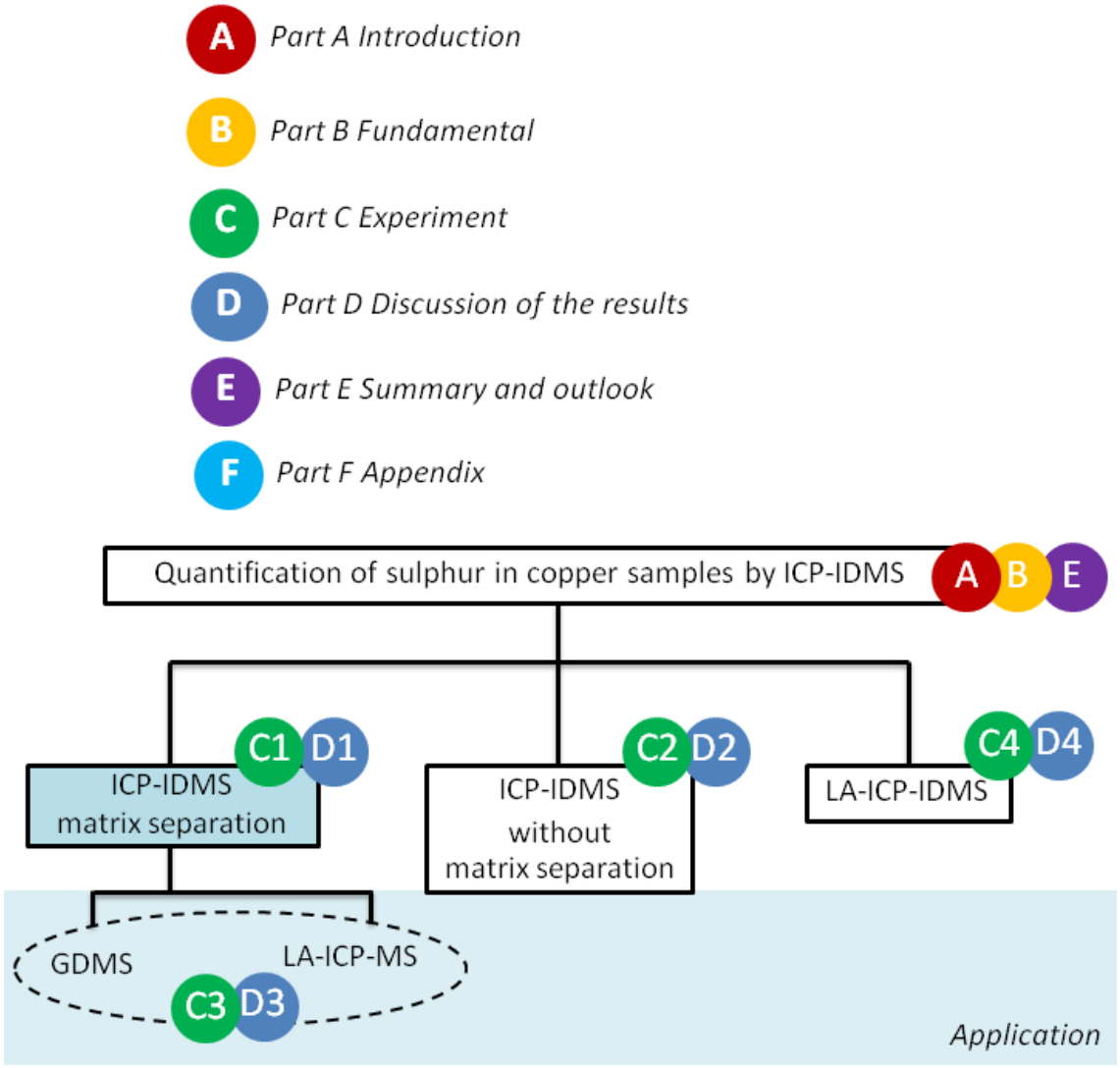

Part A Introduction

Copper (Cu) is an essential element and the third most important metal in industrial applications. It is widely used in electricity and energy, building constructions, engineering, and transportation. The value of the copper industry in Europe has an estimated turnover of about €45 billion in the past decade.[1] The world's copper supply comes from two origins: mining/refining and recycling. In natural deposits copper is mainly associated with sulphur and oxygen forming minerals such as *chalcocite* (Cu_2S, copper sulphide), *chalcopyrite* ($CuFeS_2$, copper iron sulphide) and *cuprite* (Cu_2O, copper oxide) from which copper can be extracted. Consequently, **sulphur (S)** is a major impurity in copper and directly influences chemical, physical, and mechanical properties such as colour, hardness, and tensile strength.[2] Therefore, the determination of the sulphur content in copper is necessary for many technological applications. Maintaining the quality of copper and copper alloys in technology requires specific reference materials.

To produce reliable measurement results, reference materials are needed, whose quality can be guaranteed when **chemical metrology** is properly applied. Actually, chemical metrology overlaps with analytical chemistry to a large extent but differs in detail. Normally, analytical chemistry answers the question of "how much or how many of something is in something?" (here: how much sulphur is in copper). Chemical metrology research goes beyond this and focuses on the basic principles and on additional questions such as "how to perform *correct* measurements?" and "can we trust in the measurement results?" Typically, these questions arise after "how much?", but in practice they (should) come first. Therefore, to answer those questions higher order analytical techniques and powerful instruments are requested, in other words analytical reference procedures.

In recent years, **inductively coupled plasma mass spectrometry (ICP-MS)** has been used for sulphur determination at concentration low level. Martinez-Sierra *et al.* reviewed the technical problems of sulphur analysis by ICP-MS such as isobaric interferences and high sulphur background on the basis of various publications.[3] The majority of the applications are focused on organic samples such as fuels, proteins, and pharmaceuticals. Nearly two decades before Matschat *et al*. investigated the analysis of high-purity metals (including copper) by high

resolution ICP-MS.[4] They found that the copper matrix shows strong matrix effects on the sensitivity resulting from Cu deposition on the cones. The sensitivity decrease amounts to about 70 % when aspirating a 5,000 $mg \cdot L^{-1}$ copper solution.[4] Lange *et al*. also compared analytical methods for analysing impurities in pure copper, but unfortunately the number of reported data sets was rather small while the reported standard deviations for sulphur analysis were quite large caused by the different sample dissolution techniques.[5] Summarizing their findings, the major challenge for quantifying sulphur in copper (pure/alloy) by ICP-MS is the copper matrix itself, causing severe matrix effects which require an extensive cleaning (cones, extraction lens) after each measurement. Most commonly these matrix effects in ICP-MS are reduced by sufficient dilution, often with dilution factors of 10,000 and higher. In the case of sulphur measurements, however, such dilution is ineffective, because sulphur is consequently diluted to the medium to low $ng \cdot g^{-1}$ range, which is close to the sulphur background and thus close to the resulting detection and quantification limit. Consequently, reliable sulphur determination with sufficiently low measurement uncertainties being fit for purpose is not possible under these conditions. Therefore, a reliable quantification of low sulphur levels in a copper matrix requires a sulphur-matrix separation procedure before measurements are carried out to avoid matrix induced bias.

Ion exchange chromatography is employed to develop the required **sulphur-matrix separation procedure**, which enables the removal of the copper matrix, by which sulphur is being pre-concentrated. Copper alloys can be complex matrices. After dissolution of the metal/alloy the copper and the sulphur can be present in different oxidation states. The mass fraction ratio copper-to-sulphur in the investigated materials was typically ≥ 10,000. This requires several separation steps to enable a nearly complete copper separation (> 90 %), while the sulphur recovery is high (> 50 %). Every step, however, can lead to analyte loss, which requires a quantification method which is tolerant to analyte losses.

The application of **isotope dilution mass spectrometry (IDMS)** can overcome some of these limitations, as it applies the perfect internal standard. Since sample losses will not affect the accuracy of the results once equilibration between sample and spike is established, IDMS facilitates the use of matrix separation techniques. Additionally, IDMS enables smallest measurement

uncertainties (typically ≤ 1 %) and traceability to the international system of units (SI) of the measurement results; therefore, it is perfectly suited for this analytical task.

Typically, the characterizations of copper **reference materials (RMs)** can be divided in two parts: RMs focused on the copper mass fraction or its purity and RMs focused on elemental impurities. Very recently copper reference materials with reference values for the total sulphur mass fraction have been reviewed by Phukphatthanachai *et al.*[6] Roughly half of the listed materials are certified for their sulphur mass fractions with relative measurement uncertainties of 7-30 %, whereas the other half of the reference materials provide only information values with relative standard deviations of the inter-laboratory comparison or no uncertainty data at all. The reviewed information emphasizes the lack of reference procedures, which can provide sufficiently small measurement uncertainties and which are suitable as reference procedures, especially for the certification of reference materials.[6]

The developed procedure shall be capable of being used as a **reference procedure** for the accurate quantification of sulphur in copper metals and its alloys and for enabling SI-traceable results. It should enable reference material characterization, calibration of other analytical methods, and the assignment of reference values for inter-laboratory comparisons. To achieve these aims, a higher order method is required, which yields reliable measurement results, establishes the metrological traceability to the SI via an unbroken chain of calibrations and which clearly expresses the measurement uncertainty and its individual contributions. IDMS combined with ICP-MS is one of the very rare higher order techniques for trace element analysis, which can reach these targets.

One benefit of IDMS is the validation and calibration of other analytical methods due to its superior performance which has been invest here as well. An important **application of the IDMS measurement results** is the calibration two direct analytical methods: glow discharge mass spectrometry **(GDMS)** and laser ablation inductively-coupled plasma mass spectrometry **(LA-ICP-MS)** procedures, which are routine analytical techniques in industrial laboratories and thus require suitable calibration materials. Both techniques are very powerful for the determination of sulphur in metal samples. Advantages of these direct

techniques are shorter analysis time and a simple sample preparation process, both making it fit for routine analysis. The disadvantages of GDMS and LA-ICP-MS, however, are relatively high measurement uncertainties of ≥ 20 % and the requirement of matrix matched standards for obtaining reliable results. Due to a lack of suitable CRMs most of the measurement results are traceable to commercial standards, which themselves often lack SI traceability; therefore, the application of IDMS results to calibrate these instruments can provide reliable results and traceability to the SI.

An analytical procedure based on the combination of the isotope dilution technique with LA-ICP-MS **(LA-ICP-IDMS)** was developed in this work to reduce the sample preparation procedure of ICP-IDMS and to eliminate the sulphur-matrix separation steps. The advantages of this method are a significantly reduced time and a significantly reduced complexity while SI traceability of the measurement results is maintained, and the accuracy of the results is comparatively high for LA-ICP-MS procedures. An new approach is introduced by employing a polyethylene (PE) frit-based sample preparation for the quantification of sulphur in copper samples by LA-ICP-IDMS.[7] The key parameters are investigated such as the absorption efficiency of the PE frit and the isotope ratio variation within and between loaded frits. The method was fully validated by using reference samples with reference values assigned by the previous developed ICP-IDMS procedure. The accuracy of the measurement results was maintained and ranges within the target measurement uncertainty. Moreover, the metrological traceability and the measurement uncertainty budget are clearly expressed.

The **aim** of this research is the quantification of sulphur in copper samples (unalloyed/alloyed) by applying the principles of chemical metrology. The work is divided into three parts which are (1) development of sulphur-matrix separation for ICP-IDMS, then (2) applying the obtained measurement results for calibrating GDMS and LA-ICP-MS and (3) the development of a LA-ICP-IDMS method by employing PE frits for sample preparation

A1. Objectives

The aim of this research is to:

1. Develop a sulphur-copper separation procedure which enables the quantification of sulphur in pure copper and its alloys by ICP-IDMS

2. Apply the measurement results from the developed procedure to the calibration of GDMS and LA-ICP-MS

3. Develop a fast approach for the quantification of sulphur in pure copper and its alloys by LA-ICP-IDMS

4. Express measurement uncertainty and the metrological traceability chain for each technique

Part B Fundamentals

B1. Summary

Chemical metrology is the science of chemical measurements. One focus definitely is on the transparency of the measurement procedure and a clearly demonstrated traceability to the SI, which of course can also be subsumed under the term quality of analysis. The majority of chemical measurements are quantitative determinations or absolute quantifications, which allow the conversion of instrumental response into mass fractions and which in turn can be traced back to the "kilogram" or the "mol". In elemental analysis, National Metrology Institutes (NMIs) and Designated Institutes (DIs) in the past years increasingly rely on ICP-IDMS, because it has been proven useful to the certification of reference materials (RMs), the successful participation in international-laboratory comparisons, the assignment of reference values for proficiency testing scheme, and the validation/calibration of other methods.

Isotope dilution mass spectrometry (IDMS) is a higher order calibration technique, which provides high accuracy, small measurement uncertainty (below 2 % in relative) and traceability of the measurement results to the SI. In combination with inductively coupled plasma mass spectrometry (ICP-MS), which offers high sensitivity, high precision and a wide linear dynamic range, it is a perfectly suited technique for performing elemental analysis. These characteristics make ICP-IDMS, the combination of both techniques, isotope dilution mass spectrometry (ICP-IDMS) especially useful for the detection of impurities in metal samples, which are present at varying mass fractions from the low $mg \cdot g^{-1}$ range to the $\mu g \cdot g^{-1}$ range or even below. Sulphur is an important impurity in copper metals and its alloys and it plays an important role for the chemical, physical and mechanical properties of copper.[2] Being present at trace levels of sulphur in high-purity copper the direct measurement by ICP-IDMS is hampered. The copper matrix reduces the sensitivity and affects the mass discrimination of the ICP-MS measurement, and therefore, a sulphur-copper separation procedure is required to eliminate the matrix and maintain the benefits of IDMS.[6, 8]

GDMS and LA-ICP-MS are direct solid sampling techniques and have been widely applied for direct elemental analysis in solid samples due to the short analysis time, simple and fast sample prepare, the sensitivity and the wide dynamic range.[9] It is

well known, that these techniques require matrix matched standards to calibrate the instrument and that in most cases the measurement results still lack SI traceability, because most companies do not provide SI traceability for their commercial standards. Thus, the implementation of SI traceability, in GDMS and LA-ICP-MS requires the application of matrix-matched standards with SI traceable reference values.

The combination of LA-ICP-MS and IDMS has been applied and further developed for nearly two decades, mainly to improve the accuracy of LA-ICP-MS analysis. However, nearly all applications of **LA-ICP-IDMS** lack a complete uncertainty statement and the results are not SI traceable. Therefore, the sample preparation and the isotope dilution step require further development to allow uncertainty calculation and SI traceability.

B2. Chemical Metrology

B2.1 General

"**Metrology** is the science of measurement, embracing both experimental and theoretical determinations at any level of uncertainty in any field of science and technology". as defined by International Bureau of Weights and Measures **(BIPM)**.[10] The BIPM is an international organization established by the Metre Convention, through which Member States act together on matters related to measurement science and measurement standards. The science of measurement plays an important role in scientific discovery and innovation, industrial manufacturing and international trade, in improving the quality of life and in protecting the environment. The **international system of units (SI)**, the metric system, has been published in 1960. The SI defines the seven base units: length (m), mass (kg), time (s), electric current (A), thermodynamic temperature (K), amount of substance (mol), and luminous intensity (cd). The base quantity used in chemistry and biology is **'mol'** or amount of substance, which is coupled to the kilogram via the molar mass of an element or compound.

The **goal of metrology** is "once measured, accepted everywhere". The sense of this quote is reliability, which requires quality and comparability of the measurement result as a main subject. To demonstrate equivalence of the measurement results emphasis is put on the measurement uncertainty, the traceability, and the quality system. **National Metrology Institutes (NMIs)** and **Designated Institutes (DIs)** respond to establish the measurement or calibration of their own country. The equivalence of the measurement or

calibration will be published to serve the customer, known as Calibration and Measurement Capabilities **(CMCs)**. CMCs contain the description of each specific calibration or measurement service, the entries in the key comparison database[11] show the measurand, the range, the method and the measurement uncertainty that the national metrology institute provides to their customers. These characteristics of each CMC are then published as one dataset in a publicly available database maintained by the BIPM and known as the "key comparison database" (KCDB).

Metrology in Chemistry is concerned with the development of a structured support system based on traceable standards. A key organization is the *Comite Consultatif pour la Quantite de Matiere* **(CCQM)**, which has been established in 1994. The CCQM is responsible for developing, improving and documenting the equivalence of national standards (certified reference materials and reference methods) for chemical and biological measurements.[10] This work is divided in working groups; the inorganic analysis working group (IAWG) is such a working group under CCQM, which carries out international-laboratory comparison programs (key comparisons and pilot studies) at highest metrological level in the field of elemental analysis. The aims of this group are critically evaluated competences for measurement standards and capabilities for the amount of substance fraction or mass fraction measurements of the elements.

The **quantification of sulphur** in copper samples has not yet been established at CCQM level. However, the quantification of sulphur has been an issue for the IAWG in international-laboratory comparison programs in diesel fuel twice; diesel fuel (CCQM-K35: 2007) and biodiesel fuel (CCQM-K123: 2014).[12] And the quantification of sulphur in a metal matrix was of concern in the purity assessment of pure zinc (CCQM-P149: 2017).[13] Concerning the sample matrix copper in 2007 a study on the analysis of a copper alloy was piloted by BAM (CCQM-K64: 2007),[14] but without sulphur measurement.

B2.2 Measurement Uncertainty

The **measurement uncertainty** (MU) is defined as non-negative parameter characterizing the dispersion of the quantity values being attributed to a measurand, based on the information used.[15] The estimated MU provides an interval of values where the true value is covered with 95 % confidence, when an expanded uncertainty is assumed with a coverage factor of approximately 2.

In practice, systematic and random errors can be reduced by correcting bias and repeating measurements. However, there are practical limits for repetitions as well as for corrections, and thus it is practically impossible to accurately determine or eliminate all errors, thus the true value is not accessible. The **MU concept** is designed to estimate all possible sources that contribute to the measurement results which can consist of two sources of uncertainty, those which are repeatable (systematic uncertainty) and those which vary (random uncertainty). The source of the variation, which contributes to the measurement result, will be estimated when setting up an uncertainty budget and finally it can help to identify the limitations and it can provide opportunities to improve the analytical method.

EURACHEM and CITAC have developed a **guidance** document, which gives detailed guidance for the evaluation and expression of uncertainty in quantitative chemical analysis. It illustrates how to estimate measurement uncertainty step by step and includes examples from routine analysis to basic research and to empirical and rational methods.[16] For more detail see reference[16].

The process of **measurement uncertainty estimation** is shown in Figure B2-1. It consists of 4 steps being described in the following;[16]

1. *Specify measurand*: A statement of what is the quantity intended to be measured including matrix and unit. For example, quantifying mass fraction of sulphur in pure copper by IDMS, expressed in $\mu g \cdot g^{-1}$

2. *Identify uncertainty sources:* A list of possible sources that contribute to the measurement uncertainty. A mathematical equation or equation system is the best way to express the relationship between measurand and contributing quantities.

3. *Quantify uncertainty components:* Estimation of the range of the uncertainty component associated with each potential source of uncertainty identified. Define types of uncertainty sources as type A (statistical evaluation) or type B (other).

4. *Calculate combined uncertainty:* Combination of the contributing quantities from step 3 according to the appropriate rules.

Hence: here '±' in brackets represent the expanded measurement uncertainty (k =2), '±' without brackets represent the standard deviation

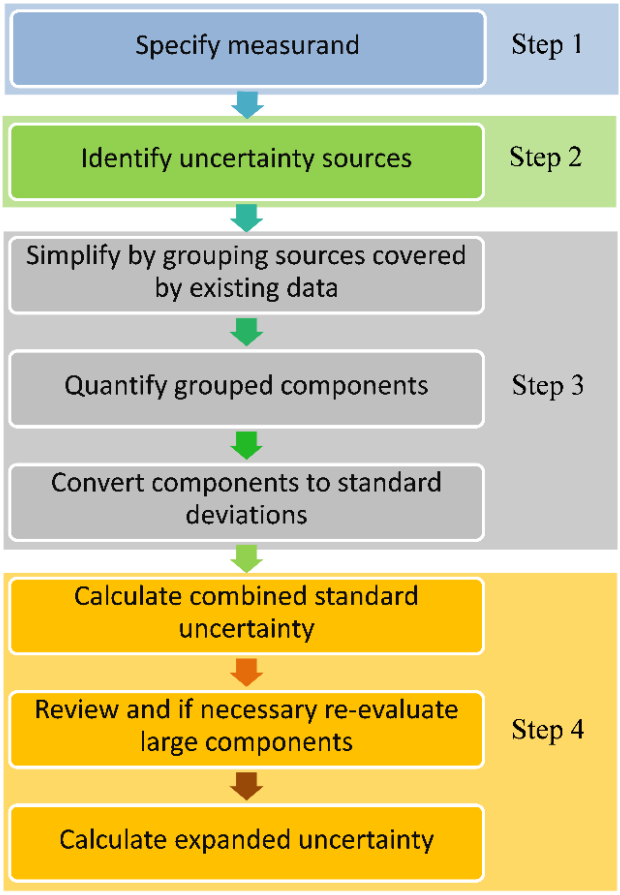

Figure B2-1 The process of measurement uncertainty estimation

B2.3 Metrological Traceability

"**Metrological traceability** is the property of a measurement result whereby the result can be related to a reference through a documented **unbroken chain** of calibrations, each contributing to the measurement uncertainty".[15] This definition illustrates the calibration of measuring systems in a **calibration hierarchy**, its link and relations between measurement results at different levels of the hierarchy. In simple terms, the metrological traceability is a direct link between a measurement result from a testing laboratory via the result from an NMI or primary laboratory finally to the SI or any other international accepted reference. It ensures that different measurement methods and instruments used in different laboratory at different times produce reliable and comparable measurement results, when being traceable to the same reference. A basic requirement of metrological traceability is a full understanding of the measurement uncertainty of the entire measurement procedure. Measurement uncertainty and traceability are interconnected as of the traceability chain only can be built up when a

method is available to evaluate the measurement uncertainty for each individual calibration step.

Therefore, metrological traceability is one of the most important requirements of ISO/IEC 17025 to assure that measurement results agree with national or international standards within the stated measurement uncertainty. Figure B2-2 displays the **metrological traceability pyramid** in which the traceability of the measurement results for an unknown sample to the SI is visualized. The top of the pyramid is an internationally defined and accepted reference, in most cases the SI. At the national level, the main tasks of NMIs or DIs are to maintain national primary standards (primary calibrators being traceable to the SI), to inter-compare them periodically, and to declare quantitative equivalence statements being published in the key comparisons database of the BIPM. The next levels are the calibration or reference laboratories, which are responsible for the calibration of secondary calibrators versus primary calibrators. Furthermore, they have to ensure that the calibration methods they employ are appropriate and well accomplished and provide that the unbroken chain of calibrations is well reported. The bottom shows any testing or field laboratory, which produce measurement results accompanied by a measurement uncertainty for the entire measurement procedure. The traceability of the measurement result is guaranteed by a documented, unbroken chain, from the testing or field laboratories, all the way up the metrological hierarchy/pyramid to the primary standard.

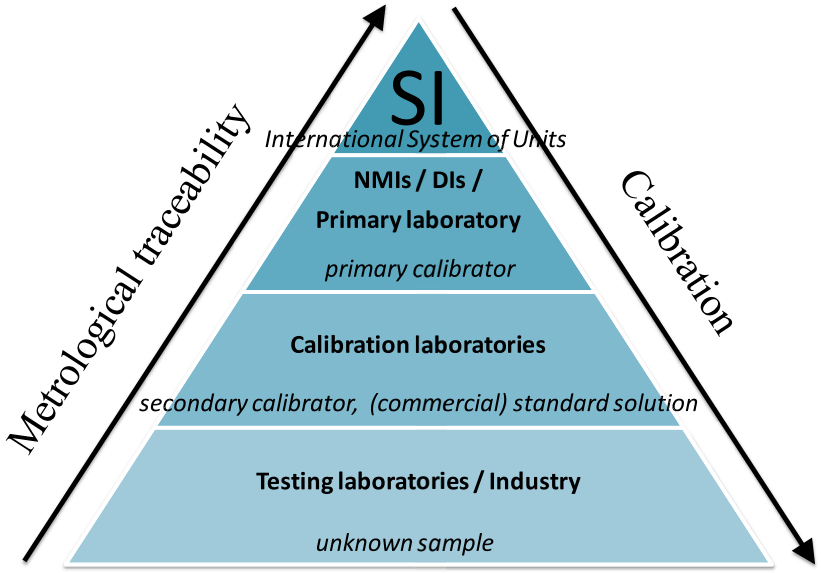

Figure B2-2 Metrological traceability pyramid

In chemical analysis the instrument must be calibrated with the use of certified reference materials, or other suitable reference materials which are traceable. Thus, certified reference materials (CRMs) plays a key role in establishing traceability of measurement results at the field level: they are a tool for validation of the measurement procedure as well as instrument calibration. To ensure reliable and comparable chemical measurements, it is necessary to demonstrate the comparability and traceability of their measurements.

B2.4 Comparability and Compatibility

Metrological comparability of measurement result is "comparability of measurement results, for quantities of a given kind, that are metrologically traceable to the same reference".[15] Simplified it means the ability to compare two measurement results with each other, not the fact that both results necessarily are of the same magnitude. This, of course, requires that both results are expressed as the same quantity using the same unit and being traceable to the same reference. Comparability of measurement results is key of metrology which "once measured, everywhere accepted", this is special importance for world-trade. Figure B2-3 illustrates metrological comparability and compatibility (see next paragraph). It shows the comparison of the measurement results with associated MU from four laboratories measuring the same material. The results of the four laboratories can be compared when all results are traceable to the same international standard and are expressed in the same unit.

Metrological compatibility is defined as "property of a set of measurement results for a specified measurand, such that the absolute value of the difference of any pair of measured quantity values from two different measurement results is smaller than some chosen multiple of the standard measurement uncertainty of that difference".[15] In simple terms, it expresses the agreement of two comparable measurement results with each other within the stated MUs. It is used to express significant or insignificant differences between two or more measurement results. In numerical way, the E_n number is used to demonstrate compatibility of the results (more details in section D2-1). Following this definition, the measurement results displayed in Figure B2-3 have to be assessed as follows: The measurement results from laboratories 1 and 2 (Case A) are compatible with each other, because the difference is less than the associated uncertainty, whereas the results of laboratory 3 and 4 (Case B) are incompatible, because the difference is larger than the associate MU.

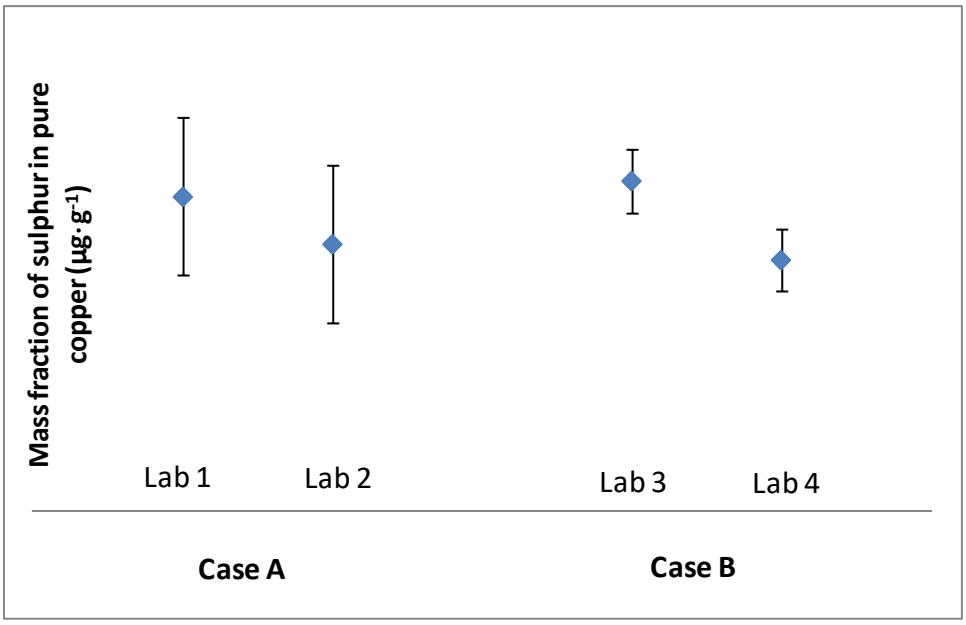

Figure B2-3 Comparability and compatibility of the measurement results

B3. Plasma Based Mass Spectrometric Techniques

B3.1 ICP-MS

The ICP-MS technique was pioneered by Houk and Gray in the 1980s, then commercialized in 1983.[17] Nowadays, ICP-MS is well-known as a technique for elemental analysis, which offers a wide working range from the percent level of the main components down to the ultra-trace level (pg·g^{-1} or even below). This is one of the reasons why it covers a broad range of environmental, geological, industrial, clinical and bioanalytical applications,[9, 17, 18] since its introduction ICP-MS is the fastest growing technique for trace elemental analysis.

An overview of the **basic instrumental** components of an **ICP-MS** is given in Figure B3-1. The ICP-MS consists of seven mains components: *1)*The *sample introduction system* converts a liquid sample to an aerosol and delivers it to the plasma. *2)* The *plasma generation system* generates an Argon plasma with high temperatures of up to 10,000 K. *3)* The *interface* allows the transfer of ions from the atmospheric pressure ion source to the high-vacuum mass analyser. *4)* The *ion optics* focuses the ion beam and eliminates neutral species and photons. *5)* The *Mass analyzer* separates the ions by their mass-to-charge ratio. *6)* The *detector* converts ions into electric pulses and amplifies them such that the signal is proportional to the number of ions in the sample. *7)* The *vacuum*

system enables the transition of the ions from the plasma at ambient pressure to the mass spectrometer in high-vacuum.

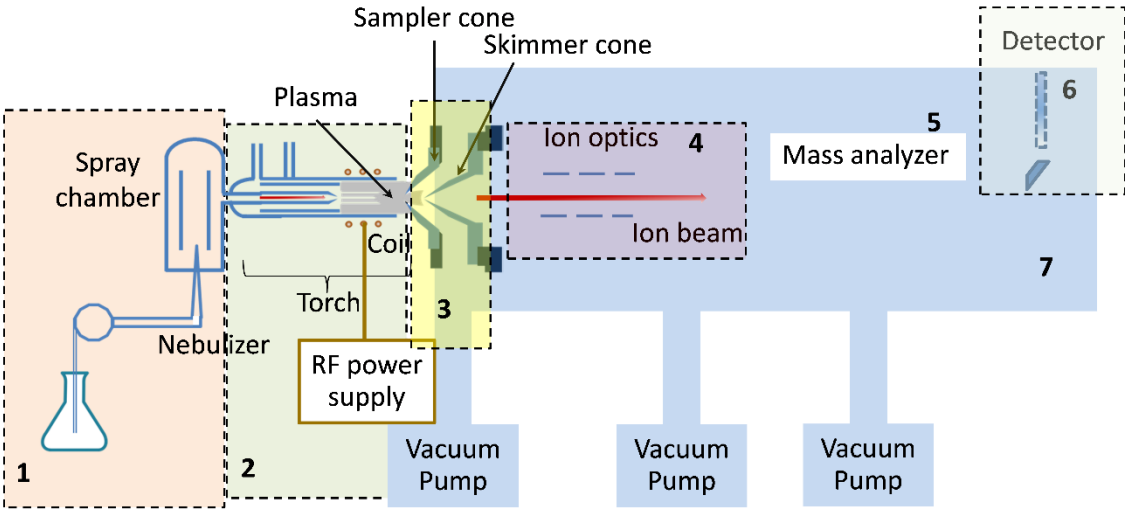

Figure B3-1 Scheme of ICP-MS, including 1) sample introduction system, 2) plasma generation system, 3) interface, 4) ion optics, 5) mass analyser, 6) detector and 7) vacuum system. Adapted from reference[17].

B3.1.1 Sample introduction

Gaseous, liquid and solid samples can be introduced into the ICP-MS. Gaseous samples can be introduced directly via the sample injector or by using gas chromatography coupled to the ICP-MS, solid samples can be introduced via laser ablation (for more detail refer to section B3.2 and B3.3) or electrothermal vaporization systems. Liquid samples are transported via a peristaltic pump, a syringe pump or self-aspiration into the nebulizer. Then the liquid sample is converted into a fine aerosol by the pneumatic action of the gas flow. The aerosol from the nebulizer is directed into the spray chamber, where large droplets (> 10 µm) are separated by inertia; they exit through the drain tube. The fine droplets are transported into the plasma via the sample injector of the plasma torch, where the plasma is maintained by the interaction of an electromagnetic radio frequency (RF) field with the flow of the argon gas. The sample aerosol is dehydrated, vaporized, atomized and ionized along the sample introduction from the tip of the injector to the end of plasma. Then the ions are directed into the mass spectrometer through an interface (sample cone and skimmer cone) and the ion optics. Figure B3-2 shows the generation of analyte ions in the plasma.

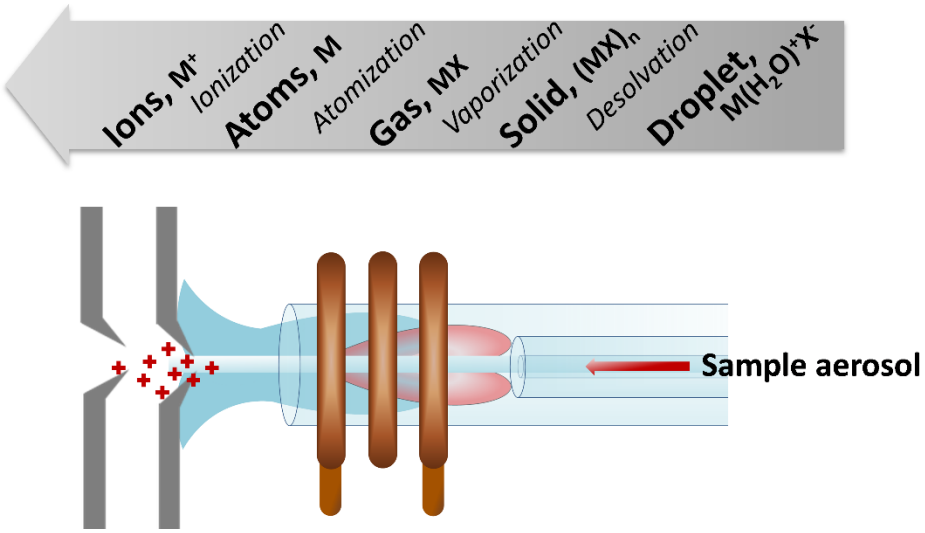

Figure B3-2 Generation of positively charged ions in the plasma.

B3.1.2 Plasma generation

The composition of the plasma torch is shown in Figure B3-3. It consists of three concentric tubes, which are made from quartz. At the end of the torch it is surrounded by the coil which is connected to the RF generator. A flow of plasma gas (usually Ar) is passed between outer and middle tube of the torch and then the RF power is applied to the load coil, producing an electromagnetic field. A high-voltage spark releases free electrons from the Ar gas, which are accelerated by the RF field and induce a cloud of electrons by collisions and subsequent ionization of the argon gas. Therefore, the ICP is formed at the end of the torch with very high temperatures of up to 10,000 K. The temperature is sufficient to ionize analyte atoms to ion (+1 or +2) which depends on ionization potential of the element. In case of sulphur, the first ionization potential is 10.357 eV[19] leading to a relatively low ionization efficiency in an argon-based plasma (about 14%). This contributes to the lower sensitivity of this element in ICP-MS.[20]

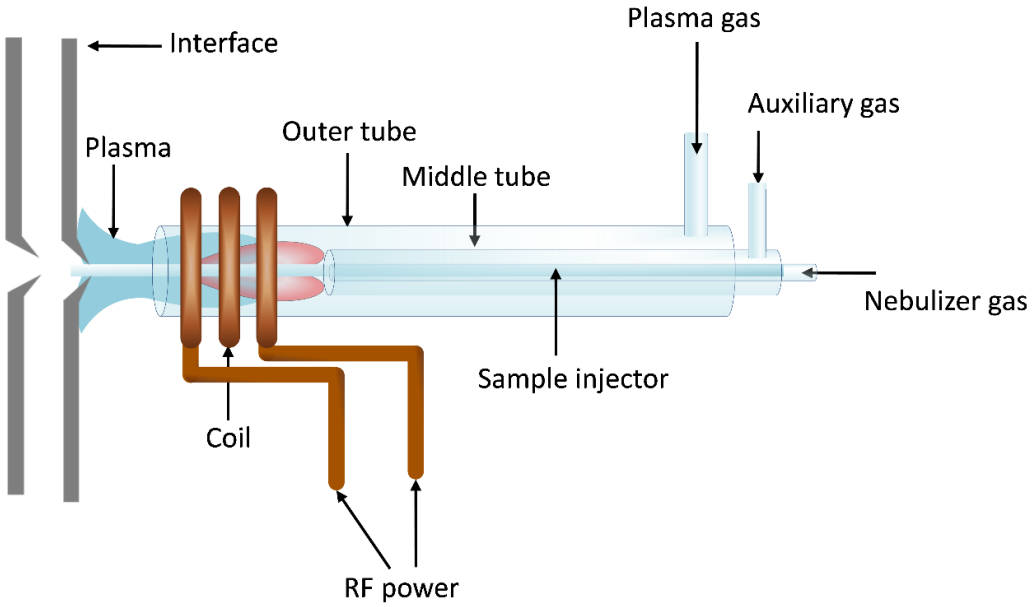

Figure B3-3 Schematics of an ICP torch and load coil.

B3.1.3 Interface

The interface consists of two cones, the sampler cone and the skimmer cone, both with small orifices (0.4-0.7 mm). The sampler cone is located directly after the plasma torch in a short distance of a few millimeters; behind the sampler cone is the skimmer cone separated by a small interface chamber. The role of the interface is to transfer the ions from the plasma at atmospheric pressure to the high vacuum in the mass analyzer. The pressure is reduced in two stages: 1) from atmospheric pressure to a vacuum of some mbar in the interface chamber by rotary pumps and 2) from the interface chamber to the high vacuum of the mass separator ($< 10^{-5}$ mbar) by a combination of rotary pumps and turbomolecular pumps. This incremental pressure reduction causes the expansion of the ion beam.

B3.1.4 Ion transfer optics

The ion transfer optics or ion lenses are positioned between the skimmer cone and mass analyzer. The function of this part is the transport of the analyte ions to focus the ion beam. When the ions pass the skimmer cone a rapid expansion and defocusing occurs, due to the pressure reduction; the positively charged ions repel each other, which is known as a space-charge effect. Ions with higher mass-to-charge ratio (m/z) tend to influence the middle of the ion beam and repel the lighter ions to the outer part of the beam or even out of the beam leading to instrumental mass discrimination or so-call mass

bias, which results in a bias of measured isotope ratios where the lighter isotopes are discriminated against. This phenomenon plays an important role when the matrix is high and has a higher mass than the analyte. The degree of loss depends on the kinetic energy (E_{kin}) of the ions which is related to the mass of the ions and their velocity as expressed in equation 1. By varying the potentials on each of the ion lenses, the analyte ions are directed back into the centre of the ion beam; by this means the ion beam can be focused.

$$E_{kin} = {}^{1}/_{2}\, mv^2 \quad , \qquad \text{Equation 1}$$

where m is the ion mass and v is the velocity.

B3.1.5 Mass spectrometer

The mass analyser is the heart of the system. It separates the analyte ions from others according to their mass-to-charge ratio. Basically, in ICP-MS three different kinds of mass analyser are used: quadrupole mass filter, double-focusing magnetic sectors, and time-of-flight mass analyser. In this work, double-focusing magnetic sectors have been used and will be described in following.

High resolution double-focusing magnetic sectors mass spectrometers, coupled to inductively coupled plasma (HR-MS-ICP-MS) source have been mostly employed for the analysis of complex samples. The instrument provides limit of detection in the $fg \cdot mL^{-1}$ (for noninterfered isotopes) to main components of the sample and it provides a mass resolution up to 10,000. The ICP-MS instruments used in this work were double focusing sector field instruments with reverse Nier-Johnson geometry (Element 2 and Element XR, Thermo Fisher Scientific, Bremen, Germany), which in most cases were operated in medium and high mass resolution mode.

The design principle of the instrument is the so-call Nier-Johnson geometry due to it was designed by Nier & Roberts, 1951 and Johnson & A.O., 1953,[21] where the magnetic sector is located in front of the electrostatic sector (ESA) as shown in Figure B3-4.

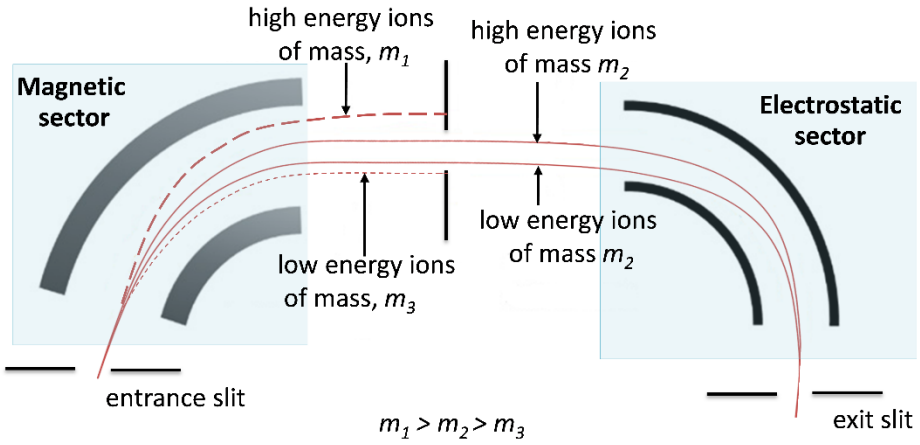

Figure B3-4 Operation principle of a double-focusing mass analyzer.

In magnetic sector analyzers ions are accelerated through a flight tube, where the ions are separated by mass-to-charge ratio. When an ion enters a magnetic field, under the influence of this force, it is deflected from its initial straight path to a circular motion of a unique radius in a direction perpendicular to the applied magnetic field. Ions in the magnetic field are forced on a circular plight path due to the magnetic field (F_B) and centripetal force (F_c).

$$F_B = zvB \quad , \qquad \text{Equation 2}$$

$$F_c = \frac{mv^2}{r} \quad , \qquad \text{Equation 3}$$

Rearrange equation 2 and equation 3 to give:

$$\boldsymbol{v = \frac{Bzr}{m}} \quad , \qquad \text{Equation 4}$$

when B = magnetic field strength

z = mass of ion

v = velocity

r = radius of the magnetic field

m = mass

The ions entering the magnetic field, usually are accelerated beforehand through a cascade-like potential difference V, which lead to an increase of the potential energy of the ion. This potential energy is equated with the kinetic energy (equation 1). Leading to equation 5.

$$\boldsymbol{zV = \frac{mv^2}{2}} \quad , \qquad \text{Equation 5}$$

when V = potential difference

Substitution of equation 4 into equation 5 gives:

$$\frac{m}{z} = \frac{B^2 r^2}{2V} \quad , \qquad \text{Equation 6}$$

The ions of a certain mass-to-charge ratio will have a specific path radius, which is described by equation 6. There are two options to scan the mass range: (i) scan the magnetic field via B, while holding V and r constant, (ii) scan the acceleration voltage V, while holding B and r constant. Usually scanning the voltage is preferred because it is much faster than the magnetic field due to the hysteresis of the magnet. When similar ions travel through the magnetic field, they will be deflected to the same degree and have the same trajectory path. Those ions whose m/z ratio do not correspond with the chosen V and B values will not pass through the slit between magnetic and electrostatic sector. Actually, the magnetic sector is dispersive with respect to mass and energy and performs the first focusing, which is the focus by the ion angle.

The selected ions from the magnetic sector are subjected to subsequent energy focusing (second focusing). The electrostatic sector or electrostatic analyser field is used to compensate for the energy dispersion of the ions. The electrostatic sector consists of two curved plates of equal and opposite potential with a voltage (V) applied between them. When ions pass through, they are deflected by the electrostatic field. The force on the ion due to the electric field is equal to the centripetal force on the ion (as equation 3 but r is radius of the electrostatic field). Here, the ions of the same kinetic energy are focused.

When magnetic and electrostatic sector analysers are employed in an instrument, both, first and second focusing are combined and the combination consequently is called a double-focusing mass spectrometer: the ion beam is focused both with respect to the energies and the angular dispersions, while being dispersive for m/z only. Double-focusing mass spectrometer allows significant improvement in resolution and sensitivity when the suitable geometry is selected. For the inverse Nier-Johnson geometry this is fulfilled, and the angular focus coincides with the energy focus. Additionally, the all m/z ions leave the electrostatic analyser at the same place, when corresponding B and V values are chosen, which makes it highly suited for scanning single collector mass spectrometers,

while forward Nier-Johnson geometry is best suited for simultaneous detection of multiple ions like in multi-collector instruments.

The mass resolution, R, which describes the ability of separating two neighboring peaks in the mass spectra, is defined in equation 7, where Δm is the mass difference between the two peaks of equal peak height both separated from each other by a valley of 10 % peak height and m is the mass of the analyte ion. The double focusing mass analyser is capable of differentiating between masses of analyte ions and interfering molecular ions, which is a significant analytical limitation of quadrupole type mass spectrometers. However, even a mass resolution of 10,000 has limitations; isobaric interferences such as $^{40}Ar^{+}$ of $^{40}Ca^{+}$ generally cannot be resolved. In case of sulphur the mass resolution is sufficient and the main interferences such as $^{16}O^{16}O^{+}$, $^{31}P^{1}H^{+}$, $^{14}N^{18}O^{+}$, $^{15}N^{16}O^{1}H^{+}$, $^{64}Zn^{2+}$ on $^{32}S^{+}$ and $^{16}O^{18}O^{+}$, $^{32}S^{1}H^{1}H^{+}$, $^{16}O^{16}O^{1}H^{1}H^{+}$, $^{68}Zn^{2+}$ on $^{34}S^{+}$ can be separated by applying the medium resolution mode (> 4,300).

$$\boldsymbol{Resolution, R} = \frac{\boldsymbol{m}}{\boldsymbol{\Delta m}} \quad , \qquad \text{Equation 7}$$

The mass resolution is realized by means of two variable mechanical slits, which are located between the acceleration lenses and the mass analyzer (entrance slit) and another slit between the mass analyzer and the detector (exit slit) and a third invariable slit between the magnetic and the electrostatic sector. Both slit units can be set in parallel to three different slit widths, corresponding to three resolution values: low resolution ($m/\Delta m$ = 400), medium resolution ($m/\Delta m$ = 4,000) and high resolution ($m/\Delta m$ = 10,000).

B3.1.6 Ion detection

After passing the exit slit, the ion must be detected and amplified. This is realized by projecting the ion beam onto the entrance slit of the detector(s). In the case of a secondary electron multiplier (SEM) the basic concept is that the ions hit the surface of the first conversion dynode and thus release secondary electrons. Then the secondary electrons from the first dynode hit the second dynode and generate more secondary electrons. Typically, nineteen dynodes are arranged in a cascade sequence. Each dynode focuses the secondary electrons onto the next dynode, thus increasing the number of electrons in the cascade sequence by a factor of 2 until the electrons reach the output electrode where the signal is extracted. Each electron cascade in the SEM creates an electrical pulse that is counted with digital counter or timer electronics. The signal intensity of a m/z peak consequently is measured in counts per second (cps). The signal

can be collected at the end of dynodes and a midpoint dynode which are so-called counting mode and analog mode, respectively. Some instruments such as Element XR and GDMS, a Faraday collector is added to extended linear dynamic range through the combination with the SEM. Dynamic range of quantification is extended from 10^9 up to 10^{12}.[22] Ion detection systems are demonstrated in Figure B3-5.

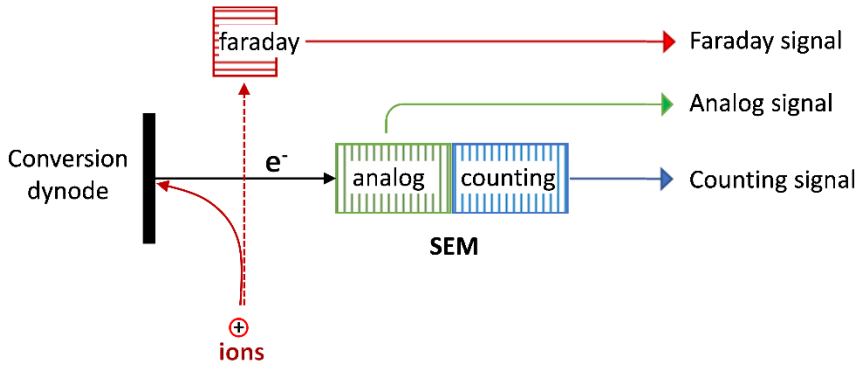

Figure B3-5 Ion detection system

The signal generation in SEMs unfortunately is negatively affected by dead time effects. The dead time is that time after the impact of an ion, for which the detector is blind to further incoming ions. The higher the count rate, the more often an ion hits the detector during the dead time. As a consequence, higher intensities experience higher loss rates than lower count rates. This leads to a bias in isotope ratio measurements, which increases the higher the measured isotope ratio deviates from unity. This phenomenon affects only ion counting system or detectors run in an ion counting mode. During this research a dead time correction according to equation 8 was applied whenever ion counting systems were used.[18, 23, 24] For more detail please see section C1.3.3

$$I_t = \frac{I_0}{(1 - I_0.\tau)} \quad , \qquad \text{Equation 8}$$

where I_t is the true ion count rate in cps

I_0 is the measured count rate obtained in cps

τ is the dead time of the detection system in ns

B3.2 LA-ICP-MS

The combination of laser ablation system (solid sample introduction) and ICP-MS is a powerful technique for direct elemental analysis. In LA-ICP-MS a high-power

laser is used to interact with the solid sample and ablate the surface of this solid sample. As a result of this interaction, small particles, atoms, and ions of the analyte, but as well of the sample matrix are dissociated from the sample surface in the form of an aerosol. This aerosol is transported to the ICP-MS by an inert gas flow (typically He gas) and is being ionized in the plasma.[18] This technique has the following benefits:[17]

- direct analysis without dissolution
- low contamination risk
- low sample consumption
- electrical conductivity of the sample is not required
- wide variety of solid samples can be analysed; even powder or liquid samples are accessible by pelletizing and solidification

Figure B3-6 gives an overview of a typical LA-ICP-MS setup. It consists of 6 parts: *1) sample observation* is used to observe the surface of the sample, to position the ablation point and to program the sampling. *2)* The *Laser generator* is the part which generates laser pulses. Different types with different wavelength and pulse width are available but the most widely used system are the solid-state lasers Nd:YAG at 266 nm and 213 nm wavelength. *3) Gas supply: typically* inert gas such as Ar and He are used; these gases transport the sample aerosol to the ICP-MS as a sample flow. 4) *Beam definition* during the ablation process, the laser beam is directed through a wavelength-transparent quartz glass window. *5) Sample chamber* laser beam is focused onto the surface of the sample in the ablation chamber to generate the sample aerosol and *6) the ICP-MS* ionizes the analyte and separates the ion masses and then detects the ion.

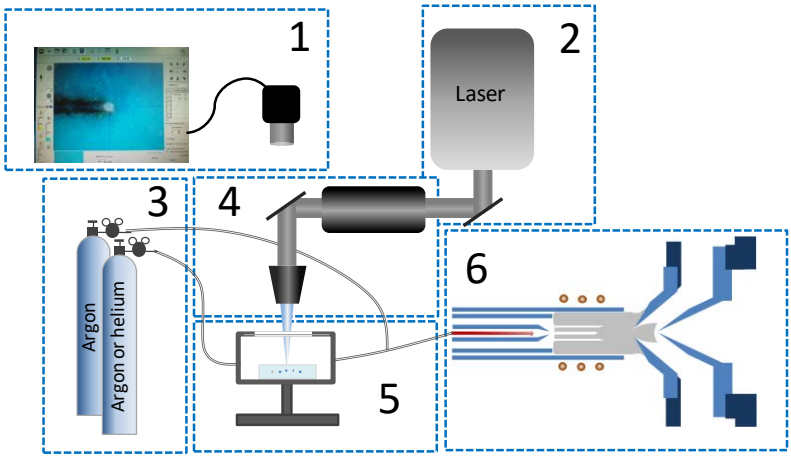

Figure B3-6 LA-ICP-MS general setup 1) Sample observation, 2) Laser generator, 3) Gas supply, 4) Beam definition, 5) Sample chamber, 6) ICP-MS, adapted from reference [9]

Pisonero *et al.* reviewed recently, critical points of solid analysis by GDMS, LA-ICP-MS and SIMS such as the general capabilities and applied calibration strategies, and provided critical comments on each technique.[25] **Quantitative analysis by LA-ICP-MS** can be realized using an external calibration approach because it remains simple, rapid and suitable for routine analysis. In case of non-matrix matched calibration methods, silicate glass (mostly NIST SRM 610 series) was employed as standard for the quantitative analysis of different elements in a wide variety of matrices by using one of the matrix elements as internal standard. This method enables, precision down to 10 % to 20 % RSD.[18] The achievable trueness is at least of the same magnitude.

Therefore, one of the main disadvantages of the direct solid sampling is the lack of suitable calibrators or certified reference materials which are required to calibrate the instrument and to produce reliable measurement results. In nearly all cases the measurement results obtained with those techniques still lack in metrological traceability. To overcome these drawbacks the combination of isotope dilution and LA-ICP-MS was considered (e.g. on-line,[26-29] and off-line[30-35]), however, successful strategies and validated analytical procedures are still under development.

This study used LA-ICP-MS as a routine analysis to quantify sulphur in copper materials; thus, instrumental optimization is not a main issue. The focus here is on the calibration strategy on one hand the application of external calibration by using suitable samples with reference values as calibrator and on the other the application of IDMS yielding SI-traceable values.

B3.3 GDMS

Glow discharge mass spectrometry (GDMS) is a reliable and sensitive analytical technique for the direct analysis of the elemental composition of solid samples. It is a mature and versatile technique for the **direct elemental analysis** (matrix to trace) in a variety of materials. A glow discharge is a type of plasma. It occurs when a DC potential difference under reduced pressure is applied between two electrodes in a cell filled with gas (usually Ar gas). In the high potential difference, the cathode releases a few electrons, which then react with the Ar gas. The resulting argon ions and free electrons induced the plasma. The phenomena continuously occur, and then the plasma stream is created. The surface of the sample, which itself is the cathode, is sputtered by collision with Ar ions. The sputtered neutral atoms are ionized downstream in the plasma

and transferred to the mass analyser to be separated according to their mass-to-charge ratio (for more detail refer to section B3.1.5). The ionization mechanism is presented in Figure B3-7.

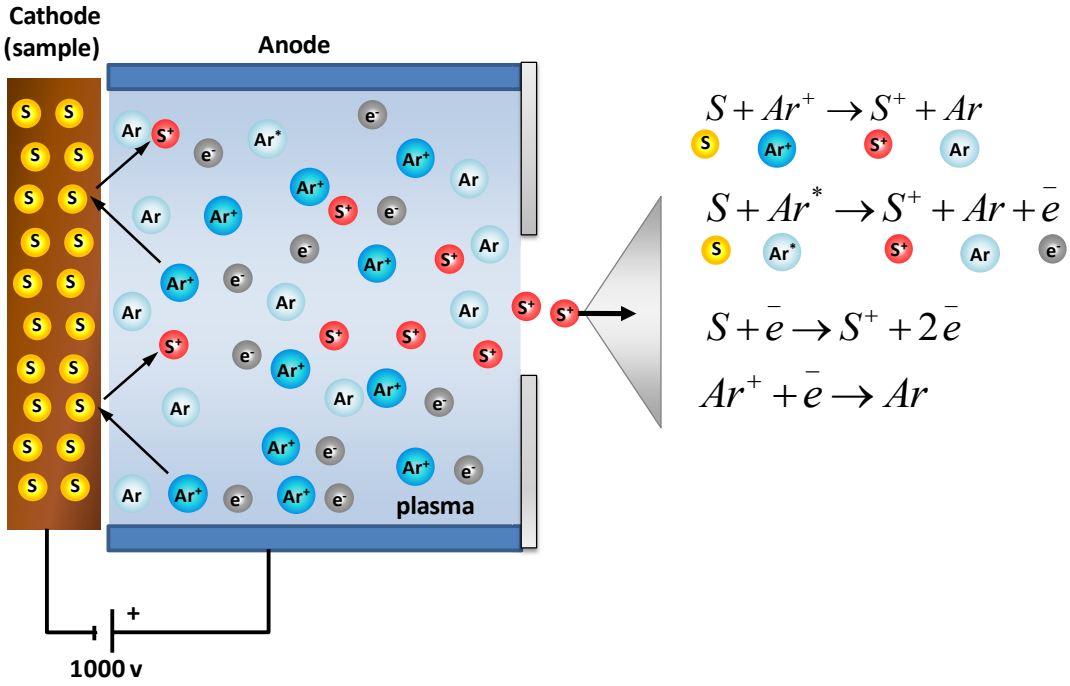

Figure B3-7 The glow discharge process, adapted from reference[36]

Operation modes, generally, the GC source can operate in three modes: 1) Direct Current mode produces a stable and stable ion source, which is a simple, inexpensive and commonly used mode. 2) Radio frequency (RF) mode requires complex materials to generate electron oscillation in the RF field. 3) Pulse mode, applying high amounts of short-term power to enhances the sputtered atom yield. Consequently, more analyte atoms are excited and ionized which provides better sensitivity. Therefore, this research employed pulse operation mode to quantify sulphur in copper samples.

Quantitative analysis by GDMS, often is carried out by using the **ion beam ratio (IBR)** method, which in fact is a semi-quantitative method. The underlying principle of the IBR is the ratio of the analyte's ion signal I_A to the matrix's ion signal I_M both corrected with the corresponding isotope abundances f_A and f_M of analyte A and matrix M, respectively. The mathematical definition of the IBR is shown in equation 9. In this equation, the matrix element serves as a kind of internal standard and thus, instabilities or fluctuation deriving from the plasma, the sputtering process or other effects cancels down, because this affects both ion beams approximately the same way.

Nevertheless, this approach contains several assumptions and therefore was defined as semi-quantitative analysis.[37, 38]

$$IBR = \frac{I_A/f_A}{I_M/f_M} = \frac{C_A}{C_M} \quad , \qquad \text{Equation 9}$$

when IBR = ion beam ratio

I_A = analyte's ion signal

I_M = matrix's ion signal

f_A = abundance of analyte isotope

f_M = abundance of matrix isotope

C_A = analyte's mass fraction

C_M = matrix's mass fraction

Relative sensitivity factor (RSF). This quantification often is applied when matrix-matched calibration is available, which of course is more accurate than IBR. RSF is defined as the inverse slope of the calibration line, (where the known mass fractions of the calibration materials are plotted versus the corresponding IBRs including the origin. The related mathematical relationship is shown in equation 10, leading to equation 11 which gives the analyte mass fraction w_A in the unknown sample.

$$RSF = \frac{1}{slope} \quad , \qquad \text{Equation 10}$$

$$w_A = RSF \cdot IBR \quad , \qquad \text{Equation 11}$$

where w_A is mass fraction of the analyte (here is sulphur in copper sample)
and IBR is the ion beam ratio of the analyte in the sample

Sometime the RSF concept is normalized to the iron matrix and named standard RSF. The reason for that is the large number of available iron reference materials and the wide distribution of iron in the earth crust; thus, a high percentage of every analysed sample is covered.[37]

Several publications discuss the requirements of a matrix matched specific elements for a GDMS and lead to the weaknesses of GDMS still lack of traceability.[9, 25, 37] Most of the reference materials used in GDMS analysis are not traceable, the especially occurs for sulphur mass fractions. Therefore, a new calibration approach based on doped synthetic tablets on basis of metal powder and element solutions has been developed to

obtain SI traceability of the measurement result.[37, 39] Gusarova *et al.* compared different calibration methods such as IBR, standard RSF, matrix-matched RSF and doped synthetic standards. The doped synthetic standard was the best calibration method, it provided relative expanded uncertainties of < 30 %.[37] While Zhou *et al.* reported measurement uncertainty in the range from less than 10 % to more than 200 %.[39]

Within this study GDMS was applied as a routine analytical method to quantify sulphur in copper materials. Thus, the instrumental optimization was not in the focus, but the calibration procedure, the measurement uncertainty and the SI traceability of the measurement results. The applied calibration approach was a matrix matched calibration based on reference values obtained by IDMS.

B4. Isotope Dilution Mass Spectrometry (IDMS)

B4.1 Theory of IDMS

The Consultative Committee for Amount of Substance (CCQM), considers IDMS as the most important "**Primary Method of Measurement**" for amount of substance determination. A primary method of measurement is a method having the highest metrological qualities, whose operation can be completely described and provides a logical framework of understanding, and for which a complete uncertainty statement can be written down in terms of SI units. Within the past years more and more of NMIs / DIs installed IDMS as a reference method for elemental quantification.

Isotope dilution mass spectrometry (IDMS) is an analytical method for the quantification of chemical compounds. The isotope dilution concept was invented by Havesy and Paneth in 1913 for the determination of the solubility of lead salts by using a radioactive isotope of lead.[40] The concept was also used in zoology in the 1930s for counting Tse-Tse flies.[23] The isotope dilution principle was further developed and applied to elemental analysis by using Thermal Ionization Mass Spectrometer (TIMS) during the 1950s. In the early 1990s the IDMS concept was combined with ICP-MS measurements. With increasing availability of ICP-MS instruments, the number of published applications has been continuously increased since then.

Indeed, IDMS can be described as an **internal standard method** which uses one isotope of the analyte itself as internal standard. The isotopic analogue is added to the

sample at the beginning of the analytical method and then both are thoroughly blended until the isotopic equilibrium is reached. After this, the accuracy of the results is not affected by losses of analyte. Sargent *et al.* summarized the guidelines for high accuracy measurements by IDMS.[41] The guideline contains a general introduction to IDMS, the principles, the advantages and disadvantages and critical factors to the accuracy of measurements by IDMS. Vogl and Pritzkow reviewed the history and the basic theory of IDMS and clearly explained the details of the IDMS equation system and the calculation of measurement uncertainties including correction factors.[23]

Figure B4-1 illustrates the **IDMS principle**. Sample x (here a copper sample) contains the analyte (here sulphur): the analyte must have at least two naturally occurring isotopes labeled as isotope *a* and isotope *b*. Natural sulphur has four isotopes as shown in Table B4-1. Two criteria for choosing both isotopes based on isotopic abundance and interference. The high abundance and without interference required for precise and accurate isotope ratio measurement. In most cases, such as sulphur, there is no free interferences, and then choosing the best one while the presence of the interferences is considered (more detail see section B3.1.5)

The quantification of sulphur by IDMS requires the measurement of ^{32}S (*a*) and ^{34}S (*b*) only, when isotope variations are neglected and the IUPAC tabulated isotopic composition of sulphur is being used.[42] The isotope ratio of the sample x is expressed as R_x which is the number of isotopes *a* (N_{xa}) divided by the number of isotopes *b* (N_{xb}). The spike solution is indexed with the letter y and, of course, also contains the isotopes *a* and *b*, but in a different isotopic composition than x. Mostly, the spike solution contains the isotope *b* with an enrichment above 90 %; its isotope ratio is defined as R_y. The concept of IDMS is that an accurately known amount of spike y is directly added as an internal standard to a sample x. After the complete blending of the sample and spike, a new isotope ratio in the so-called sample-spike blend is obtained (R_{xy}). Both, sample x and spike y contribute to the number of isotopes *a* in the sample-spike blend (or simplified to sample blend); the same occurs for the

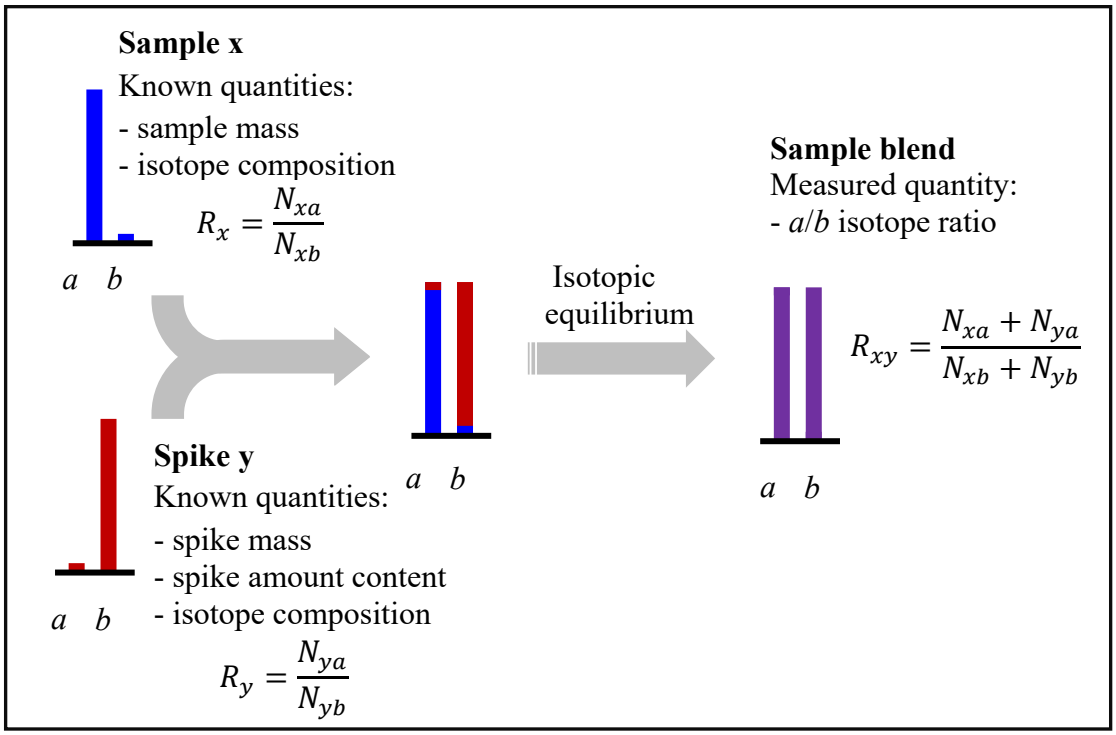

Figure B4-1 Schematic IDMS principle, adapted from reference [23]

Table B4-1 Isotopic composition of sulphur

Isotope	Abundance[42]	Atomic mass[43]	Interference[44]
^{32}S	0.9499(26)	31.972070	$^{16}O^{16}O^+$, $^{31}P^1H^+$, $^{14}N^{18}O^+$, $^{15}N^{16}O^1H^+$, $^{64}Zn^{2+}$
^{33}S	0.0075(2)	32.971458	$^{15}N^{18}O^+$, $^{14}N^{18}O^1H^+$, $^{15}N^{17}O^1H^+$, $^{16}O^{17}O^+$, $^{16}O_2{}^1H^+$, $^{32}S^1H^+$
^{34}S	0.0425(24)	33.967866	$^{16}O^{18}O^+$, $^{32}S^1H^1H^+$, $^{16}O^{16}O^1H^1H^+$, $^{68}Zn^{2+}$
^{36}S	0.0001(1)	35.967080	$^{36}Ar^+$

of isotopes *b*. The ratio of the two isotopes *a* and *b* (in this work $^{32}S/^{34}S$) is measured using mass spectrometry. The determined isotope ratios then enable the calculation of the analyte mass fraction in the sample. Details of the calculation and the labelling and description of the individual quantities are given in Figure B4-1. The resulting IDMS equation (equation 12) consists of isotope ratios obtained from measurements, masses of sample and spike, the procedural blank as well as known quantities such as isotope abundances and atomic weights.

Typically, in IDMS 4 different calibration approaches are applied; single IDMS, double IDMS, exact matching IDMS and triple IDMS.[45] The simplest approach is **single IDMS**, where a certified or calibrated spike is used. This certified spike is added to the

sample and both are mixed well until the isotopic equilibrium is reached. The isotope ratios of the sample, the spike and the sample-spike blend are measured then within the same sequence. The mass fraction of the analyte in the sample can be calculated from equation 12. Consequently, the measurement uncertainty associated with the mass fraction of the spike solution contributes to the uncertainty budget. Typically, certified or calibrated spikes offer relative expanded measurement uncertainties in the range between 0.2 % and 2 %. This limits the overall uncertainty and therefore, the measurement uncertainty in single IDMS typically is larger than for the other approaches; irrespective of the larger measurement uncertainty single IDMS provides metrological traceability direct to the SI.

$$w_x = w_{y,b} \frac{M_x m_y}{M_b m_x a_{x,b}} \frac{(R_y - R_{xy})}{(R_{xy} - R_y)} - ProcBlank \quad , \qquad \text{Equation 12}$$

w_x = mass fraction of the analyte (sulphur) in the sample (copper) ($\mu g \cdot g^{-1}$)

$w_{y,b}$ = mass fraction of the spike isotope b in the spike (^{34}S solution) ($\mu g \cdot g^{-1}$)

M_x = standard atomic weight of analyte (sulphur) in the sample[46]

M_b = atomic weight of the spike isotope

$a_{x,b}$ = isotope amount fraction of the spike isotope in sample

m_x = mass of sample (g)

m_y = mass of spike (g)

R_x = isotope ratio in the sample

R_y = isotope ratio in the spike

R_{xy} = isotope ratio in sample-spike blend

ProcBlank = procedural blank (μg)

In **double IDMS** a primary standard (primary assay) or so-called back spike (indexed with z) is used to characterize the spike solution in a first IDMS experiment. Then the exact mass fraction of the spike solution is calculated by equation 13; this step is named reverse IDMS. After that, in a second IDMS experiment, the characterized spike solution is used to quantify the analyte in the sample analogue to single IDMS. As two IDMS experiments are combined this approach is named double IDMS; this is illustrated in Figure B4-2. The measurement uncertainty in double IDMS is smaller than that of single IDMS, because equation 12 and equation 13 are combined and thus some quantities cancel down (e.g. M_b), especially isotope variations are excluded (e.g. $M_x = M_z$) and do not contribute to the measurement uncertainty. The measurement result is traceable to the

SI through the primary standard in a more direct way than for single IDMS. In this research the double IDMS approach was employed, because it provides smaller measurement uncertainty.

$$w_{y,b} = w_z \frac{M_b m_z a_{z,b}}{M_z m_y} \frac{(R_{zy} - R_z)}{(R_y - R_{zy})} - ProcBlank \quad , \qquad \text{Equation 13}$$

w_z = mass fraction of the analyte in the back-spike ($\mu g \cdot g^{-1}$)

$w_{y,b}$ = mass fraction of the analyte in the spike ($\mu g \cdot g^{-1}$)

M_z = standard atomic weight of sulfur in back-spike

M_b = atomic weight of the spike isotope

$a_{z,b}$ = isotope amount fraction of spike isotope in the back-spike

m_z = mass of back-spike (g)

m_y = mass of spike (g)

R_z = isotope ratio in the back-spike

R_y = isotope ratio in the spike

R_{zy} = isotope ratio in the spike-back-spike blend

ProcBlank = procedural blank (μg)

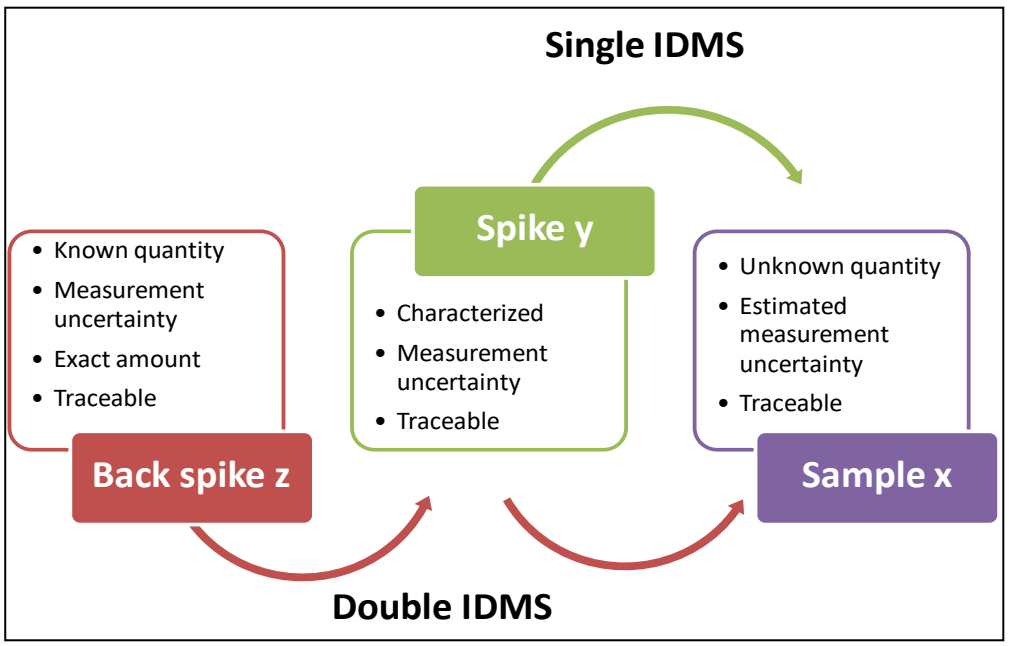

Figure B4-2 Single IDMS vs. double IDMS

Matching IDMS is a special from of single IDMS and double IDMS when the exact mass fraction of the spike solution is not required. The spike solution is added to sample and back spike until the blend isotope ratios and the signal intensities are matched.

For the **triple IDMS** a third blend is introduced to avoid contamination of the mass spectrometer with the isotopically-enriched spike, an additional blend of the back spike and the spike can be measured instead of measuring the enriched spike directly (R_y).

B4.2 Performance of IDMS

IDMS is a very important analytical method, because it is the only method for trace analysis in complex matrices having the potential to be a primary method of measurement. The **benefits** that make IDMS a universally accepted method are:

- ✓ high accuracy method
- ✓ small measurement uncertainty
- ✓ traceable to SI
- ✓ wide range of quantitative analysis from ultra-trace ($pg \cdot g^{-1}$) to major component (%)
- ✓ losses of analyte do not affect the accuracy of the result after complete equilibrium
- ✓ applicable to element, species and compound analysis

However, IDMS has the following **restrictions**:

- × lack of isotopic material (in some cases)
- × time consuming
- × destructive method
- × complete isotopic equilibrium is required
- × two isotopes are needed, which are free from interferences, or where the interferences can be separated

Due to the above listed advantages the IDMS methodology is highly suited for the aim of this research, which is the development of a reference procedure for quantifying sulphur in pure copper and copper alloys. As typically for a reference procedure the accuracy and reliability of the measurement are prioritized to produce reliable results.

B5. Sulphur-Copper Separation

Quantification of sulphur in copper materials by ICP-MS entails severe problems due to the copper matrix itself, which cause matrix effects and makes an

extensive cleaning (cones, extraction lens) necessary after each measurement session. Therefore, a sulphur-matrix separation procedure is required.

Sulphur- copper separation is a method used to **purify sulphur** or to isolate sulphur from the matrix (Cu) to avoid measurement problems caused by the matrix as described above.

Table B5-1 shows sulphur-matrix separation procedures, which have been applied in IDMS and isotope ratio analysis. The procedures are categorized into two main groups. The first group with the generation of gaseous sulphur in H_2S form, and consequently the formation of solid precipitates such as As_2S_3[8, 47] or Ag_2S.[48] The procedure based on the generation of H_2S gas generally are complicated, laborious and time consuming. Pritzkow *et al*. generated H_2S then precipitated in As_2S_3 as a method to separate sulphur and measure sulphur by TIMS.[8] They found that the method had

Table B5-1 Sulphur-matrix separation followed by mass spectrometric detection

Author	**Das *et al.*[49]**	**Craddock *et al.*[50]**	**Pritzkow *et al.*[8]**	**Kelly and Paulsen[47]**	**Burke *et al.*[48]**
Year	2012	2008	2005	1984	1982
Analysis	$\delta^{34}S$	$\delta^{34}S$	isotope ratio, IDMS	isotope ratio, IDMS	IDMS
Sample	seawater, CRM	sediment, CRM	fossil fuels	copper-based and iron-base materials	NBS standard reference materials
Sulphur-matrix separation	AER (AG1X8, Cl^- form) & CER (AG50-X8, H^+ form)*	CER (AG50-X8, H^+ form)	generate H_2S then precipitate as As_2S_3	generate H_2S then precipitate as As_2S_3	generate H_2S then precipitate as Ag_2S
Recovery (%)	100 ± 2	98 ± 4	-	82 % (73-90)	good recovery
Instrument	MC-ICP-MS, Neptune	MC-ICP-MS, Neptune, NewWave UP213	MC-TIMS, Sector	TIMS, NBS single sector	SSMS JEOL model 01BM-2
Resolution	high resolution	high resolution	-	-	-
LOD	-	-	0.2 $\mu g \cdot g^{-1}$	-	0.1 µg theoretical
Mass fraction of sulphur	2 $\mu g \cdot mL^{-1}$	-	40-4000 $\mu g \cdot g^{-1}$	3-54 $\mu g \cdot g^{-1}$	23-360 $\mu g \cdot g^{-1}$
^{32}S background intensity /blank	6-9 mV	30-50 mV	< 0.3 µg	0.27 ± 0.22 µg	0.5 ± 0.1 µg
Application	isotope ratio	isotope ratio	isotope ratio & IDMS	isotope ratio & IDMS	IDMS

* AER = anion exchange resin, CER = cation exchange resin

disadvantages for routine analysis concerning time and effort; especially the apparatus for the sulphur conversion allows only the preparation of one sample in parallel. The second group uses ion exchange chromatography to remove matrix.[49, 50] Das *et al.* published a sulphur separation procedure based on anion chromatography for the determination of $\delta^{34}S$ values in standards and seawater by MC-ICP-MS.[49] This method required less processing time, less consumption of chemicals and it offered lower procedural blanks (12-250 ng of sulphur) compared to previously published methods. The recovery calculated for sulphur standard solutions reached 100 % ± 2 %. For low or simple matrix containing samples the separation procedure of Das *et al*. is well suited. Therefore, the ion exchange chromatography was chosen as starting point for development of the sulphur-copper separation method in this research.

Ion exchange is applied as a form of column chromatography in which analyte ions in a solution pass through a resin packed into column, and where active exchange sites react with the ions bound to resin beads. The mechanism of separation is based on the different affinities of the (analyte) ions to the resin. An ion with lower affinity will be displaced by an ion of greater affinity at the active site. The displaced ion is then washed out or collected. Two different types of ion-exchange resins can be used for this purpose, depending on the nature of the ions under investigation: cation exchange (CER) and **anion exchange resin (AER)**. Craddock *et al.* employed CER (AG-50-X8) which is a strongly acidic cation exchange resin to purify sulphur from sediment samples.[50] The resin adsorbed cations such as Zn, Cu, Fe and Ca in the matrix while sulphur easily passed through the resin. The AG 50W resin is composed of sulphonic acid functional groups (as an active site) attached to a styrene divinylbenzene based polymer.[51] Thus, the use of this resin is critical concerning the sulphur background. Das *et al*. used AER (AG1X8) to purify sulphur in sea water.[49] The sulphur is retained on the resin, then the matrix is washed off and subsequently sulphur is eluted. This resin is composed of quaternary ammonium functional groups attached to a styrene divinylbenzene based polymer; thus, it is expected to have low sulphur blanks from the resin.[52]

The ideal sulphur-copper separation by **anion exchange chromatography** is schematically shown in Figure B5-1. The column is filled with AG1X8 resin, then the sample solution is added. Sulphur is expected to remain on the resin while the copper matrix moves through the resin, and then rinse resin to remove copper by eluent 1, after that elute sulphur from the resin by eluent 2. Unfortunately, the intended, ideal separation

yields insufficient recovery and matrix separation. More details on this will follow in the results section.

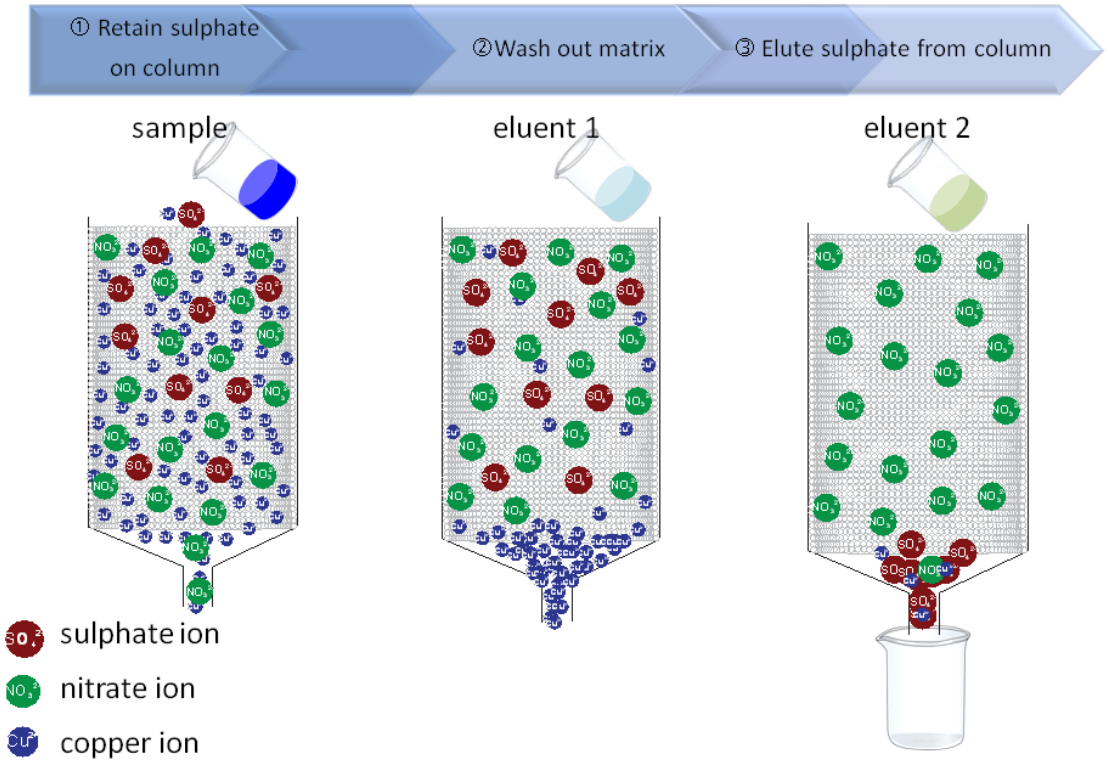

Figure B5-1 Ideal concept of sulphur-copper separation process by AER

B6. Quantification of Sulphur Mass Fraction in Copper Samples by GDMS and LA-ICP-MS

Normally, in the **routine analytical laboratory** glow discharge mass spectrometry (**GDMS**), X-ray Fluorescence (XRF), X-ray diffraction (XRD), carrier gas hot extraction elemental analyzer (CGHE) and laser ablation inductively coupled plasma mass spectrometer (**LA-ICP-MS**) are applied to screen and quantify trace elements in solid samples. These methods are proven useful for fast qualitative and semi-quantitative analysis. Such, **direct solid analysis techniques** do not require complicated sample preparation such as dissolution/digestion or even matrix separation, which are time-consuming and laborious prior to analysis.

Quantitative analysis of GDMS: D. M. McClenathan and G. M. Hieftje analysed accuracy based on concentration of the impurity in iron, nickel, cobalt and copper 27 samples.[53] They divided the analyte concentrations into 3 ranges; greater than 10 %, 1.0 % - 10 %, and 0.10 % - 0.99 % and they evaluated the mean error which were

21 %, 53 % and 65 %, respectively and for copper matrix were 22 %, 105 % and 150 %, respectively. The matrices play an important role to the % error, especially copper, whose % error is significantly higher than others.

Usually, quantitative analysis with GDMS yield accuracy values in the order of 15 % - 20 % without matrix matched calibration, whereas matrix matched calibration gives 5 %.[54] Matschat *et al.* reported relative measurement uncertainty within the order of 5 - 10 % for multi-elemental analysis by matrix matched calibration.[55]

Quantitative analysis of LA-ICP-MS: when no matrix matched standards are available, silicate glass standards (mainly the NIST SRM 610 series) is typically being used in LA-ICP-MS for the quantitative analysis of elements in a wide variety of matrices. This calibration approach may provide accuracy and precision between 10 % to 20 % RSD for simple matrices being close to the silicate glass in composition.[18] However, this non-matrix matched calibration is not suited for a more complex matrix or matrices differing from the glass standard. Craig *et al.* reported negative bias (up to 30%), when geological reference materials were analysed by using a non-matrix matched calibration approach.[18]

Traub *et al.* analysed pure copper by nanosecond-[56] and femtosecond-[57] LA-ICP-MS. They compared two types of calibrator (CRMs produced by BAM and doped copper powder) for calibrating the instrument. The results show that using a matrix matched calibration based on suitable CRMs yields measurement uncertainties of 20 %.

Part C Experiment

Part C consists of four main sections. The first part contains the quantification of sulphur in copper samples by ICP-IDMS with matrix separation and the development of the sulphur-copper separation procedure describing the separation process in detail. The second part describes the quantification of sulphur in copper samples by ICP-IDMS without matrix separation. The third part describes how the measurement results from IDMS are applied to validate and calibrate GDMS and LA-ICP-MS techniques and to quantify sulphur in copper samples. The fourth and the last part concern the development of a LA-ICP-IDMS based procedure for the quantification of sulphur in copper samples.

C1. Quantification of Sulphur in Copper Samples by ICP-IDMS With Matrix Separation

The **IDMS Laboratory** (Division 1.1, BAM) is an ISO/IEC17025 accredited laboratory. Consequently, its environmental conditions are controlled and monitored continuously, e.g. temperature and relative humidity are set at (21 ± 1) ºC, (50 ± 10) %, respectively. The analytical balances were annually calibrated, and they were tested with standard weights before each use to ensure they are working with in their specification. Weighing plays a crucial role to the accuracy of IDMS analysis and metrological traceability of the method.

C1.1 Material, Reagent and Sample

Material and reagents In order to keep the sulphur blank as low as possible all reagents were used in the highest available purity. Nitric acid, used for sample digestion and sulphur-matrix separation, was purified by a two-stage sub-boiling procedure in the clean room. It is widely known that sulphur is an ubiquitous element found at elevated concentrations levels everywhere in the environment. This causes a high **risk of contamination**. To reduce this risk the determination of sulphur, especially at the low $\mu g \cdot g^{-1}$ level, clean working space and specialized sample handling equipment are required to avoid contamination risk. Therefore, all sample preparation processes were carried out in a clean room. All used reagents and apparatus are summarized in Table C1-1. In case of plastic

Table C1-1 A list of the used reagents and apparatus

Reagent	Grade	Supplier
Ammonia solution	Suprapur®	Merck KgaA, Darmstadt, Germany
hydrogen peroxide	Ultrapur®	Merck KgaA, Darmstadt, Germany
NIST SRM 3154	primary standard, high purity standard	NIST, USA
^{34}S spike	-	Sciences International Inc., Delaware USA
Sodium sulphide ($Na_2S.9H_2O$)	ACS reagent	ACROS Organics, USA
Sodium sulphite (Na_2SO_3 anhydrous	ACS	Bernd Kraft der Standard, Duisburg, Germany
Equipment	**Model**	**Company**
High pressure asher, HPA	Anton Paar, HPA-S	Anton Paar GmbH Graz, Austria
Analytical balance	Mettler Toledo AX205	Giessen, Germany
Hot plate	-	Pico Trace GmbH, Goettingen Germany
Metal free clean room	Class 10 (Fed STD 209E)	Pico Trace GmbH, Goettingen Germany
Automatic shaker	IKA HS 260 C	IKA®-Werke GmbH & Co. KG, Staufen, Germany
Micropipette	100, 1000 and 5000 µL	Eppendorf
PFA beaker	15, 30 mL	AHF Analysentechnik AG, Tübingen, Germany
Column	2 mL Eichrome	Triskem International, SAS, France
Centrifuge tube	15, 50 mL with self-standing	Different supplier

labware, they were soaked in 10 % HNO_3 at least 60 hours, whereas PFA beakers and quartz vessels were cleaned by an acid stream cleaning system, where nitric acid vapours continuously leach any contaminations from the labware; after the acid cleaning all labware were soaked in

Milli-Q water overnight. Finally, the labware were dried by air flow in the cleanroom cabinets. When drying was completed the labware either was stored in a cleaned plastic box or in a zip lock bag, in both cases labelled "ready to use".

NIST SRM 3154 was used as primary assay, or so-called **back-spike** in IDMS. The **enriched isotope ^{34}S** was dissolved in HNO_3 to prepare the ^{34}S enriched spike solution. The exact mass fraction of the ^{34}S spike solution was characterized by using the back-spike solution for performing a so-called reverse IDMS. Secondary **stock solutions** were prepared from the parent solutions of NIST SRM 3154 and the ^{34}S spike solution. They were kept separately, stored under controlled conditions and they were monitored for their weight before and after each withdrawal to enable correction of evaporation loss. From the secondary solutions working standards were diluted gravimetrically with 2 % HNO_3.

Sodium sulphide ($Na_2S.9H_2O$), sodium sulphite (Na_2SO_3 anhydrous) and sulphuric acid (H_2SO_4, back-spike) were used to investigate the effect of different sulphur species on the sulphur-matrix separation. Three different ion-exchange resins were used within this study. The details of these resins are shown in Table C1-2.

Table C1-2 Information of the ion exchange resins

Property	Amberlite CG50[58]	AG1X8[52]	Chelex-100[59]
Company	Sigma-Aldrich	Biorad labs	Biorad labs
Resin type	weak cation exchange	strong anion exchange	weak cation exchange
Functional group	carboxylic acid	quaternary ammonium	carboxylic acid
Ionic form	H^+	Cl^-	Na^+
Size (mesh)	100-200	200-400	200-400
Total exchange capacity ($mmol \cdot mL^{-1}$)	3.5	1.2	0.4
Selective to copper	high	none	very high
Function in separation procedure	remove copper	retain sulphur on resin	remove copper
Amount of resin used (mL)	2*	1	1

*depends on amount of copper (2 mL for copper ≤ 20 mg)

All resins were activated and cleaned before use by applying the cleaning procedures which are summarized in Table C1-3. After packing the resins in columns, they were rinsed again before sample loading using Milli-Q water of approximately five times the resin volume.

Table C1-3 Activation and cleaning of resins

Step	Amberlite and Chelex-100 resin
1	put the resin in a PP bottle
2	add Milli-Q water
3	shake by automatic shaker about 30 minutes
4	let the resin precipitate and remove the water
5	repeat step 2-4 until the water is clear or transparent
6	label “ready to use”
AG1X8 resin	
1	put the resin in a PP bottle
2	add Milli-Q water
3	shake by automatic shaking device about 30 minutes
4	let the resin precipitate and remove water
5	add 1 M HNO_3 to modify active site of the resin from Cl^- to NO_3^-
6	shake by automatic shaker about 30 minutes
7	let the resin precipitate and remove the acid
8	repeat step 5-7, three times
9	repeat step 2-4, three times
10	label “ready to use”

Sample NIST SRM 1034 and NIST SRM 494 are certified reference materials produced by NIST whereas BAM-M385, BAM-M376a, BAM-228, BAM-227 are certified reference materials produced by BAM. They were selected to serve as well-defined samples for the development of the sulphur-matrix separation procedure (for details see Table C1-4). For the NIST SRM they were etched by an acid mixture (10 mL of 65 % HNO_3 + 10 mL of 85 % H_3PO_4) for 1 minute then rinsed by Milli-Q water 3 times, followed by drying overnight in an oven at 45 ºC before cutting them to small pieces.

Table C1-4 Copper reference materials (CRMs/RMs) with reference values for the total sulphur mass fraction

Material No.	Type	Copper mass fraction in $g \cdot g^{-1}$ [a,b]	Sulphur mass fraction	U_{rel} in %[c]	Representative range of sulphur
NIST SRM 1034	Pure	99.96, IV	(2.8 ± 0.2) $\mu g \cdot g^{-1}$, CV	7.1	very low
NIST SRM 494	Pure	(99.91 ± 0.01), CV	(15 ± 3) $\mu g \cdot g^{-1}$, CV	20.0	low
BAM-M385	Pure	-	(31.2 ± 1.5) $\mu g \cdot g^{-1}$,CV	4.8	low
BAM-M376a	Pure	-	133 ± 19 $\mu g \cdot g^{-1}$, IV	14.3	low
BAM-228	Alloy	85.34 ± 0.03, IV	360 ± 40 2SD, IV	11.2	medium
BAM-227	Alloy	85.57 ± 0.03, IV	1,220 ± 100 2SD, IV	8.2	high

[a] CV = certified value, IV = information value

[b] Here '±' in brackets represent the expanded measurement uncertainty (k =2),
'±' without brackets represent the standard deviation

[c] U_{rel} = Relative expanded measurement uncertainty of the sulphur mass fraction

C1.2 Development of a Sulphur-Copper Separation Procedure

C1.2.1 Dissolution and digestion/oxidation/equilibration of copper samples

Copper samples were processed to yield small pieces, 0.1 g to 0.25 g of which were weighed into HPA vessels. In case of IDMS analysis, the spike ^{34}S solution was added before sample dissolution was carried out, aiming at a $^{32}S/^{34}S$ ratio of 1. Then 5 mL of conc. HNO_3 was slowly added. This step must be carried out carefully and work shall be performed in a fume hood due to the strong reaction between metal and conc. HNO_3 producing large amounts of toxic gas (NO_x). After this step it was required to wait until the copper was completely dissolved. Then 1 mL of H_2O_2 was added before digestion, which was carried out by applying the HPA.

Digestion was accomplished using an HPA equipped with a heating block holding 5 quartz digestion vessels of 90 mL volume. The digestion program lasted 4 h at a maximum temperature of 320 ºC and a maximum pressure of about 130 bar. The temperature was raised from room temperature to 150 ºC in 30 min and then up to 320 ºC in 60 min. This temperature was kept for 150 min followed by a cooling step down to room temperature with a period of 60 min. The heating program of the digestion is displayed in Figure C1-1.

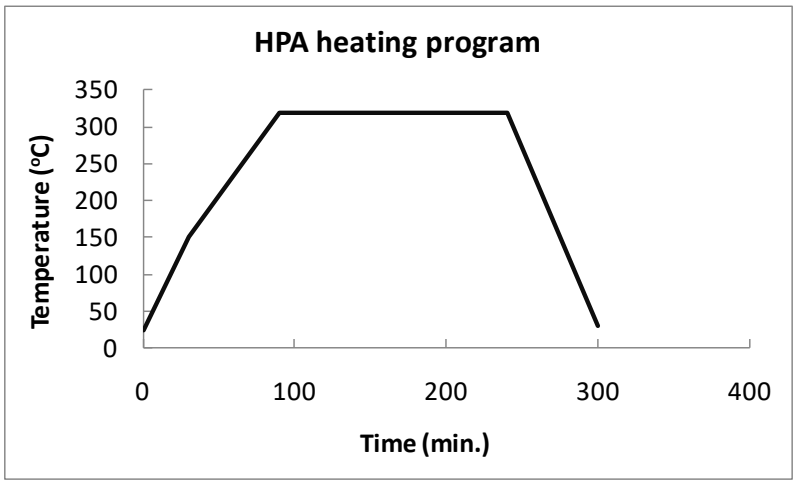

Figure C1-1 High pressure asher heating program

C1.2.2 Sulphur-copper separation

The complete sulphur-copper separation process is summarized in Table C1-5 and visualized in Figure C1-2. The developed procedure for sulphur-copper separation consists of three subsequent separation steps and is described in the following in detail.

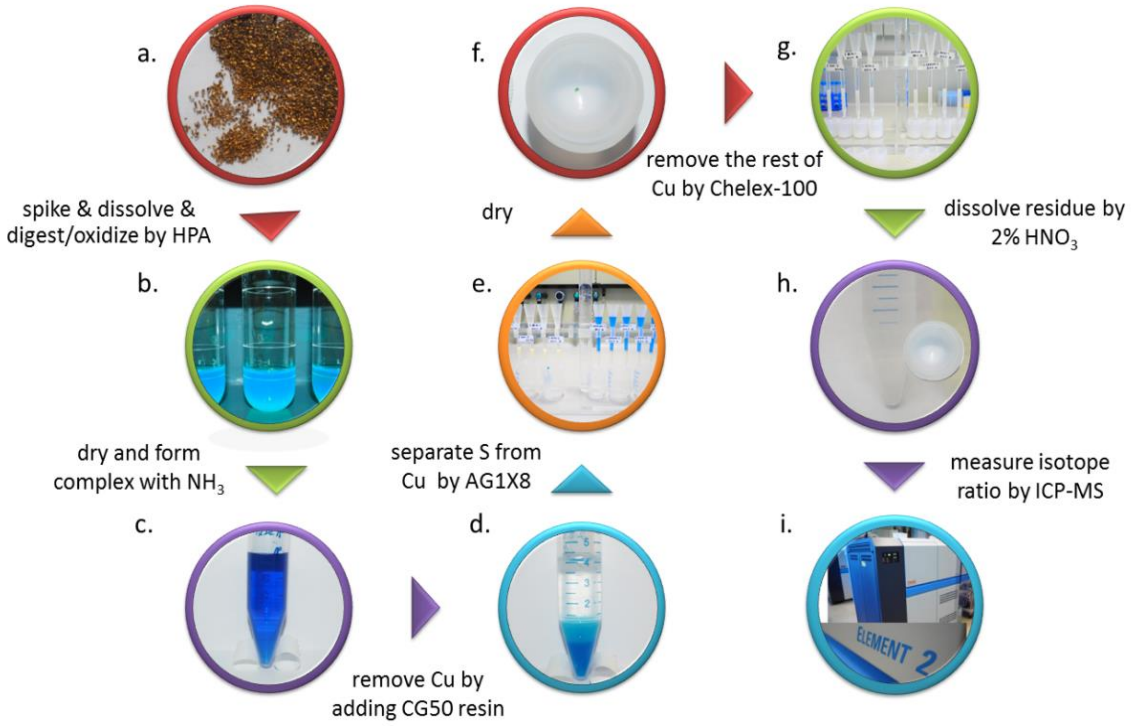

Figure C1-2 Sulphur-copper separation process

Table C1-5 The developed procedure for the sulphur-copper separation

11	Procedure	Remarks
1	weighing 1.0-1.5 g of the digested sample solution into PFA beakers	light blue colour of the solution (Figure C1-2b), sample weight depends on amount of sulphur
2	evaporating to dryness at 110 ºC	using hotplate
3	dissolving the residue by 8 mL of 0.028 M HNO_3	
4	addition of conc. ammonia in excess at room temperature at least > 10 times **Step 1**	amount calculated on stoichiometric basis of the chemical reaction per mole of copper, the colour of the sample solution turns into a deep blue due to the formation of the copper-ammonia complex (Figure C1-2c)
5	addition CG50 resin (white) in excess	1 mL per 10 mg Cu
6	mixing well by using an automatic shaker for 3 h	the resin turns light blue whereas the solution is clear and transparent (Figure C1-2d)
7	packing 1 mL of AG-1X8 resin in a column	(Figure C1-2e)
8	rinsing with Milli-Q water, 5 mL	
9	closing the lower end of the column by parafilm	
10	loading the clear solution from no. 6	let the CG50 precipitate
11	removing the parafilm to let the remaining matrix pass through, after about 20 min **Step 2**	
12	rinsing CG50 resin from no.6 with 4 mL Milli-Q water	
13	loading the solution onto the AG1X8 column	
14	repeating no.11 to no. 12, 4 times	
15	eluting the sulphur fraction from the AG1X8 resin by addition of 12 mL of 0.25 mol·L^{-1} HNO_3 onto the column	collecting this fraction, requires new PFA beaker
16	evaporating the eluted fraction to dryness at 110 ºC	evaporating overnight
17	check the residue, normally, it is blue or green	which means that remains from the copper matrix are still present (Figure C1-2f)
18	dissolving the residue with 2 mL of Milli-Q water	
19	packing 1 mL of Chelex resin into the column	(Figure C1-2g)
20	rinsing the resin with 5 ml of Milli-Q water	
21	closing the lower end with parafilm	
22	loading the residue solution from no. 18 onto the column **Step 3**	
23	removing the parafilm, after 20 minutes	
24	rinsing the PFA beaker with 2 mL Milli-Q water and loading it onto the column	the sulphur is eluted, collected this fraction, new PFA beaker is required
25	repeating no. 24, 4 times	
26	evaporating the eluted fraction to dryness at 110 ºC	(Figure C1-2h)
27	dissolving the residue by 2 % HNO_3	final sulphur mass fraction is aimed at 2 µg·g^{-1} for each isotope
28	spiking ^{34}S into the procedure blank by gravimetric method	final sulphur mass fraction is aimed at 2 µg·g^{-1} for ^{34}S
29	measuring $^{32}S/^{34}S$ by ICP-MS	

To ensure the reproducibility of the separation, every parameter was kept constant as far as possible, even the volume of the resins. Column packing is one of the critical steps and has to be carried out as reproducible as possible. The column was cleaned before use (see details in Table C1-3) then a frit was inserted into the column, followed by the addition of 1 mL or 2 mL Milli-Q water. The Milli-Q water was only used to mark the filling level of the later loaded resin volume. The resin was added into the column by pipetting up to the mark, then the resin was rinsed with Milli-Q water at least 5 times of the resin volume. In case of CG50, the resin was mixed with the sample solution before loading it into the column, then the subsequent treatment was the same as described above.

C1.3 Measurement by ICP-MS

C1.3.1 Challenges of the sulphur measurement by ICP-MS

The aim of this research is the development of a reference procedure for the quantification of sulphur in copper. Intrinsic part of a reference procedure is the consideration of metrological principles. This leads to a number of challenges impeding the development of such a reference procedure. To enable a successful method development these challenges were investigated, solutions were found and cross-checked with the aims of this work. Table C1-6 lists the major challenges and the found solutions.

Table C1-6 A list of challenging and solving in sulphur measurement

Challenge	Detail	Solution
high background on ^{32}S and ^{34}S	10th most common element	effective cleaning, high purity reagents, work in clean laboratory
polyatomic interferences	$^{32}S \rightarrow {}^{16}O^{16}O$	use ICP-MS in medium or high resolution (m/Δm >
isotopic interferences	$^{64}Zn^{2+}$ on ^{32}S, $^{68}Zn^{2+}$ on ^{34}S	
high first ionization potential	10.36 eV[19]	use instrument with high sensitivity
difficult matrix	metal matrix leads to bias in mass discrimination	sulphur-matrix separation
low sulphur content	mg·g^{-1} level	pre-concentration of sulphur
SI traceability required	procedure available which enables traceability	Double IDMS
low measurement uncertainty (MU) required	most calibration strategies provide high MU	Double IDMS

C1.3.2 Instrument

All mass spectrometric measurements were performed using the sector field ICP-MS instrument Element 2 (Thermo-Fisher Scientific, Germany), unless stated otherwise. The instrument was tuned to obtain the highest efficiency in daily use by aspirating a multi-element tuning solution (1 $\mu g \cdot L^{-1}$(. For quality assurance pruposes the performance criteria were set as follows:1) intensity for 1 $\mu g \cdot L^{-1}$ indium > $1x10^6$ cps (low resolution), medium resolution > 4,300, precision of signal intensity within one measurement < 1.5 % and 2.5 % RSD for low and medium resolution. Table C1-7 shows the operating conditions of the instrument after tuning.

Table C1-7 Instrument operating parameters for sulphur measurements

Instrument type	Element 2
Autosampler	Cetac ASX 100
Aspiration mode	Self-aspirating
Nebulizer	MicroMist 100 µL
Spray chamber	Cyclonic spray chamber
Interface	Jet interface
Cones	Ni sampler and skimmer X-cone
Cool gas flow rate	16 $L \cdot min^{-1}$
Auxiliary gas flow rate	0.8-1.0 $L \cdot min^{-1}$
Sample gas flow rate	0.9-1.25 $L \cdot min^{-1}$
RF power	1200 W
Guard electrode	On
Mass resolution mode	Medium
Acquisition mode	Pulse and analog mode
Runs / passes	10 / 40
Sensitivity in cps/($\mu g \cdot g^{-1}$)	$1x10^7$ for ^{32}S
Drift correction	Yes

C1.3.3 Measurement

The separation of the major interferences requires the **medium mass resolution** mode (m/Δm > 4,300). Martínez-Sierra *et al.* showed a mass spectra of $^{32}S^{+}$ and $^{16}O_2^{+}$ where both peaks clearly separated from each other at mass resolution of approximately 4000.[3] However, also doubly charged Zn ions ($^{64}Zn^{2+}$ and $^{68}Zn^{2+}$) can affect the sulphur measurement. To resolve this interference a mass, resolution above 4,300 is required.

Regarding the **interferences from doubly charged Zn ion**, the mass fraction of zinc in copper materials is relevant and need to be checked. The copper samples in this study contain zinc in the range from less than 10 $mg \cdot g^{-1}$ to 300 $mg \cdot g^{-1}$. Due to this high mass fractions of Zn the intensities of $^{64}Zn^{+}$ and $^{68}Zn^{+}$ were monitored to observe any potential problems with high intensities of doubly charged Zn isotopes interfering on the sulphur masses 32 and 34. After sulphur-matrix separation, the Zn mass fraction was below 50 $ng \cdot g^{-1}$ which was close to total **zinc removal** (> 99.999%). One-point calibration with 50 $ng \cdot g^{-1}$ Cu-Zn standard was used to quantify the remaining Cu and Zn after the separation. The intensities of $^{63}Cu^{+}$ and $^{65}Cu^{+}$ were used to investigate matrix removal efficiency, as well as, the intensities of $^{64}Zn^{+}$ and $^{68}Zn^{+}$. The intensities of $^{63}Cu^{+}$, $^{65}Cu^{+}$, $^{64}Zn^{+}$ and $^{68}Zn^{+}$ after separation were $6x10^5$ cps, $3x10^5$ cps, $3x10^5$ cps, and $2x10^5$ cps, respectively. Therefore, concerning problems with high intensities doubly charged of Zn isotopes can be neglected.

Sulphur IDMS analysis was measured in a sequence of 122 analysis by applying a modified **bracketing method**. The sequence started with 24 measurements of back-spike solution, followed by 6 measurements of the natural sample, 24 measurements of the sample blends, 12 measurements of the procedural blanks and finally 6 measurements of the spike solution. The nitric acid blank (2 % HNO_3) was measured in between every sample, whereas the back-spike solution was monitored after every 6 sample measurements along the sequence to allow for a later drift correction.

In general, the **observed intensities for ^{32}S** in 2 % HNO_3, in the procedural blank and in a 2 $\mu g \cdot g^{-1}$ sulphur standard were in the range of 0.2-1.3$x10^6$ cps (n = 106), 0.4-2.5$x10^6$ cps (n = 22) and 2-3$x10^7$ cps (n = 94), respectively. As a consequence, the signal 2 $\mu g \cdot g^{-1}$ sulphur standard was 20 times above those of the blank in all cases. The standard deviation of the sulphur isotope ratio of back spike for a complete sequence over 17 hours was around 1.3 %

relative, which included the reproducibility of the isotope ratio measurement, the instrumental drift and wash-out effects during the measurement sequence.

Mass bias is the common, although inaccurate term for instrumental mass discrimination / fractionation can contain drift effects thereof and detector efficiency.[23] In ICP-MS mass bias leads to a bias in the measured isotope ratio at the expenses of the isotope compared to the "true" isotope ratio. In IDMS mass bias typically is corrected using the so-called *K*-factor (see below), which requires the measurement of a sample with known, "true" or absolute, isotope ratio. In this work the back spike which was prepared from the certified reference material, NIST SRM 3154 was used for this purpose. The back-spike was regularly measured in between the samples and blends along the whole sequence to enable both corrections, those of the mass bias correction as well as the drift thereof. Drift corrections are important in ICP-MS, especially when long sequences over several hours are measured. However, drift corrections have to be applied carefully, because over corrections can easily occur: e.g. when the overall standard deviation of a sequence is only slightly larger than the typical standard deviation of a single measurement in fact no drift is present, and a drift correction will only increase the spread of results and the measurement uncertainty.

Correction factor *(K*-factor) is used to correct for the instrumental mass discrimination / fractionation. It is simply calculated as the "true" or absolute isotope ratio of a reference divided by the measured isotope ratio of this reference. The reference is either an isotopic reference material certified for its isotope ratio, a reference sample with known absolute isotope ratio or a representative sample realizing the natural isotopic composition, which is tabulated by IUPAC. The mathematical relationship for the *K*-factor is given in equation 14.[18, 23] The reference value for the $n(^{32}S)/n(^{34}S)$ ratio in NIST SRM 3154, which was used as isotope reference in this work, was taken from Pritzkow *et al.* 2005.[8]

$$K = \frac{R_{ref}}{R_{obs}} \quad , \qquad \text{Equation 14}$$

where *K* is correction factor

R_{ref} is the absolute isotope ratio of the reference

R_{obs} is the observed or measured isotope ratio of the reference

Deadtime correction: As described in section B3.1.6 the deadtime is required to correct any deadtime effects which lead to a bias in the ion intensity and the isotope ratios when

ion counting mode is used. Lutetium (Lu) standard solutions with different mass fractions were used to determine the deadtime: 0.2, 0.4, 0.6, 0.8 and 1.0 $\mu g \cdot g^{-1}$. The ion intensities were recorded and the resulting measured isotope ratio $^{75}Lu/^{176}Lu$ was plotted versus the Lu mass fraction. Then the deadtime was calculated by equation 8 in section B3.1.6.

C1.4 Data Processing

Excel was usually used in this research for data processing such as management of raw data, drift correction and calculation of average values and their standard deviations or their standard uncertainty. Excel was used not only for pre-calculation but also for post-calculation, for summarizing data, for comparing measured values and for plotting graphs. The main calculations, however, leading to the mass fractions of sulphur and their measurement uncertainty were carried out by using the GUM Workbench software. [60]

Gum workbench is a software, which allows to calculate the uncertainty of any measurement, test or analysis, including calibrations, physical testing and chemical analyses. The statistical and mathematical analysis and computations follow the rules of the ISO Guide to the Expression of Uncertainty in Measurement and the requirement document EA 4/02 of the European Cooperation for Accreditation. It is compatible with other GUM based documents for example the NIST Technical Note 1297, the Eurachem/CITAC Guide and UKAS M3003. GUM Workbench was used in this research in its version 2.4.

Figure C1-3a shows the mathematical model used in this work as it appears in GUM Workbench. This model was used to quantify the mass fractions of sulphur in the copper samples and all contributing quantities, which affect to the measurement result. In the table at the bottom of Figure C1-3a, the definitions of the quantities are listed. The result of the analysis is a transparent table of the uncertainty budget (see Figure C1-3b). This table lists all used quantities with values, uncertainty contribution and % contribution. The associated standard uncertainty and the sensitivity coefficient automatically are obtained from the model equation. The result of the calculation (in the bottom) expresses the mass fraction of sulphur with its expanded uncertainty. In the drop-down list box of the expanded uncertainty, it can be selected between different types such as expanded uncertainty, standard uncertainty or relative measurement uncertainty. A complete example of an uncertainty budget calculated with GUM Workbench is displayed in Part F Appendix.

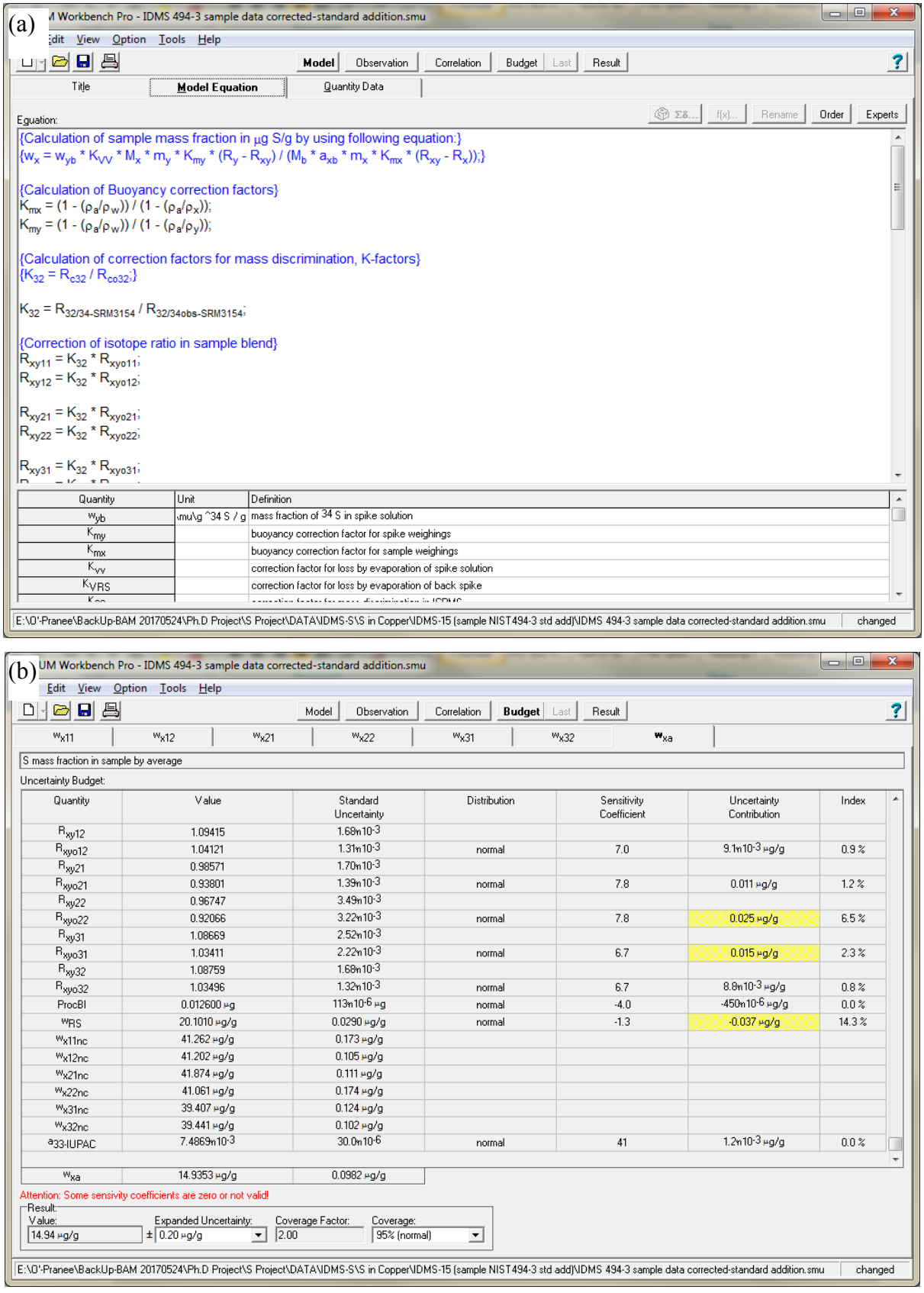

Figure C1-3 Excerpt of an uncertainty budget for the IDMS analysis of sulphur in copper as calculated by GUM Workbench. (see Part F Appendix for more information)

C2. Quantification of Sulphur in Copper Samples by Direct ICP-IDMS Analysis (Without Matrix Separation)

C2.1 Material, Reagent and Sample

Material, reagents and sample Same as section C1.1 except only three copper sample were measured which were BAM-M376a, BAM-228 and BAM-227.

C2.2 Sample Preparation

Typically, sulphur analysis by conventional ICP-MS is straightforward, that is the direct measurement of the sample after dissolution and dilution. Table C2-2 shows the calculation and the resulting mass fractions for the sample preparation process of an IDMS analysis without matrix separation. Approximately 0.1 g to 0.25 g of copper samples were accurately weighed into 50 mL centrifuge tubes; then an exact amount of the ^{34}S spike was added, which was calculated beforehand to yield a $^{32}S/^{34}S$ isotope ratio of 1. Next, the conc. HNO_3 was slowly added to dissolve the copper. As mentioned before the reaction between copper and conc. HNO_3 generates a large volume of NO_x then the system must be loosen to release the pressure. After that the solution was mixed well manually. The sample blend solution was diluted to realize an upper limit of $\mu g \cdot g^{-1}$ copper. Therefore, BAM-M376a, BAM-228 and BAM-227 sample solutions contained differences in total sulphur mass fractions of approximately 0.13 $\mu g \cdot g^{-1}$, 0.34 $\mu g \cdot g^{-1}$ and 1.16 $\mu g \cdot g^{-1}$, respectively.

Table C2-2 Data of the sample preparation for an IDMS analysis of sulphur in copper without matrix separation

Sample name	BAM-376a	BAM-228	BAM-227
copper mass fraction ($g \cdot g^{-1}$)	~1.00	~0.85	~0.85
sulphur mass fraction ($\mu g \cdot g^{-1}$)	133	360	1220
sample mass (g)	0.25	0.15	0.10
mass of sulphur (µg)	33.25	54	122
mass of ^{32}S (µg)	31.58	51.29	115.89
mass of ^{34}S	1.41	2.30	5.19
natural $^{32}S/^{34}S$ isotope ratio	22.35		
aimed $^{32}S/^{34}S$ ratio in sample blend	1	1	1
volume of the spike solution (mL)*	0.33	0.53	1.20
amount of ^{34}S (µg)	30.17	49.00	110.70
total sulphur in sample blend (µg)	63.42	103.00	232.70

Sample name	BAM-376a	BAM-228	BAM-227
volume of the conc. HNO_3 (mL)	6	6	6
concentration of the sulphur in sample blend ($\mu g \cdot mL^{-1}$)	10.57	17.17	38.78
concentration of the copper in sample blend ($\mu g \cdot mL^{-1}$)	41,666	25,000	16,667
sample volume of the sample blend	0.10	0.16	0.24
mass of sulphur (μg)	1.06	2.75	9.31
mass of copper (mg)	4.17	4.00	4.00
final volume (dilute by 2% HNO_3) (mL)	8.3	8.0	8.0
concentration of the total sulphur ($\mu g \cdot mL^{-1}$)	0.13	0.34	1.16
concentration of ^{32}S ($\mu g \cdot mL^{-1}$)	0.06	0.17	0.58
aimed concentration of the copper ($\mu g \cdot mL^{-1}$)	500	500	500

* mass fraction of sulphur in spike solution is (92.21 ± 0.19) $\mu g \cdot g^{-1}$

C2.3 Measurement

For measurement and data processing, please refer to section C1.3 and C1.4, respectively. This part of the study, sulphur is quantified without matrix separation. Thus, the matrix correction is required.

Matrix correction: To correct the matrix effect, a matrix correction factor was determined and applied, which is similar to the correction factor for mass discrimination defined in equation 15. This matrix correction factor was obtained by dividing the measured $^{32}S/^{34}S$ isotope ratio in the unspiked, natural copper samples by the measured $^{32}S/^{34}S$ isotope ratio in the back-spike; sulphur isotope variations in natural samples were not considered as they are expected at the per mil or sub per mil level, which is far below the here obtained isotope ratio precision. The idea behind is that when natural isotope variations are insignificant, the occurring bias between the isotope ratio in the matrix-containing sample and those in the matrix-free back-spike can only be derived from matrix effects. Subsequently, this matrix correction factor was applied to correct the isotope ratio of the sample blends.

$$K_c = \frac{R_{obs(back-spike)}}{R_{sample}} \quad , \qquad \text{Equation 15}$$

where K_c is the correction factor

$R_{obs(back\text{-}spike)}$ is the observed isotope ratio in the back-spike solution

R_{sample} is the observed isotope ratio in the unspiked, natural sample

C3. Quantification by GDMS and LA-ICP-MS as Demonstrated for Sulphur in Copper and Copper Alloys

GDMS and LA-ICP-MS are direct techniques for elemental analysis. This study used both as a routine analysis; instrumental optimization is not a main issue. The techniques will be validated by IDMS values (with matrix separation) as reference values or calibrator. After that, sulphur in other copper materials can be quantified on the basis of the different calibration approaches. Consequently, the measurement results are traceable to the SI through the IDMS results. Measurement uncertainty will be estimated for different calibration strategies.

Table C3-1 is a list of pure copper and copper alloy samples / calibrators which were used in this study. Matrix-matched calibration was the preferred calibration approach for the quantification of sulphur. To realize this BAM-M385 and BAM-376a were used as a calibrator for pure copper samples, whereas BAM-228 and BAM-227 were used for copper alloy. Cross calibration between pure copper and copper alloy was validated as well.

C3.1 Sulphur Measurement by GDMS

GDMS is a well-established technique which require little sample preparation. However, it is important to realize that the presence of residual gases (air and water) on the sample surface can affect the performance of the GDMS measurements in terms of absolute sensitivity and spectral interferences. Thus, the samples were cleaned with absolute ethanol before each measurement; in the vacuum the samples were pre-sputtered for about 9 minutes before measurements were started. The purpose of the pre-sputtering is not only cleaning the surface, but also waiting for signal stabilization. For tuning the instrument, the reference material BAM-M376a was used to check the mass position, peak shape and resolution of copper and sulphur. The measurement parameters resulting from this tuning are shown in Table C3-2. GD source was operated in Pulse mode for high sensitivity to sulphur measurements. The sample cone was changed for every sample to avoid cross-contamination.

Table C3-1 List of studied copper materials

Name	Institute/company	Year of issue	Type	Cu (%)	Mass fraction of sulphur (µg·g^{-1}), CV / IV*	Mass fraction of sulphur (µg·g^{-1}) by IDMS	GDMS	LA-ICP-MS
SRM1034	NIST	1982	Pure Cu	99.96	(2.8 ± 0.2), CV	-	No	Yes
BAM-Y001	BAM	2004		99.99	(5.4 ± 3.2), IV	-	No	Yes
SRM 494	NIST	1986		99.91	(15 ± 3), CV	-	No	Yes
M385	**BAM**	**2013**		**99.96**	**(31.2 ± 1.5), CV**	**(37.8 ± 0.2)**	**Yes**	**Yes**
M376a	**BAM**	**2016**		**99.59**	**(133 ± 19), IV**	**(133.7 ± 0.8)**	**Yes**	**Yes**
429	Kabel-und Metallweisse (KM)	-		99.95	20, IV	-	Yes	Yes
422	Kabel-und Metallweisse (KM)	-		99.55	154, IV	-	Yes	Yes
S26	Weiland Wecker (WW)	-		99.85	466, IV	-	Yes	Yes
BAM-228	**BAM**	**1979**	Cu alloy	**85.34**	**360 ± 40, RV**	**(385.5 ± 2.2)**	**Yes**	**Yes**
BAM-227	**BAM**	**1979**		**85.58**	**1220 ± 100, RV**	**(1376.7 ± 5.1)**	**Yes**	**Yes**
826	CTIF (Centre Technique des industries De La Fonderie)	1977		87.05	750, IV	-	Yes	Yes

* CV = certified value with expanded uncertainty (k=2), IV = information value, Bold = calibrator

Table C3-2 Instrument operating parameters for sulphur measurements

Instrument type	Thermo Fisher Scientific Element GD plus
Operation mode	Pulsed
Pulse duration	40 μsec
Frequency	4 kHz
Discharge voltage	1000 V
Discharge gas	462 $mL \cdot min^{-1}$
Discharge current	Approximately 23 mA
Cones	Ni cones
Measurement repeatability	14 times
Pre-sputtering	9 min. (in average)
Mass resolution mode	Medium
Acquisition mode	Triple mode

Table C3-3 shows the ion beam ratio (IBR) of calibrators and samples which were used for result evaluation. The obtained precision for the IBR of the calibrators and sample are below 4 % RSD, when measurements were repeated 14 times, except for sample no. 422 (7.4% RSD). The RSD value not only represents the stability of the measurements, but also the homogeneity of the materials. This variation will be included in the uncertainty budget.

Table C3-3 Ion beam ratio of ^{32}S in calibrators and samples

Sample no.	Type	IBR	SD	RSD
BAM-M385	pure copper	30.109	0.238	0.8 %
BAM-M376a		104.699	2.363	2.3 %
429		14.7059	0.090	0.6 %
422		99.1979	7.377	7.4 %
S26		487.868	19.249	3.9 %
BAM-228	copper alloy	347.136	4.365	1.3 %
BAM-227		1155.556	33.180	2.9 %
826		692.4663	4.489	0.6 %

C3.2 Sulphur Measurement by LA-ICP-MS

LA-ICP-MS is a well-established direct analysis technique for solid samples with minimal sample preparation. Typically, the LA-ICP-MS is optimized by tuning the system during the continuous ablation of a suitable CRM (after tuning the ICP-MS with tuning solution). In this work the NIST SRM 005a, a glass reference material, was used for tuning the ICP-MS. Unfortunately, this SRM did not contain sulphur; thus, the BAM-M385 reference material was used in addition to optimize the parameters such as peak position, mass offset and peak shape specifically for sulphur.

Before the samples were placed into the sample chamber their surfaces were cleaned with ethanol. After that the sample chamber was connected to the laser system and the ICP-MS. The sample chamber was flushed with He gas about 10 minutes before the measurement started. The instrumental parameters are listed in Table C3-4.

Table C3-4 Instrumental operating parameters for sulphur measurements by LA-ICP-MS

Parameter	Element XR
Interface	Normal
Cones	Ni
Cool gas flow rate	16 $L \cdot min^{-1}$
Auxiliary gas flow rate	0.95 $L \cdot min^{-1}$
Sample gas flow rate	0.59 – 0.80 $L \cdot min^{-1}$
RF power	1350 W
Guard electrode	On
Mass resolution mode	Medium
Acquisition mode	Triple mode, S measured with SEM
Drift correction	Yes
Measured isotopes	^{32}S, ^{34}S, ^{63}Cu, ^{65}Cu
Laser system	Cetac LSX-213
Laser energy	1.4 mJ, fluence 4.5 $J \cdot cm^{-2}$
Laser wavelength	213 nm
Pulse width	< 6 ns
Repetition rate	20 Hz
Carrier gas	He
Carrier gas flow	0.9 $L \cdot min^{-1}$
Sampling mode	Line scan
Spot size	200 μm
Scan rate	25 $\mu m \cdot s^{-1}$
No. of line scan/sample	3

Parameter	Element XR
Sample chamber	Large volume chamber (ETH Zürich)
Ablation duration	10 s laser warm up followed by 1 min ablation for stabilization before starting the measurement depending on the analysis time

The raw data were corrected for the gas (flow) blank and for drift by using the QC sample (BAM-M376a) which was measured before and in between each measurement. The intensity of ^{32}S and $^{32}S/^{65}Cu$ (^{34}S intensity was too low) were plotted versus the mass fractions (IDMS reference values) of the materials and linear regression lines were calculated and the slope, the intercept and the corresponding determination coefficient, R^2, were obtained (Table C3-5). The R^2 value of ^{32}S and $^{32}S/^{65}Cu$ for sulphur in pure copper were 0.9977 and 0.9999, respectively. The isotope ratio of $^{32}S/^{65}Cu$ provides slightly a better linearity which is well suited for external calibration matrix-matched calibration, because instabilities which occur during the measurement are corrected by using ^{65}Cu as internal standard.

Table C3-5 Results from the linear least square fit for different calibration strategies

CRM	Type	Reference Value*	^{32}S	$^{32}S/^{65}Cu$
SRM494	Pure Cu	(14.97±0.20)	4,564.0	4.108×10^{-5}
BAM-M385		(37.76±0.2)	6,869.3	5.164×10^{-5}
BAM-376		(133.7±0.8)	14,255.2	9.384×10^{-5}
		Slope	80.3	4.465×10^{-7}
		Intercept	3575.4	3.46×10^{-5}
		R^2	0.9977	**0.9999**
228	Cu alloy	(385.5±2.2)	32,946.5	3.652×10^{-4}
227		(1376.7±5.1)	139,194.9	1.390×10^{-3}
		Slope	102.3	7.770×10^{-7}
		Intercept	-2719.1	2.80×10^{-5}
		R^2	0.9978	**0.9960**

* from IDMS analysis

The mass fraction of sulphur in each copper sample was calculated by using the linear relationship as shown in equation 16. The parameters (slope and intercept) of this

linear equation were obtained from least square fit performed for different external calibration strategies.

$$y = ax + b \quad , \quad \text{Equation 16}$$

when y is the measured ratio $^{32}S/^{65}Cu$ in the copper sample

x is the sulphur mass fraction in the sample

a is the slope of the calibration curve obtained from the least square fit

b is the intercept of the calibration curve obtained from the least square fit

C4. Method Development for the Quantification of Sulphur in Copper Samples Using LA-ICP-IDMS

C4.1 Material, Reagent and Samples

Polyethylene (PE) frits are normally used for separation in column chemistry. The frits were selected as a support material in this work because of their properties which suits the purpose best: thermoplastic (melting point > 100 °C) and chemical resistance, especially with nitric acid (> 70 %, depending on type of PE). The frit is a product from Triskem International Company (Bruz, France), with diameter 7 mm, thickness 2 mm and pore size 20 µm. Reagents, material and equipment are listed in Table C1-1, section C1.1. Three reference materials were used to validate the method which were BAM-M376a, BAM-228 and BAM-227. Several support materials were tested such as sodium silicate (Th. Geyer GmbH & Co. KG, Germany), Nitrocellulose membrane (Thermo Scientific, USA) whereas gelatine, epoxy glue and cotton were obtained from market.

C4.2 Selection of Support Material

A pellet or tablet form is highly suitable for laser ablation based analysis. The transfer of the liquid sample solution into a pellet requires a support material which has the ability to absorb the liquid or to solidify the liquid. For this purpose, several potential support materials were tested such as sodium silicate, epoxy glue, gelatine, nitrocellulose and, cotton. All these materials proved unsuitable to form homogeneity and solid pellets which can be used for LA-ICP-MS measurements of sulphur in trace levels. **Sodium silicate** and **epoxy glue,** formed an acceptable pellet when mixed with Milli-Q water, but when mixing with the digested copper solution they created agglomerates and the resulting

pellets were not suitable for LA measurements. **Gelatine** has good physical properties leading to suitable pellets, but the sulphur blank levels ($2.5x10^6$ cps for ^{32}S) were unacceptable high. **Nitrocellulose membranes** provide low absorption efficiency for the digested copper solution and high sulphur background. The sulphur intensity was $1.2x10^5$ cps for ^{32}S for nitrocellulose membrane blanks as well as samples, making this material completely unsuitable. **Cotton** is not resistant to concentrated nitric acid (contained in the digested copper sample). During the laser ablation process it contaminates the sample cell and tubing. The **PE frit was the best** choice because of its low sulphur content, high absorption efficiency, optimum size and shape, high stability against concentrated nitric acid and relatively high temperatures. The PE frits shows a good and uniform ablation behaviour. Moreover, a significant number (n = 13) of samples fits into the sample cell, so there is no need to interrupt the measurement for each individual sample. The sample cell with 13 frits is shown in Figure C4-1.

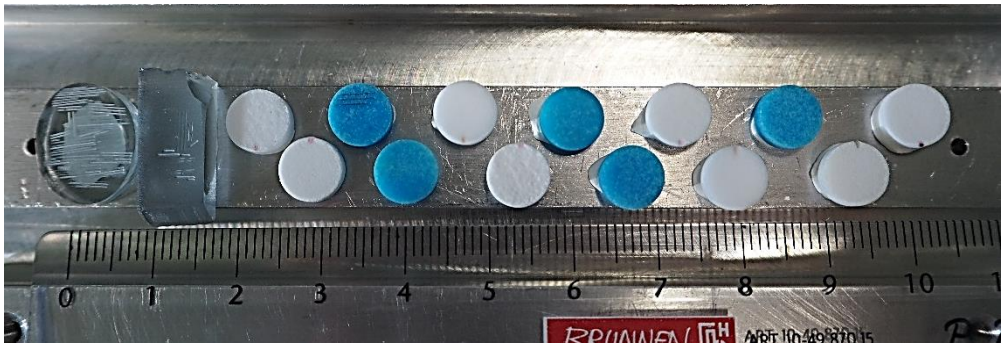

Figure C4-1 PE frit samples in the sample cell of LA-ICP-MS

Characteristic of Polyethylene frit: Most commonly, polyethylene (PE) frits are used for column chromatography in analyte-matrix separation: here, the PE frit retains any sample or resin particles and avoid the wash-out of these particles into the analyte fraction. In this project the PE frit was selected as a support material due to its specific properties: thermoplastic material with a melting point > 100 ºC and chemical resistance, especially against nitric acid (> 70 %, depending on the type of PE). The frit is produced by Triskem International Company, with a diameter of 7 mm, a thickness of 2 mm and a pore size of 20 µm. The porous characteristics directly affect the absorption efficiency of the sample solution, which will be taken up into the cavities of the frit.

C4.3 Investigation of the PE Frit Performance

As this PE frits were used the first time for sample preparation in LA-ICP-IDMS for elemental analysis, the performance criteria must be reviewed prior to LA-ICP-IDMS analysis.

C4.3a Sulphur background

The sulphur background of the LA-ICP-MS system was investigated by measuring the sulphur intensity in the gas flow blank without any laser ablation. The intensity of the gas flow was in the range of 1.3-1.8x10^4 cps for ^{32}S, while the blank intensity of the ablated PE frit was 2.3-4.0x10^4 cps for ^{32}S (n = 8). Comparing to the all other tested support materials the PE frit shows the lowest sulphur background which is approximately twice the intensity of the gas flow blank.

C4.3b Absorption efficiency

Absorption efficiency was determined by the indirect method as follows.

1. The frit samples were doped by sulphur standard solution, which were weighed into 15 mL PFA beakers such that increasing a sulphur masses of 2 µg, 5 µg, 10 µg, 20 µg, 40 µg and 80 µg in individual beakers were obtained.
2. The beakers were filled up with 1 mL of 2 % HNO_3, the solutions were mixed well, and then a PE frit was dropped into every beaker.
3. The solution with the PE frit was evaporated to dryness on a hot plate at 100 ºC.
4. 2 % HNO_3 was added to the beakers, swirled them and the acid was evaporated on the hot plate again. This step was repeated three times.
5. After drying, the PE frits were marked on one side to recognize the side to be ablated by the laser. As the frits typically float on the surface of the sample solution, the downside preferentially adsorbs the sample compared to the upside.
6. The frits were analyses by LA-ICP-MS to investigate the sensitivity, the isotope ratio precision, the limit of detection (LOD), the limit of quantification (LOQ) and the dynamic range by external calibration strategy. In parallel, the PFA beakers were weighed and rinsed well by the addition of 1 g of 2 %

HNO_3. The rinsing solution was quantified for the remaining sulphur mass fraction by external calibration ICP-MS (Element 2).

7. The absorption efficiency of the frit was determined by subtracting the remaining sulphur in the beaker from the original sulphur amount as shown in section D4.1a.

C4.4 Sample Preparation

The sample preparation process was summarized in Figure C4-2. Copper samples were processed as described in section C1.2. After digestion, a volume of 1 mL to 2 mL of the sample solutions was subsampled into a PFA beaker. Then the PE frit was added, and the sample was evaporated at 100 ºC until dryness. The frit absorbs the sample solution inside their cavities. Figure C4-3b shows the resulting frit surface; some residual particles deriving from the evaporated sample stick on surface of the frit and show a significant inhomogeneity of the sample dispersion. About 40 µL of 2 % HNO_3 were added to re-dissolve the residue on the surface. After drying this step was repeated until the frits show smooth surface (normally three times). The magnification of the frit's surface is illustrated in Figure C4-3c.

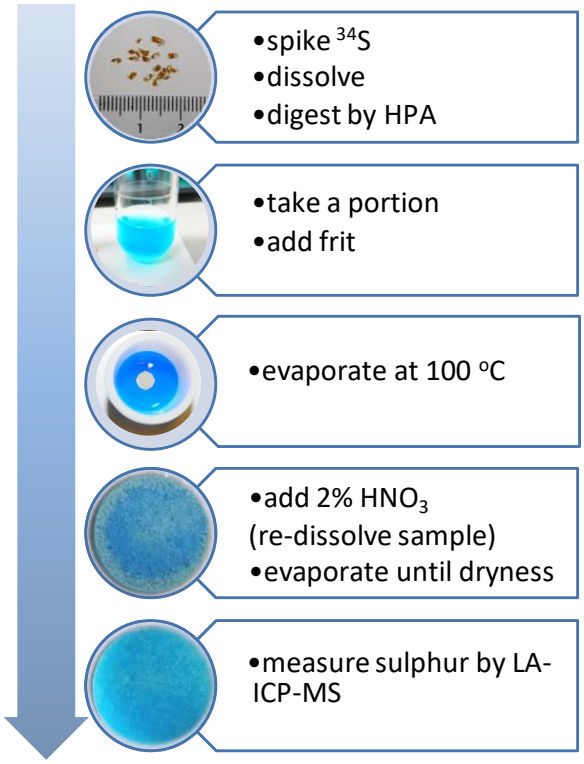

Figure C4-2 Sample preparation scheme

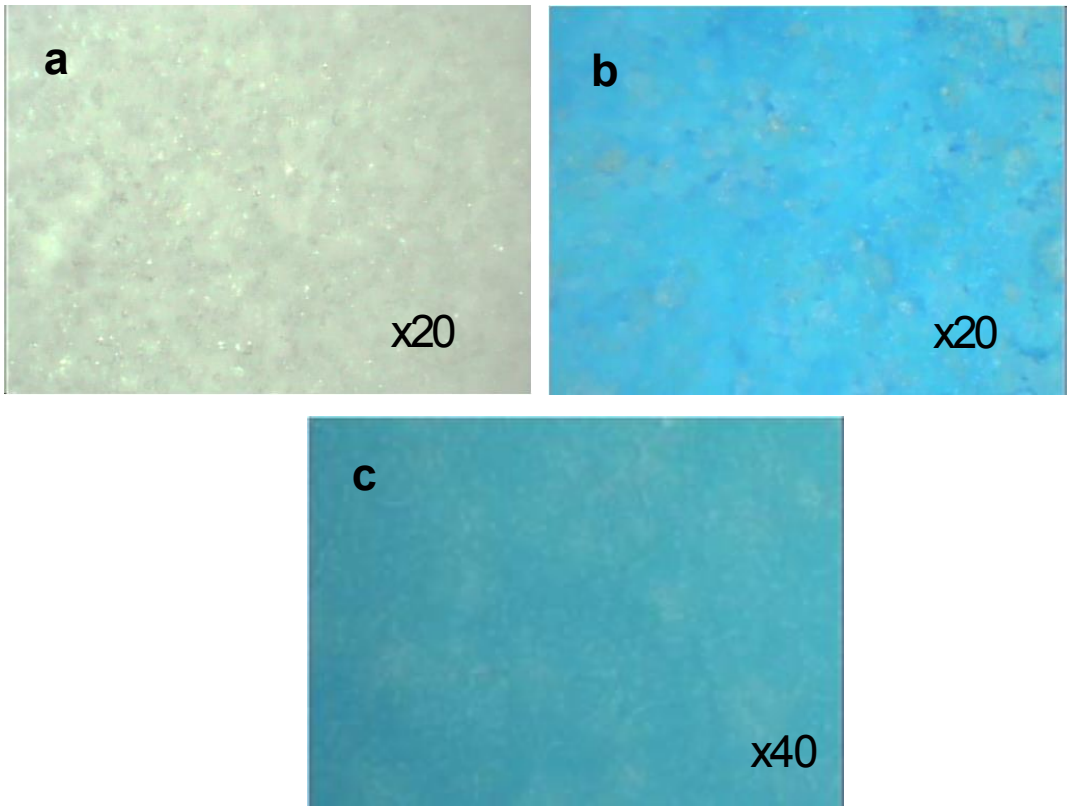

Figure C4-3 Sample preparation surfaces a) frit's surface without sample b) without re-dissolving and c) surface after re-dissolving

C4.5 Sequence of LA-ICP-IDMS Analysis and Data Processing

The sequence of analysis was similar to conventional IDMS as shown in Table C4-2. The analysis was started with a gas flow blank, a frit blank and followed by the back spike. The different numbers of the back-spike mark different frits. This is necessary, because the frit has a limited area for ablation, allowing eight line scans in maximum. Then the unspiked sample offering natural isotopic composition of sulphur was ablated followed by the sample blends. To avoid memory effects and cross-contamination the spike (^{34}S isotope) was measured at the end, leading to a sequence from natural isotopic composition, via spiked sample and finally the pure spike. For every sample three line scans were performed. A gas flow blank and a frit blank were measured between each two samples to control memory and cross-contamination effects. The back-spike sample was measured every two samples to monitor drift effects and allow for drift correction along the sequence. Back spike and spike samples were prepared such that the same sulphur amount is on the frit as in the frits with the sample blends. Information about data processing is provided in section C1.4.

Table C4-2 Sequence of isotope dilution LA-ICP-MS analysis

gas flow	gas flow	gas flow
frit	frit	frit
back spike 1	sample blend 2	Procedure blank
gas flow	gas flow	gas flow
frit	frit	frit
sample-natural isotope	sample blend 3	back spike 3
gas flow	gas flow	gas flow
frit	frit	frit
sample blend 1	back spike 2	spike
gas flow	gas flow	gas flow
frit	frit	
back spike 1	sample blend 4	

C4.6 Sulphur Measurement

All mass spectrometric measurements were performed using the sector field ICP-MS instrument Element 2 (Thermo Fisher Scientific, Germany) for solution method and Element XR (Thermo-Scientific, Germany) coupled to the laser ablation system LSX-213 (Cetac, Omaha, Nebraska, USA) for solid sample analysis, unless stated otherwise. The LSX-213 was equipped with a large volume ablation chamber developed by the group of D. Günther at ETH Zürich. The LA chamber is similar to the one described by Fricker *et al*.[61], but the dimensions are comparatively smaller (outer dimensions length 28 cm, width 10 cm, height 5.5 cm plus cap with 8 cm diameter and 2 cm height into which the laser aerosol expansion takes place). Up to 13 PE frits plus the glass CRM used for tuning can be analysed without opening the LA chamber. The operating parameter for ICP-MS shows in Table C1-7 in section C1.3.2 and that for LA-ICP-MS shows in Table C3-4 in section C3.2, while Table C4-3 shows more detail when measure sulphur in the frits.

For LA-ICP-MS helium was used as a carrier gas and argon was added before the ICP torch using a Y-piece. The ICP-MS Element XR was tuned daily for maximum ion intensity and good signal stability (RSD < 5 %), keeping the oxide ratio (ThO/Th) below 1 % during ablation of NIST SRM 612 (Trace Elements in Glass). Additionally, CRM BAM-S005A (Multielement Glass) containing sulphur trioxide was used for sulphur optimization in medium mass resolution and for mass offset determination.

Table C4-3 Characteristic of sulphur measurement in the frits (more detail refer to Table C3-4, section 3.2)

Instrument type	LA Element XR
Measured isotopes	^{32}S, ^{34}S and ^{13}C (for external calibration)
Sensitivity on ^{32}S	$3x10^4$ cps·µgS^{-1}
Sulphur content / mass fractions	0 – 80 µgS per frit
Drift correction	Yes (by back spike sample)

Part D Results and Discussion

This part consists of four sections: (1) development of a sulphur-copper separation procedure, (2) quantification of sulphur in copper metals and its alloys by ICP-IDMS, (3) application of IDMS values to GDMS and LA-ICP-MS, and (4) development of a LA-ICP-IDMS procedure for the quantification of sulphur in copper. Figure D1 gives an overview of this part.

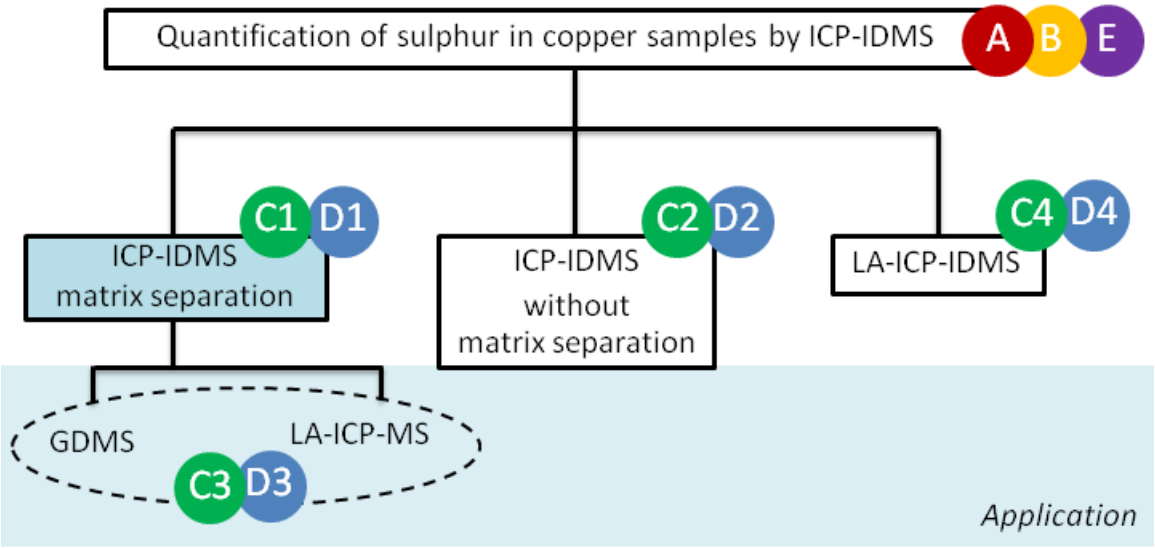

Figure D1 Overview of result and discussion part

D1. Quantification of Sulphur in Copper Samples by ICP-IDMS with Matrix Separation

The development of the sulphur measurement procedure in copper and the results are discussed in this section. The focus is on the sulphur-copper separation procedure and metrological issues, such as method validation, measurement uncertainty, and metrological traceability. The target value for the relative measurement uncertainty aims at below 2 %.

D1.1 Sample Digestion/Oxidation/Equilibration

Most copper is produced by mining and/or extracting from copper sulphide (Cu_2S, *Chalcocite*) and copper iron sulphide ($CuFeS_2$, *Chalcopyrite*). Consequently, the pure copper obtained after roasting and purification contains traces of sulphur in different species such as sulphide, sulphite, and sulphate. Unfortunately, the anion exchange resin (AG1X8), which is used to separate sulphur from the matrix, is selective to sulphate and

sulphite but less-selective to sulphide.[52] In order to avoid any measurement bias and sulphur loss during the separation process, the **different species of the sulphur** need to be oxidized to sulphate prior to the sulphur-copper separation on the AG 1X8 resin. Consequently, the three different sulphur species were oxidized under two different conditions and the separation procedure using AG1X8 was carried out. The recovery of the oxidation and separation was determined by ICP-IDMS. Stock solutions for **sulphate, sulphite, and sulphide** were gravimetrically prepared from sulphuric acid, sodium sulphite and sodium sulphide, respectively. A portion of each species standard containing an accurately determined amount of about 10 µg sulphur was oxidized in two different ways:1) addition of 3 mol·L^{-1} HNO_3 and H_2O_2 (30 %, w·w^{-1}), hot plate at 120 ºC for 3 h; 2) addition of 3 mol·L^{-1} HNO_3 and H_2O_2 (30 %, w·$w^{-1)}$, digestion by HPA. After that the samples were applied to the AG1X8 separation procedure. Then the samples were analysed by ICP-IDMS and the recovery for each sample was calculated referring to the gravimetrically determined amount of sulphur (Table D1-1). The recovery of sulphate for both oxidation experiments was (100±1) %. In the case of sulphite, the oxidation by using the hotplate was insufficient (about 79 % recovery), whereas the HPA oxidation yielded quantitative recovery (100±1) %. For sulphide both oxidation experiments were insufficient, yielding recoveries below 50 %. Therefore, another oxidation experiment was carried out applying again the HPA oxidation as described above, but with concentrated nitric acid (65 %, w·w^{-1}). Here, the sulphur quantification was established by external calibration ICP-MS. The obtained recovery for sulphide was 94 % with an estimated expanded uncertainty of 10 %. Therefore, the complete oxidation of sulphide to sulphate can be assumed with a quantitative recovery for the AG1X8 separation procedure. The complete conversion from sulphide and sulphite to sulphate could be achieved only when applying the HPA oxidation with concentrated HNO_3 and H_2O_2.

Table D1-1 Oxidation conditions for the conversion of different sulphur species into sulphate with corresponding recovery rates after separation by using the AG1X8 resin

measured by ICP-IDMS or ICP-MS together with expanded uncertainties (recovery related to gravimetric value)[6]

Species	Recovery (%)		
	3M HNO_3 + H_2O_2 by hot plate (120 °C, 3 h)*	3M HNO_3 + H_2O_2 by HPA*	conc HNO_3 + H_2O_2 by HPA**
Sulphide, S^{2-}	15	37	(94 ± 10)
Sulphite, SO_3^{2-}	79	(100 ± 1)	n.a.
Sulphate, SO_4^{2-}	(100 ± 1)	(100 ± 1)	n.a.

* IDMS applied.

**% Recovery from external calibration method

D1.2 Sulphur-copper Separation

Accurate IDMS analysis requires accurate isotope ratio measurement, which in turn requires best possible matrix separation. Figure D1-1 shows the effect of increasing copper matrix on the sulphur isotope ratio measurement expressed as deviation from the measured sulfur isotope ratio without copper matrix. The diagram clearly shows that copper mass fractions of ≥ 75 $\mu g \cdot g^{-1}$ lead to a bias in the isotope ratio of sulphur of more than 1 %. Hence, the maximum allowable matrix mass fraction was set to 50 $\mu g \cdot g^{-1}$ copper to reduce the matrix induced bias to a level which is comparable to the expected precision level.

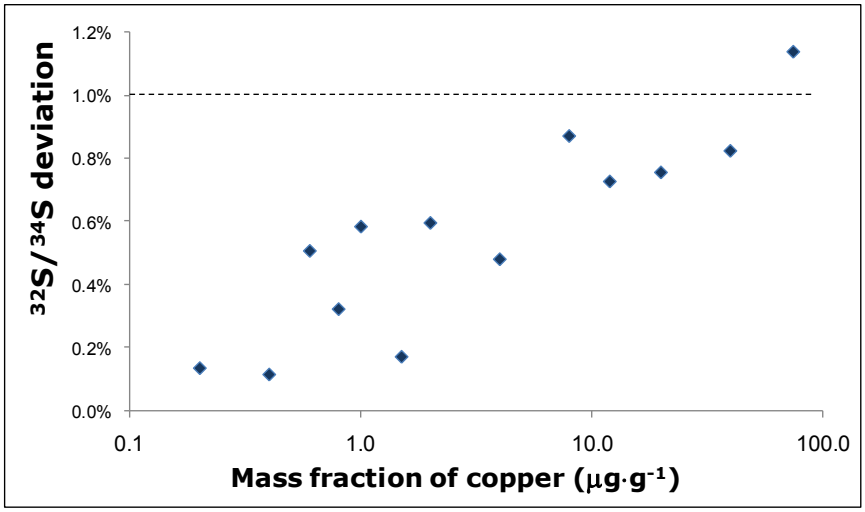

Figure D1-1 Copper matrix effect on sulphur isotope ratio measurement (sulphur mass fraction 0.5 $\mu g \cdot g^{-1}$)

In the first phase of this study, especially for the sulphur measurements in biofuel, the separation procedure published by Das *et al.*[49] was applied. This separation procedure

employs a strong anion exchange resin (AG1X8), which retains the sulphur on the column while the matrix elutes without retardation. After the matrix was completely removed, the sulphur was eluted from the resin. Figure D1-2 shows the elution curves of a sulphur standard and sulphur containing petrol sample, which both were used to evaluate the elution volume of the sulphur containing fraction. To retain sulphur as much as possible the eluent volume should be above 5 mL. Consequently, the recovery of this procedure was checked, and it was found to be 100 ± 2 %.

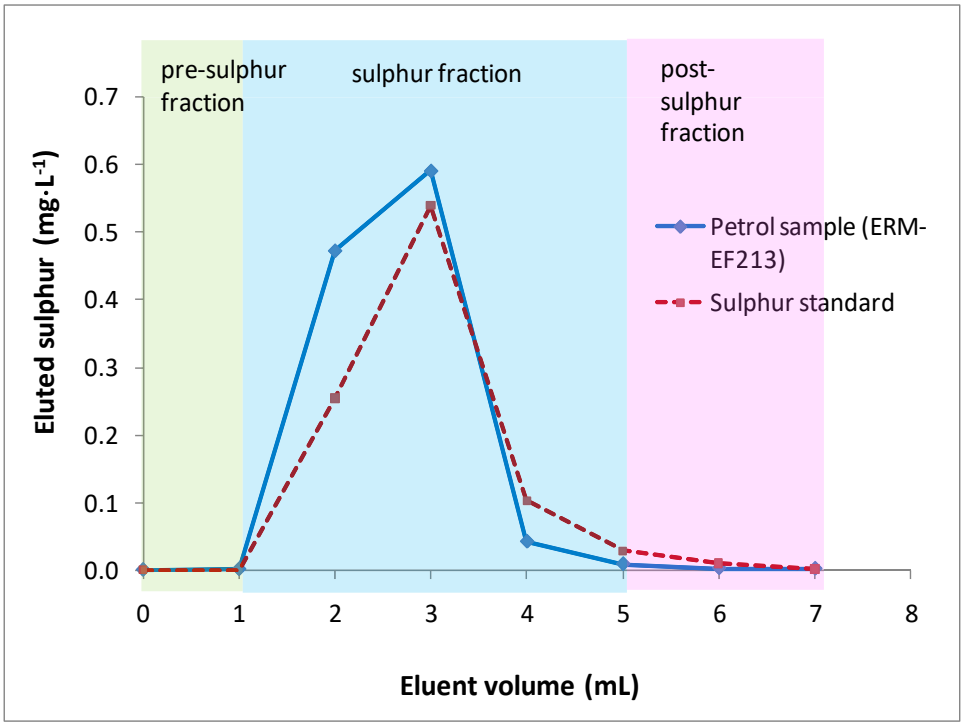

Figure D1-2 Elution curves of sulphur standard and petrol sample (ERM-EF213)

After calibrating the ion exchange column, the procedure was applied to synthetic sample solutions, which were prepared by mixing a sulphur standard (sulphate form) with a copper standard such that a sulphur mass fraction of 8 $\mu g \cdot g^{-1}$ and a copper mass fraction of 24,000 $\mu g \cdot g^{-1}$ was obtained. For this sample the recovery of sulphur dropped to 10 % – 30 %, which presumably is due to the formation of copper (II) sulphate ($CuSO_4 \cdot (H_2O)_x$) complexes formed by the reaction of sulphate with excess copper.

Therefore, **ammonia**, which is a highly selective ligand for Cu(II), was added to form a complex with copper, thus reducing the above-mentioned formation of copper sulphate. The formation of the tetraamine-copper(II) complex releases trapped sulphur and leads to increased recovery rates. The chemical reaction of ammonia and copper is well-

known and is shown in the equations *(a)* and equation *(b)* below. When applying the ammonia addition, the sulphur recovery for the synthetic sample increased to 100 ± 3 (n=4).

$$CuSO_4(aq) + 2NH_3(aq) + 2H_2O(l) \rightarrow Cu(OH)_2(s) + (NH_4)_2SO_4(aq) \quad , \quad \text{equation (a)}$$

$$Cu(OH)_2(s) + 4NH_3(aq) \rightarrow [Cu(NH_3)_4](OH)_2(aq) \quad , \quad \text{equation (b)}$$

When applying this procedure to real copper samples (pure copper and copper alloy), the recovery of sulphur dropped to 10 % – 20 % again. Possible reasons for such significant decrease are ascribed to the very high amount of the copper matrix compared to the sulphur mass fraction which is approximately 3 times higher than in the synthetic sample. It was assumed that a copper removal step prior to the AG1X8 separation will solve this problem. At first strong cation resins were considered, because they are well known for the removal of heavy metals from matrices such as waste water. Unfortunately, most cation exchange resins contain sulphonated polystyrene as exchange site, which would lead to unacceptable high procedure blanks. Then **weak acidic cation resins** could be identified as suitable material: especially the resin CG50 does not contain sulphur groups and is capable of retaining copper with a high selectivity.[62, 63] Together with its high capacity (3.5 mmol·mL^{-1}) it makes the resin highly suitable for the intended use. A new separation step was carried out by adding an excess amount of cation resin CG50 (1 mL CG50: 20 mg Cu) to the sample solution. The mixture of sample solution and CG50 resin was shaken to increase the contact time between the resin and the copper for maximum matrix removal efficiency. Consequently, the deep blue sample solution turned to a clear and transparent solution, while the resin itself turned from white to blue (Figure D1-3a). The clear solution was separated from the resin and was dried to remove the solvent and to pre-concentrate the sulphur. The residue contained large amounts of solids as shown in Figure D1-3b. This residue cannot be dissolved and used for measurements, because the first tests with the ICP-MS showed that the nebulizer blocked after a few measurements.

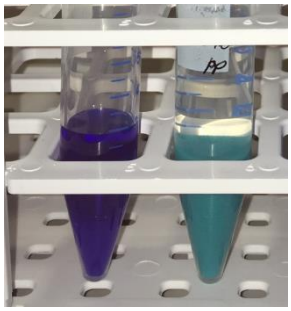

(a)

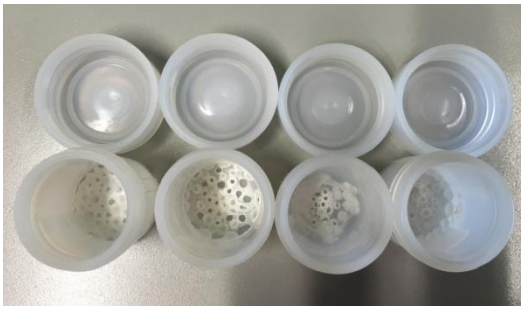

(b)

Figure D1-3 Copper removal by CG50 resin (a) before (left vial) and after (right vial) adding CG50, (b) residue of clear solution

Therefore, the residue from the CG50 separation was redissolved and the resulting clear solution was loaded onto the column which contains AG1X8 to further purify the sulphur fraction. After eluting the sulphur from the AG1X8 resin the solution was dried on a hot plate until dryness yielding a blueish green residue (by visual) which still contained copper above 100 $\mu g \cdot g^{-1}$ (see Figure D1-4a). The preset requirement for the copper separation was a maximum allowable Cu mass fraction of 50 $\mu g \cdot g^{-1}$. Therefore, a third resin was employed to remove the remaining copper: this time a chelating ion exchange resin was selected (Chelex 100) due to its strong adsorbing properties which make it possible to remove the remaining copper.[64] After this third separation the blueish green colour of the residue was removed (see Figure D1-4b).

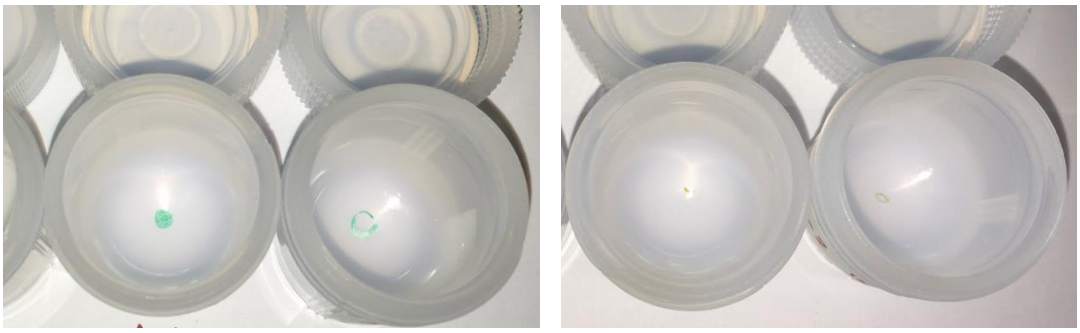

(a) (b)

Figure D1-4 Residue before (a) and after (b) Chelex resin

The ion intensities of $^{63}Cu^{+}$ and $^{65}Cu^{+}$, measured by ICP-MS in medium resolution, were used to check the matrix removal efficiency prior to the ICP-IDMS measurements. The detected Cu signal intensities were 0.04 – $2x10^{7}$ cps for ^{63}Cu and 0.02 - $1.5x10^{7}$ cps for ^{65}Cu corresponding to Cu mass fractions of less than 150 $ng \cdot g^{-1}$ in the final solution.

The copper materials investigated in this study contain copper in the range of 0.85 – 0.99 $g \cdot g^{-1}$. Approximately 0.10 g - 0.25 g of these samples were used to perform the sulphur-copper separation. After the three-stage separation procedure was applied to the copper materials, the mass fraction of copper was significantly reduced to below 150 $ng \cdot g^{-1}$ except for the high purity copper NIST SRM 1034, where the final copper mass fraction

was 370 $ng \cdot g^{-1}$. In summary, most of the **copper (> 99.999 %) was removed**, resulting in an extremely high matrix removal factor of above 10^5.

D1.3 Measurement Results for Sulphur in Copper by ICP-IDMS with Matrix Separation

The sulphur-matrix separation did not only remove the matrix but also lead to a pre-concentration of sulphur. Approximately 2 $\mu g \cdot g^{-1}$sulphur was contained in the final sample solution used for measurements. Prior to each sample and standard measurement, a blank measurement was carried out and signal intensity of sample and standard was corrected by the blank before the data were processed. Thus, the variation of the blank intensity (about 5 %) within one sequence was negligible. In summary, the sulphur background might contain minor amounts of remaining interferences. When medium resolution was applied, a very small effect was observed, as the signal to noise ratio (S/N) is above 20.

D1.3a Measurement Results of Sulphur in Copper Sample by ICP-IDMS with Matrix Separation

As described in previous sections, sulphur-matrix separation was applied and combined with the described ICP-IDMS procedure for quantification of sulphur in six different reference materials. The results and their measurement uncertainty are displayed in Table D1-2. Sample no. BAM-M385, BAM-M376a, BAM-228, BAM-227, and SRM 494 were quantified by normal IDMS. In case of SRM 494 and SRM 1034 different approaches were applied for quantification, because the amount content of sulphur was lower than the working range of the separation procedure. To extend the working range an exact amount of sulphur standard was added in the sample before ^{34}S spiking to increase sulphur amount. Then sample was dissolved and digested as usual, but in the

Table D1-2 Sulphur mass fractions in copper reference materials as obtained by ICP-IDMS with the associated measurement uncertainty and the individual uncertainty contributions[6]

List		BAM-M385	BAM-M376a	BAM-228	BAM-227	NIST SRM 494	NIST SRM 494*	NIST SRM 1034*
Measurement value and MU ($\mu g \cdot g^{-1}$), k=2*		(37.72 ± 0.19)	(133.68 ± 0.86)	(385.50 ± 2.40)	(1,376.6 ± 6.2)	(14.34 ± 0.09)	(14.97 ± 0.20)	(6.79 ± 0.36)
U_{rel} (%)		0.5	0.6	0.6	0.5	0.7	1.3	5.3
Reference value**		(31.2 ± 1.5)	(133 ± 19)	(360 ± 40)	(1,220 ± 100)	(15 ± 3)	(15 ± 3)	(2.8 ± 0.2)
Cu in final solution ($ng \cdot g^{-1}$)		< 100	< 150	< 100	< 150	< 150	< 260	< 370
Zn in final solution ($ng \cdot g^{-1}$)		< 10	< 50	< 10	< 10	< 10	< 10	< 10
Number of replicates		8	8	8	8	4	6	6
Uncertainty budget	**Type**	**% Contribution**						
Observed ratio of back spike	A	48.1	58.5	65.5	33.7	41.8	11.1	2.8
Mass fraction of spike	B	42.4	27.3	28.3	55.0	24.3	45.1	81.2
Observed ratio of sample blends	A	5.2	8.2	2.4	4.0	29.7	22.4	2.4
Observed ratio of natural	A	2.7	4.8	1.2	1.1	1.6	0.1	< 0.1
Observed ratio of spike	A	< 0.1	< 0.1	0.8	0.4	1.8	2.0	< 0.1
Weighing of samples	A	0.4	< 0.1	1.2	4.7	< 0.1	< 0.1	< 0.1
Weighing of spikes	A	< 0.1	< 0.1	< 0.1	< 0.1	< 0.1	5.0	2.3
Procedure blank	B	< 0.1	< 0.1	< 0.1	< 0.1	< 0.1	< 0.1	< 0.1
Mass fraction of back spike (standard addition)	B	-	-	-	-	-	13.2	10.7
Weighing of back spike (standard addition)	A	-	-	-	-	-	< 0.01	< 0.01
Others	-	1.2	1.2	0.6	1.1	0.8	1.2	0.6

* Combined standard addition and IDMS technique, ** For type of reference values please see table C2-4

calculation, the amount of sulphur standard added before will be subtracted. The measurement results obtained for sample BAM-M376a, BAM-228 and SRM 494 with normal IDMS agree well with the reference values, whereas for sample no. BAM-M385 and BAM-227 the results differ from the certified values. Sample BAM-227 was certified in 1979 using two methods, one of which was a photometrical method and the other method was titration by Dimethyl-p-phenylenediamines. Additionally, the reference value was accompanied by the analytical precision only. At that time, the metrological concept such as measurement uncertainty and SI traceability were not clear or even not existing. In case of sample BAM-M385, the IDMS result obtained within this work and the certified value is significantly different. The uncertainty of the certified value again, only represents the dispersion of the inter-laboratory comparison. Most of the results reported by the participants were obtained by carrier hot gas extraction method (CGHE). The basic concept of the method is that the sample is heated in an oxygen stream to release sulphur in gaseous form. When sulphur reacts with oxygen molecular species such as SO_2 and SO_3 are generated.[65] These species are transported by a gas stream (carrier gas) to an infrared spectrometer where they are detected based on the S=O bonding. In most cases, external calibration techniques are applied using pure $BaSO_4$ as calibrator. Consequently, matrix effects, different sulphur species, species interconversion and spectral interferences in the detection are critical. In case of quantifying sulphur by the ICP-OES technique, the same issues as in CGHE occur; additionally, the sulphur loss during sample preparation should be considered.

An obstacle for the quantification of sulphur in NIST SRM 494 by normal IDMS is the very high copper to sulphur ratio, which leads to a high copper amount on the resin, when aiming at the same amount of sulphur (2 µg) loaded on the resin as for the other materials. This clearly affects the sulphur-matrix separation efficiency. The recovery of sulphur for the whole separation procedure dropped to about 30 % for four replicates and for two replicates to even below 10%. The resulting samples show too low sulphur amounts for reliable ICP-MS measurements. The S/N at mass 32 was 7 in average. To enable measurements without changing the separation procedure, a combination of standard addition technique and IDMS technique was used. An exact amount of sulphur was added prior to spiking, such that the sulphur mass fraction was shifted to the optimum working range of the separation procedure.

The exact amounts of sulphur, which were added prior to spiking to enhance the mass fraction of sulphur ranged from 15 $\mu g \cdot g^{-1}$ to 40 $\mu g \cdot g^{-1}$. Thereafter, the spiking, the matrix separation and the ICP-MS measurements were performed as usual. After calculating the IDMS result, the added sulphur amount was subtracted from the total amount sulphur at the end, such that the mass fraction of sulphur in the sample was quantified. The measurement result agreed well with the certified value within the uncertainties. The measurement uncertainties were approximately the two-fold of those obtained with the normal IDMS experiment, because the measurement uncertainty of the sulphur addition has to be considered.

For sample NIST SRM 1034, the same concept of the addition of a standard solution was applied by increasing the sulphur content from 2.8 $\mu g \cdot g^{-1}$ (certified value) to 40 $\mu g \cdot g^{-1}$. Nevertheless, in this case the measurement result was significantly different to the certified value. This disagreement requires further investigation. The NIST SRM 494 measurement results, however, proved that the combination of standard addition technique and IDMS is a suitable tool to extend the working range of the separation procedure. This combination provides reliable results which are true within the stated uncertainties as shown for NIST SRM 494.

D1.3b Measurement Uncertainty

Within this study, ICP-IDMS was applied as a higher-order reference measurement procedure. The measurement process is well understood, and a measurement equation can be written down, permitting the calculation of the mass fraction of sulphur directly from the signal intensities. Consequently, measurement uncertainties were assessed based on the IDMS equation 12. Table F2 (in Part F Appendix) is an example of the measurement uncertainty sources, showing the calculation and all factors affecting the measurement result of the sample BAM-M376a in detail. The main contribution to the uncertainty is derived from the observed isotope ratio in the back spike for conventional IDMS (without standard addition); this is caused by the relative standard deviation of the sulphur isotope ratio of the back spike for a complete measurement sequence (2.6 % RSD). The second largest contribution is made up by the ^{34}S mass fraction in the spike, followed by the observed isotope ratio in the sample blend, the unspiked sample and the spike. All other quantities do not contribute significantly. This also applies to the very low procedure

blank (average value 14 ng). An overview of the main uncertainty contributions to the measurement result is given in Figure D1-5.

For the combination of standard addition and IDMS, where the exact amount of back-spike (sulphur standard) is added to the sample before spiking, the main contribution to the measurement uncertainty are made up by the mass fraction of the spike and the back spike and the isotope ratio in the sample blend as shown in Figure D1-7. Usually, the relative expanded measurement uncertainties for normal IDMS are below 1%. When combining results obtained by both standard addition and IDMS, the relative expanded measurement uncertainties are larger and amount to 1.34 % and 5.30 % as calculated for sample no. SRM 494 and SRM 1034, respectively.

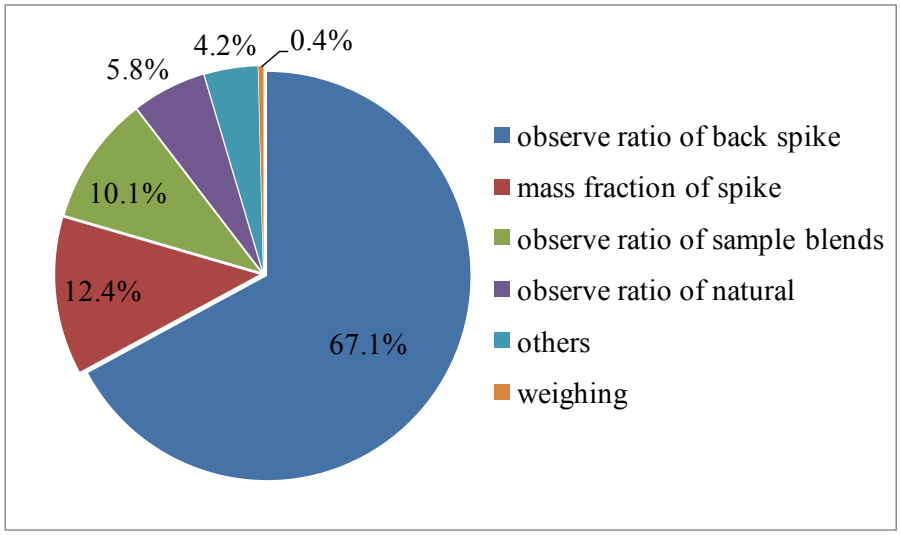

Figure D1-5 Percentage contributions to the measurement uncertainty of sample no BAM-M376a (normal double IDMS)

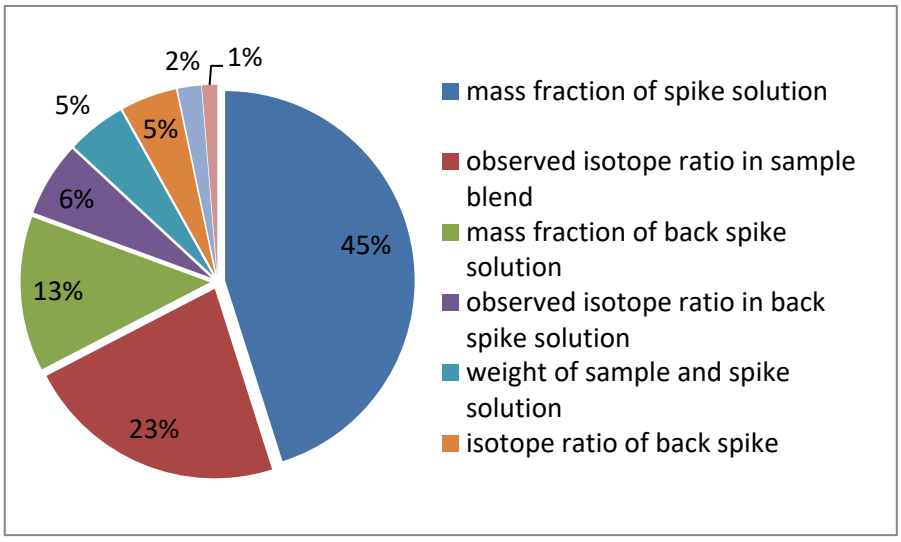

Figure D1-6 Percentage contributions to the measurement uncertainty of NIST SRM 494 with standard addition and double IDMS

The individual contributions to the measurement uncertainty listed for each sample type are displayed in Table D1-2.

D1.4 Detection Limit and Working Range

The procedural blank was determined by IDMS as well. The average of the procedure blank (n = 22) over all measured sequences was calculated and yielded a total procedure blank of 14 ng sulphur with a standard deviation of 12 ng, with procedural blanks ranging from 3 ng to 53 ng for the individual IDMS measurement sequences was ranging from 3 ng to 53 ng. When considering a sample weight of 0.25 g, the limit of detection (LOD, 3SD) was 0.20 $\mu g \cdot g^{-1}$ while the limit of quantification (LOQ, 10SD) was 0.54 $\mu g \cdot g^{-1}$.

However, for applying IDMS, the LOD and LOQ are more a theoretical concept, than a practically usable parameter, because the applicability of the IDMS procedure is more strongly defined by the working range, which is limited by the separation procedure and the measurement uncertainty aimed at. The target measurement uncertainty was aimed at less than 2 % in relative, and a working range from approximately 15 $\mu g \cdot g^{-1}$ to 1500 $\mu g \cdot g^{-1}$ could be established.

For samples containing sulphur mass fractions of below 15 $\mu g \cdot g^{-1}$ the application of the standard addition technique is necessary, as explained above for the sample NIST SRM494 leading to relative measurement uncertainties of > 2 %.

D1.5 Method Validation

The developed procedure for the quantification of sulphur mass fractions in copper materials has been validated via three different routes. First, each single step of the procedure was checked by a step-by-step validation. It was carried out during the method development. Second, a complete uncertainty budget was established which was set up as described earlier. And third, the method was validated by participating in an inter-laboratory comparison at highest metrological level.

A step-by-step validation was obtained while developing the procedure such as *sample digestion*/*oxidation*/*equilibration* (section D1.1) concerned about the species of sulphur in separation process and *sulphur-copper separation* (section D1.5) the matrix removal efficiency was observed. In case of the complete uncertainty budget, it was described in section D1.3b.

The third approach for method validation is the participation in inter-laboratory comparisons; CCQM comparisons represent the highest metrological level in this context. In CCQM comparisons the participants are NMIs/DIs of each country and they employ the best available method to quantify the measurand. This approach was used to verify that the developed IDMS procedure is capable of accurately determining sulphur mass fractions in the low $\mu g \cdot g^{-1}$ level. The inter-laboratory comparison CCQM- K123 "trace elements in biodiesel fuel" was the only-available one for low sulphur measurements during the research period.[12] The developed IDMS procedure was applied at BAM and the result was submitted as BAM result. The biodiesel matrix when compared to the copper material has the advantage that most of the matrix is oxidized to CO_2, when a suitable digestion procedure is applied (here HPA). Thus, the separation procedure required only a one-step separation by anion exchange chromatography AG1X8 resin). The biodiesel fuel sample was spiked and digested/equilibrated by using the HPA. The sulphur was isolated by anion exchange chromatography (AG1X8 resin) and then measured by MC-ICP-MS. The results of the CCQM-K123 inter-laboratory comparison is shown in Figure D1-7. BAM's result shows an excellent agreement with the other results and demonstrates that the developed procedure enables sulphur measurements at the low $\mu g \cdot g^{-1}$ level in complex matrices with sufficiently low measurement uncertainties. Even though the biodiesel sample did not really fit with a copper matrix, the comparison was on the highest metrological level and could at least validate the spiking, the ^{34}S spike solution, the digestion / equilibration step, the anion exchange step (AG1X8) and the isotope ratio measurement as well as the calculations. Moreover, it could verify the level of the obtained measurement uncertainty.

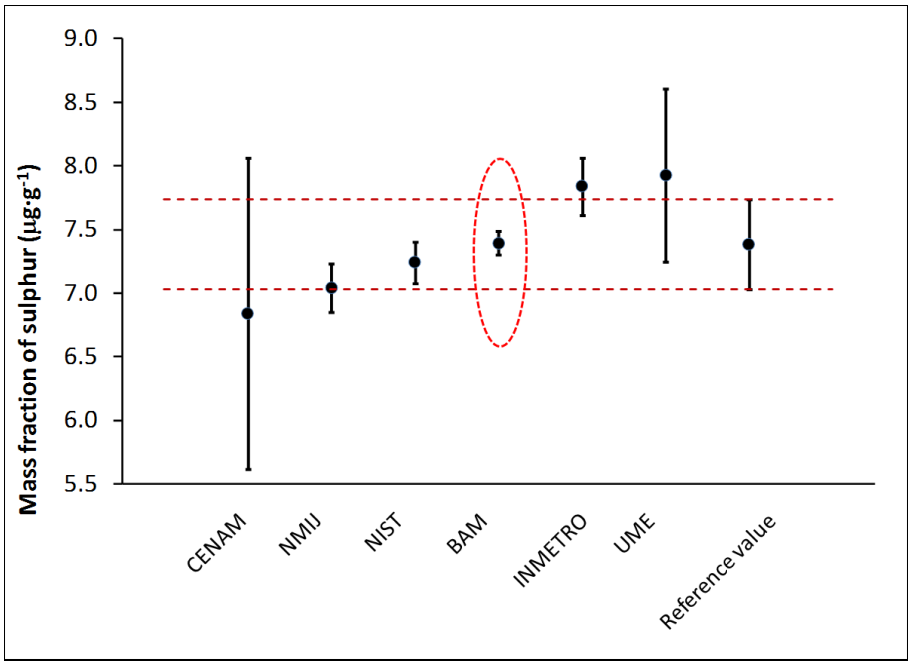

Figure D1-7 Results of the CCQM-K123 inter-laboratory comparison (from 6 participants): mass fraction of sulphur in biodiesel fuel displayed for the participating laboratories together with the reference value (all error bars represent expanded uncertainties, k=2). BAM's result was (7.39 ± 0.10) µg·g^{-1} while reference value was (7.38 ± 0.35) µg·g^{-1}.[12]

D1.6 Metrological Traceability

The metrological traceability is typically visualized by a traceability chain leading from the mol and/or kg down to the final mass fraction in the sample. For the mass fraction of sulphur, w_x, in copper samples is obtained by the here developed double IDMS technique. This has been established by an unbroken chain of comparisons, each accompanied by an uncertainty budget. Figure D1-8 visualizes the metrological traceability to the SI for the sulphur mass fraction in sample no BAM-M376a .

The symbols '▽', '○', and '□' represent SI units which contributed to the measurement procedure, which are electrical current (ampere, A), mass (kilogram, kg) and amount of substance (mole, mol), respectively. The numbers in the symbols express the measurement procedure, e.g. '③ 'represents the measurement procedure 3 (IDMS) traceable to the unit 'mol'.

The bottom line states the meaning of the boxes in each column. The measurement results with standard measurement uncertainties of calibrators or samples are expressed in the three boxes on the left-hand side, while details of the measurement systems and the

measurement procedures are shown in the two boxes on the right-hand side. The action of calibrators and measuring systems in each step is expressed by arrows in the middle of the metrological traceability chart.

As expressed in the Figure D1-8 from the top of the calibration hierarchy, NIST SRM 3154, the primary calibrator 1, was certified by two primary reference procedures which were coulometric titration and gravimetric method at NIST (the information is displayed in the certificate). The reference procedure 1 (coulometric titration) could be traced to SI units; electric current, A and mass, kg while the reference procedure 2 (gravimetric method) could be traced to S units; mass, kg and amount of substance, mol. Therefore, the sulphur mass fraction of the primary calibrator 1 is in turn metrologically traceable to the definition of the SI measurement unit mole through the quantity values for electric current and kilogram. Then, the primary standard NIST SRM 3154 was used to quantify the exact mass fraction of ^{34}S in the spike solution which was assigned as secondary calibrator 2. The mass fraction of the ^{34}S spike solution was characterized by reverse IDMS (labelled measurement procedure 3); as a result was (92.21 ± 0.19) $\mu g \cdot g^{-1}$. After that, the secondary calibrator was used to quantify sulphur in sample no. BAM-M376a by applying the IDMS approach at BAM (labelled measurement procedure 4). The mass fraction of sulphur in sample no BAM-M376a is (133.7 ± 0.9) $\mu g \cdot g^{-1}$. Figure D1-8 clearly shows the sulphur mass fraction of sample BAM-M376a, as obtained by the here described IDMS procedure, being traceable to the SI in the most direct way.

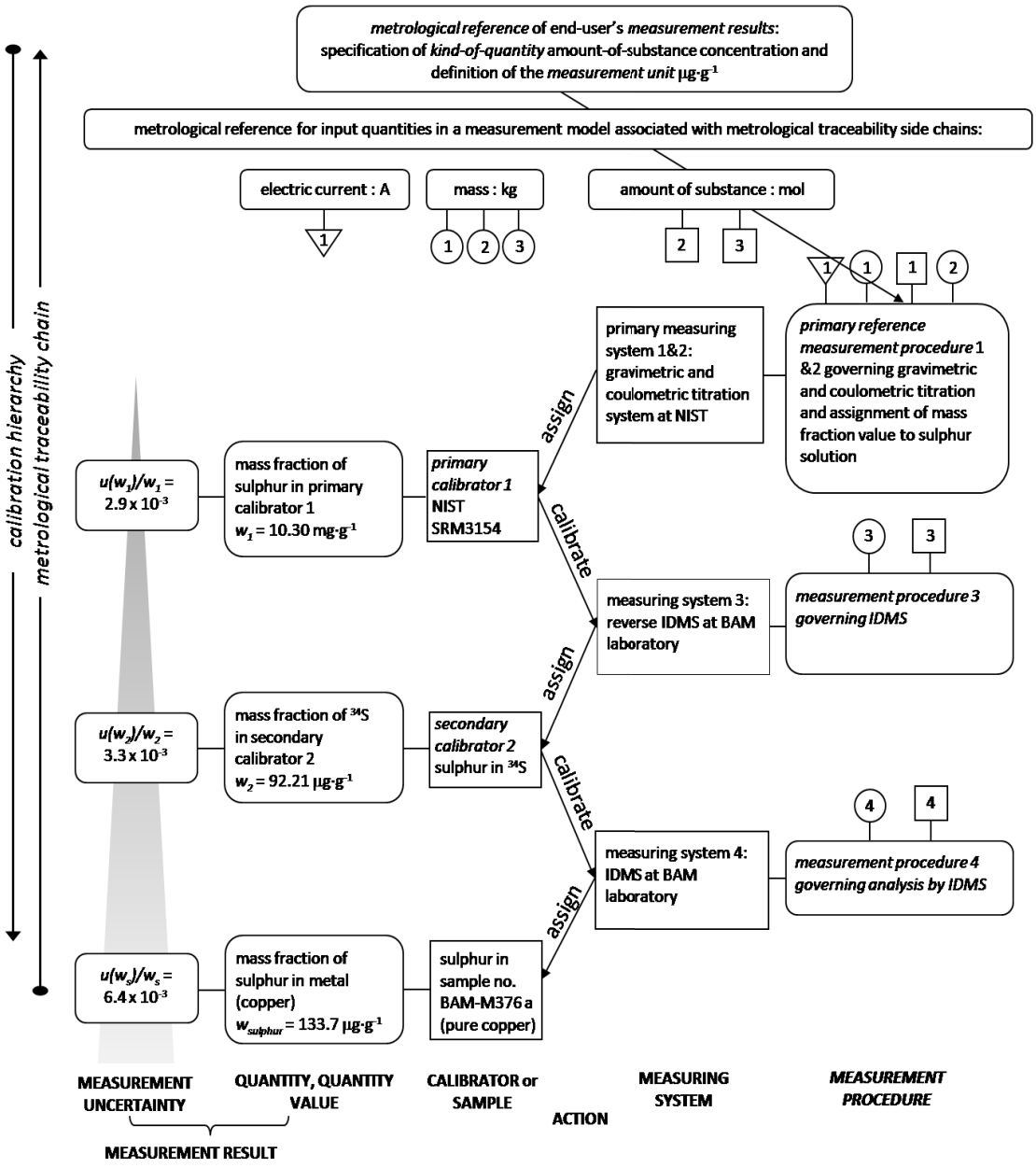

Figure D1-8 Metrological traceability chain of IDMS measurement results for mass fraction of sulphur in pure copper sample no. BAM-M376a.[6]

When establishing an unbroken chain of calibrations and thus SI traceability, the measurement result is considered reliable, acceptable and comparable. Consequently, the mass fraction of sulphur in sample BAM-M376a (and the other samples in this research) is considered reliable, acceptable and comparable.

D1.7 Comparison with Other Procedures

Procedural blanks are in the range between the maximum values of 4 ng and 53 ng, with the majority of the blank values ranging from 9 ng to 16 ng (n = 22). This is 7

times lower than a previous work which employed ID-TIMS.[8] LOD and LOQ values are 0.20 $\mu g \cdot g^{-1}$ and 0.54 $\mu g \cdot g^{-1}$, respectively being the same level as previous work but it has to be noticed that the matrix is different. As mentioned before, the LOD and LOQ are more theoretical concepts for IDMS including trace-matrix separation and have only limited practical use, because the working range of the analytical procedure is defined by the matrix separation procedure and the measurement uncertainty aimed at. Moreover, calculations of LOD values vary significantly. For this procedure a working range of approximately 15 $\mu g \cdot g^{-1}$ to 1500 $\mu g \cdot g^{-1}$ can be achieved. In addition to the low detection limits and two orders of magnitudes of working range, the procedure offers a high matrix removal efficiency, low measurement uncertainties and SI traceability.

The developed analytical procedure was successfully validated via an inter-laboratory comparison at the highest metrological level, a step-by-step validation of the whole analytical procedure, and the setup of a complete uncertainty budget. Additionally, relative expanded measurement uncertainties were estimated to range below 1 %, while metrological traceability to the SI is clearly expressed. Therefore, the procedure is well-suited to provide reference values for the total sulphur mass fraction in copper materials.

D2. Quantification of Sulphur in Copper Samples by Direct ICP-IDMS Analysis (Without Matrix Separation)

This research investigates the basic problems of sulphur quantification in copper samples using direct ICP-IDMS. Some of these problems concerning matrix effects have already been addressed in previous literature.[4] The investigation will focus on the accuracy of the measurement results, the measurement uncertainty, metrological compatibility and the LOD in pure copper and some copper alloy samples. The samples preparation was quite simple and consisted of a weighing step, spiking of the samples with ^{34}S enriched spike, a dissolution step, and a final dilution step. The obtained solutions were introduced into the instrument by continuous nebulization without matrix separation as described in section C2.

D2.1 Measurement Results for Sulphur in Copper by ICP-IDMS

As already mentioned in previous chapters, the copper matrix strongly affects the sulphur measurements. Therefore, the measurement results were corrected for matrix

effects before evaluation. This matrix correction factor was obtained by dividing the measured $^{32}S/^{34}S$ isotope ratio in the natural, unspiked sample by the measured $^{32}S/^{34}S$ isotope ratio in the back-spike; natural sulphur isotope variations are neglected, because they are significantly lower than the matrix effects. After that the matrix correction factor was applied to correct the isotope ratio of the sample blend. The effect of the matrix on the measured values was compared in Table D2-1 in the columns "with matrix correction" and "without matrix correction". When the matrix correction is applied, the results are shifted closer to the reference values by 3 % to 6 %, which demonstrates the importance of the matrix correction for the accuracy of the results. As any other correction, the matrix correction factor leads to an increase in the measurement uncertainty extended (< 1 %) when this factor is included. It makes the result more reliable. Even when including the matrix factor all measurement results are still significantly smaller than the reference values. This negative bias demonstrates that there is still an effect which is not corrected completely.

The E_n number is used to assess the comparability of the results between measured value and reference values. The E_n number is rewritten from the "Degrees of Equivalence, d_i" as shown in equation 17-19. Normally, this concept is employed for the CCQM Key Comparisons Program (international-laboratory comparison). It is applied to compare the results of a study on metrological level, which its criterion is required. Usually, for an E_n number equal to or below 1 ($E_n \leq 1$) compatibility with the reference value is demonstrated to be established.

$$E_n = \frac{|d_i|}{U(d_i)} \quad , \qquad \text{Equation 17}$$

$$d_i = \left(x_i - x_{ref}\right) \quad , \qquad \text{Equation 18}$$

$$U(d_i) = 2 \cdot \sqrt{(u(x_i)^2) + u\left(x_{ref}\right)^2} \, , here\ k = 2 \quad , \text{Equation 19}$$

The measurement results of BAM-228 and BAM-227 were not compatible with the reference values even though corrected for matrix effects. The main reasons for this incompatibility are: 1) under estimation of the measurement uncertainty, which means some major contributions are still not detected; 2) analyte and spike did not reach the equilibrium point because the digestion was carried out in a semi-closed system, which could lead to sulphur loss before the equilibrium was reached and 3) strong and incompletely corrected matrix affects. The latter was already reported by Matschat *et al.*, who observed a decrease in analyte intensity by approximately 70 % when introducing

solutions containing 5,000 mg·L^{-1} of copper.[4] This is in good agreement with the findings made in this work: the analyte intensity decreased by approximately 30 %, when the copper matrix was introduced into the system with copper concentrations of < 1,000 mg·L^{-1}. In order to keep matrix effects below 50 %, the sample solutions were diluted such that a copper matrix content of approximately 500 µg·g^{-1} was reached. In parallel the sulphur content was diluted as well, which resulted for e.g. BAM-M376a in a final sulphur mass fraction of 60 ng·g^{-1}. Typically, the instrumental background for sulphur measured in dilute (2 % m/m) nitric acid is in the range of 20 ng·g^{-1} to 40 ng·g^{-1}, leading for BAM-M376a to an analyte signal to background ratio (S/N) of 1.6 to 2.4. A common acceptance criterion for quantification are S/N values above 3. Taking this into account, the working range of the here applied procedure is limited to sulphur mass fractions above 150 mg·kg^{-1}. Thus, this approach is unsuitable for quantifying trace amounts of sulphur in metals. LOD and LOQ are 0.08 µg·g^{-1} and 0.21 µg·g^{-1}, respectively, while the procedure blank is 2 ng - 10 ng S.

Table D2-1 Results of sulphur mass fraction in copper samples and its uncertainty (*k=2*)

Sample no.	Mass fraction of sulphur in copper samples (µg·g^{-1}), U_{rel} (%), E_n		
	Reference values	Without matrix correction	Matrix correction
BAM-M376a	(133.7 ± 0.9), 0.7	(120.6 ± 1.3), 1.1, **8.3**	(123.9 ± 2.1), 1.7, **4.3**
BAM-228	(385.5 ± 2.4), 0.6	(276.2 ± 1.9), 0.7, **26.7**	(291.1 ± 2.6), 0.9, **26.7**
BAM-227	(1,376.6 ± 6.2), 0.5	(1,051.9 ± 21.2), 2.0, **8.6**	(1,110 ± 30.2), 2.7, **8.6**

D2.2 Conclusion

This part of the research was aimed at simplifying the IDMS based reference procedure by omitting the analyte-matrix separation and performing direct measurements after dilution. This was accomplished and the developed ICP-IDMS procedure without matrix separation was tested for its performance concerning sulphur quantification in copper with the following result:

- The copper matrix leads to significant matrix effects (sensitivity decrease of 30 %), which need to be corrected by a suitable correction factor.

- The copper matrix requires high dilution factors in order to keep matrix effects below 50 %. This limits the working range of the procedure to sulphur mass fractions of > 150 $\mu g \cdot g^{-1}$.
- LOD and LOQ are 0.08 $\mu g \cdot g^{-1}$ and 0.21 $\mu g \cdot g^{-1}$, respectively. And procedural blank is 2 ng S - 10 ng S. However, LOD and LOQ practically are useless, because the applicability of IDMS procedures is more strongly defined by the working range, which itself is limited by the instrument background for this case.
- Accuracy, expressed by metrological compatibility: The results show that copper matrix, sample preparation and blank level affected the measurement accuracy. Especially sensitivity decreases about 30 % when copper is introduced in the system.
- Measurement uncertainty: The relative expanded measurement uncertainty range between 1 % and 3 %. Although, matrix effects were considered, the measurement uncertainty is still underestimated as demonstrated by the E_n value. More realistic uncertainty estimates can be obtained, when setting the E_n value to 1 and calculate the necessary measurement uncertainty. This results in relative expanded measurement uncertainties of 8 % - 32 %.

This performance is not suitable for quantifying trace amounts (< 150 $\mu g \cdot g^{-1}$) of sulphur in metal matrices at uncertainty levels of a few percent. On top, the ICP-IDMS procedure without matrix separation requires an extensive cleaning (cones, extraction lens) after each measurement sequence, which nearly equals the time and costs of a matrix separation procedure. Therefore, the reliable and accurate quantification of trace amounts of sulphur in metal matrices requires the sulphur-matrix separation prior to ICP-IDMS measurements.

D3. Quantification by GDMS and LA-ICP-MS as Demonstrated for Sulphur in Copper and Copper Alloys

This section involves the application of IDMS values (from section D1) to calibrate GDMS and LA-ICP-MS by direct analysis for sulphur quantification in copper samples. Here, details on the measurement results in different calibration strategies such as the number of calibrator(s) for calibration and cross calibration between pure copper and copper alloys are given. The accuracy, measurement uncertainty and metrological traceability of the result will be discussed. The metrological traceability chain is expressed reliability of the measurement results.

In the previous work (section D1) the sulphur mass fraction in CRMs/RMs were quantified by IDMS analysis with matrix separation, where small sampling sizes were analysed. Variation of the sample on a large scale was not included. Therefore, the application of IDMS values (which are not certified value) must be considered the sample variation, which is known as homogeneity term, in the measurement uncertainty. Unfortunately, information about homogeneity of these CRMs / RMs are not available, thus, the term of homogeneity is estimated from the available data such as standard deviation of measurement between laboratories and a number of independently analysed samples. Table D3-1 shows the mass fraction of sulphur (by IDMS analysis) with their expanded measurement uncertainty which included the homogeneity term.

Table D3-1 Mass fraction of sulphur and their expanded measurement uncertainty which included homogeneity term.

Source / RMs	Measurement	Homogeneity*			Combined uncertainty	Sulphur mass fraction** ($\mu g \cdot g^{-1}$)
	u_m	SD	n	u_h	u_c	U (k=2)
BAM-M385	0.095	1.177	8	0.42	0.51	(37.7 ± 1.0)
BAM-M376a	0.43	4.9	8	1.73	2.16	(134 ± 4)
BAM-228	1.2	20	3	11.5	12.7	(386 ± 26)
BAM-227	3.1	50	2	35.4	12.7	(1,377 ± 77)

* SD / √n

** Reference values for GDMS and LA-ICP-MS

D3.1 Quantification of Sulphur in Copper and Copper Alloys by GDMS

As previous work, the result showed that the sulphur mass fraction in BAM-M385 obtained by ICP-MS was not compatible with the certified value, then GDMS was used to verify the method by using BAM-M376a as a calibrator. The result from GDMS was (38.4 ± 1.3) $\mu g \cdot g^{-1}$ which is close to the IDMS method as shown in Figure D3-1. This clearly demonstrates the IDMS result being more likely the right value, while the certified value is biased. Therefore, the reference material BAM-M385 will be used as a calibrator for the other copper materials by using the result from the IDMS analysis as reference values.

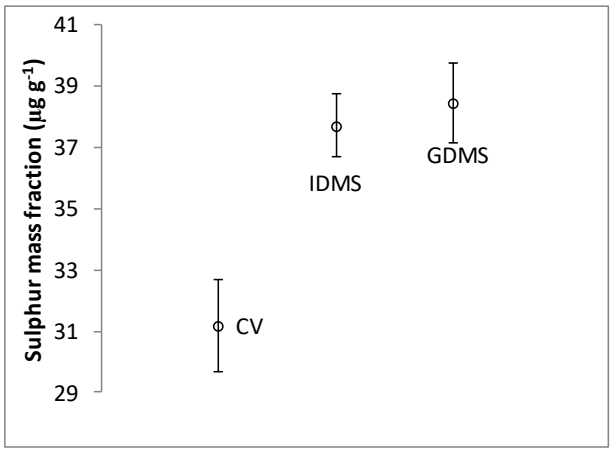

Figure D3-1 Comparison the measurement results of sulphur mass fraction in BAM-M385 to certified value.

D3.1a Method validation

The method was validated by cross calibration among the calibrators / CRMs: the results from GDMS were compared to the IDMS value, which was used as the reference values. The Table D3-2 shows cross validation when a CRM was used as a calibrator to quantify sulphur mass fraction in another CRM (as sample). Different calibration strategies were validated. These include one-calibrator, two-calibrators (with cross-type) and mixed-calibrators. The mass fraction of sulphur in each sample was calculated based on equation 11 (see section B3.3). Calibration curves were plotted between the reference values versus IBR at zero intercept. Using the same copper type as calibrator, the measurement results deviated from the reference value below 2 % and 7 % for pure copper and copper alloy, respectively. However, using the cross-type calibrator, the results deviated in the range of 5-15 %. The E_n number was calculated to observe

compatibility of measured value and reference value and they are above 1 when cross-type calibrators were used. The results show that comparability and compatibility of sulphur content in all samples. Instrumental calibration with the same matrix will yield good results as compared to different matrix results, which is worse as evidence of the larger uncertainty and in-compatible of the measurement results to the reference values.

Table D3-2 Sulphur mass fraction ($\mu g \cdot g^{-1}$) in CRMs from being cross-validated by one calibrator

Calibrator / Type	**BAM-M385 / pure**	**BAM-M376a / pure**	**BAM-228 / alloy**	**BAM-227 / alloy**	**Cross-type**
RV* / **Sample**	(37.7 ± 1.0)	(134 ± 4)	(385 ± 26)	(1,377 ± 77)	-
BAM-M385	-	(38.4 ± 1.3)	(33.4 ± 2.2)	(35.9 ± 2.1)	(36.1 ± 2.3)
U_{rel} (%)		3.4	6.6	5.8	6.4
E_n		< 1	> 1	< 1	< 1
BAM-M376a	(131 ± 4)	-	(116 ± 8)	(125 ± 7)	(125 ± 8.1)
U_{rel} (%)	3.0		6.8	5.9	6.5
E_n	< 1		< 1	> 1	< 1
BAM-228	(435 ± 12)	(443 ± 16)	-	(414 ± 24)	(444 ± 17)
U_{rel} (%)	2.8	3.6		5.8	3.8
E_n	> 1	> 1		< 1	> 1
BAM-227	(1448 ± 45)	(1475 ± 56)	(1283 ± 56)	-	(1478 ± 60)
U_{rel} (%)	3.1	3.8	4.4		4.1
E_n	< 1	> 1	< 1		> 1

* Reference value

D3.1b Quantification of Sulphur in Copper Metals and Its Alloys by GDMS

Calibration curves were plotted between IBR and the sulphur mass fraction of calibrators (from GDMS with extended MU) at zero intercept. The RSF of each calibration was calculated and expressed in Table D3-3. They were divided into 3 groups depending on the number of the used calibrator and in each group is also divided into sub-group based on copper types.

Table D3-3 RSF and linear least square of different calibration strategies at zero intercept

Calibration strategy	Calibrator(s)	Type	RSF	R^2
1 calibrator	BAM-M385	Pure copper	1.253	-
	BAM-M376a		1.277	-
	BAM-228	Copper alloy	1.111	-
	BAM-227		1.191	-
2 calibrators	BAM-M385 & BAM-M376a	Pure copper	1.279	0.9999
	BAM-228 & BAM-227	Copper alloy	1.198	0.9993
3 calibrators	All CRMs	Mixed	1.189	0.9994

Sulphur mass fraction in copper samples were quantified based on equation 11 (see section B3) by different calibration strategies as shown in the previous section. The measurement results are shown in Table D3-4 with their measurement uncertainties. Mass fraction of sulphur in each sample is comparable because all of them are traceable to the same reference system (SI units). The comparison shows small differences when using alloys, or pure copper to calibrate the instrument. For the GDMS technique, it is well known that it requires matrix matched calibration to generate accurate results.

Table D3-4 Sulphur mass fractions in copper reference materials as obtained by GDMS and their individual uncertainty contributions

List		**429**	**422**	**S26**	**826**
Measurement value and MU ($\mu g \cdot g^{-1}$), $k = 2$		(18.8 ± 0.7)	(127 ± 7)	(624 ± 27)	(830 ± 52)
Relative measurement uncertainty (%)		3.7	5.4	4.3	6.3
Reference value*		20	154	466	750
Uncertainty budget	Type	% Contribution			
Sulphur mass fraction of BAM-M385	B	0.3	0.2	0.2	-
Sulphur mass fraction of BAM-M376a	B	86.8	41.0	66.3	-
Sulphur mass fraction of BAM-228	B	-	-	-	0.8
Sulphur mass fraction of BAM-227	B	-	-	-	92.0
IBR of BAM-385	A	0	0	0	-
IBR of BAM-376a	A	12.1	5.7	9.2	-
IBR of BAM-228	A	-	-	-	0
IBR of BAM-227	A	-	-	-	6.9
IBR of sample	A	0.8	53.2	24.2	0.3

* see Table C3-1 (section C3)

D3.1c Measurement Uncertainty Budget

Measurement uncertainty is evaluated from equation 11 for the different applied calibration strategies. Figure D3-3 shows an exemplary uncertainty budget of the quantification of sample no. 422 by two pure copper calibrators. The main contributing quantities for all calibration strategies are the ion beam ratio of the samples and the calibrators and the mass fraction of sulphur in the calibrators. As shown in the figure more than 85% of the uncertainty budget are caused by the IBR value of the sample, so the repeatability of the measurement is a significant parameter. This means the characteristics of the sample are most important for the quantification of sulphur in copper by GDMS and they define the measurement uncertainty.

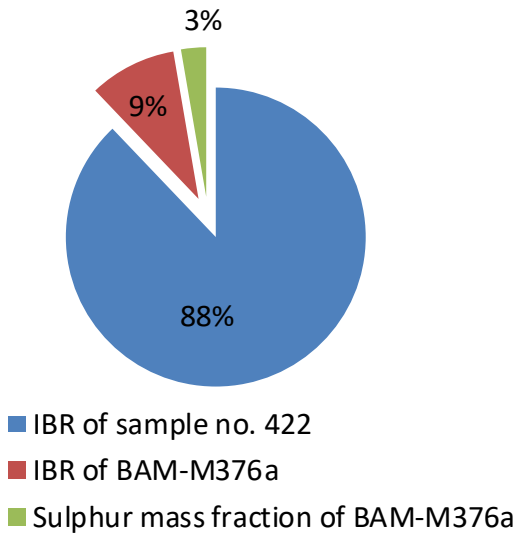

Figure D3-3 Measurement uncertainty budget of sample no. 422 in different calibrator

D3.1d Metrological Traceability

As mentioned before, for reliable measurement results, metrological traceability must be clearly demonstrated. When an unbroken chain of calibrations was established the measurement result with metrological traceability is considered reliable, acceptable and comparable. In our case the metrological traceability to the SI for the determination of the sulphur mass fraction, w_x, in copper samples by GDMS is established by an unbroken chain of comparisons, each accompanied by an uncertainty budget. This is visualized in Figure D3-4 showing the traceability from the *kg* down to the final mass fraction in the sample for the example of sample no 422. In the boxes at the bottom line the sulphur mass fraction in copper and the measurement uncertainty are presented. Both are assigned by measurement procedure 5 which employs external calibration strategy by

GDMS. Two external calibrators are used to calibrate the instrument, which for this exact sulphur content was obtained by the IDMS method as shown in the figure. The rest of the traceability chain up to the SI are the same as section D1.6.

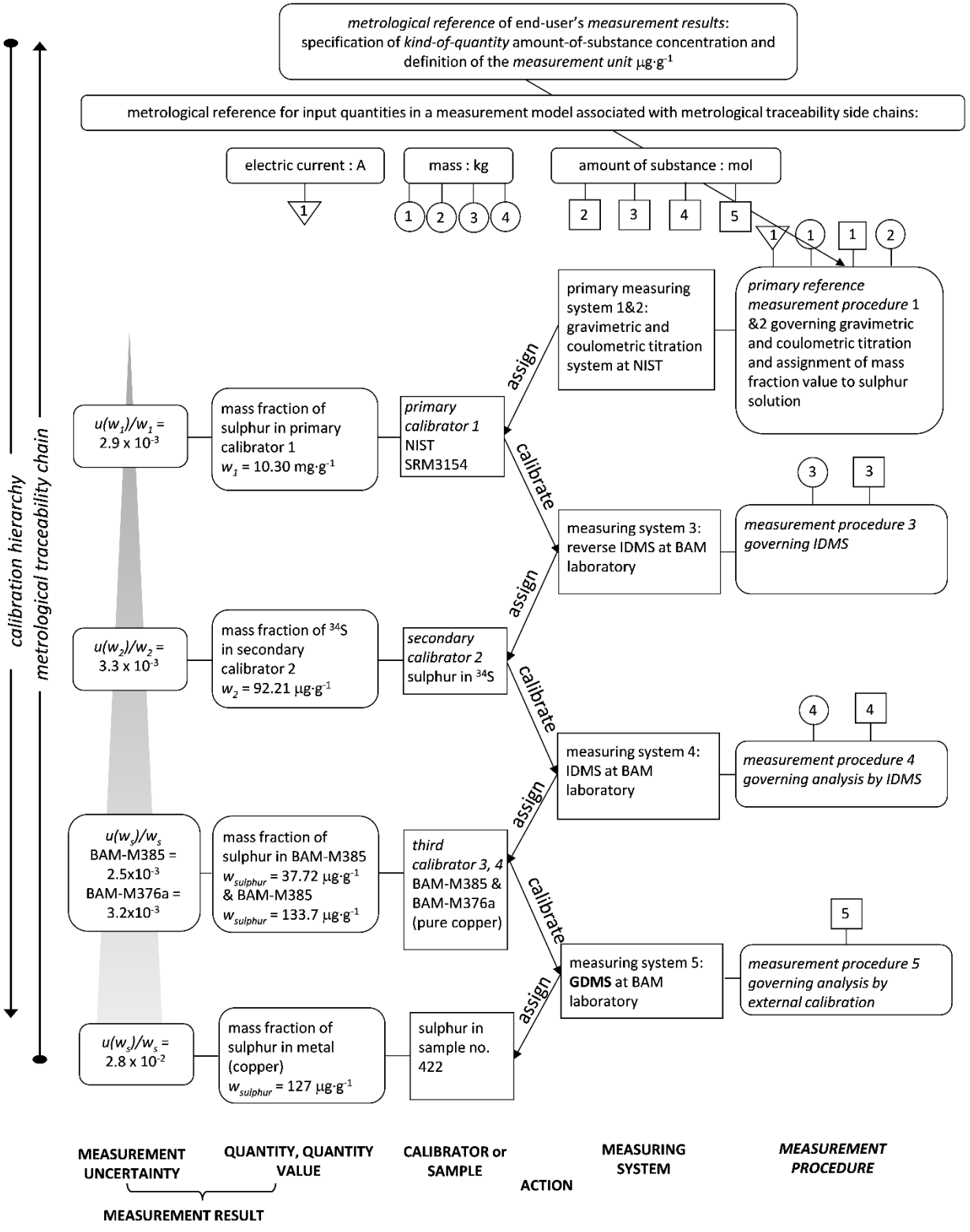

Figure D3-4 Metrological traceability chain of sample no. 422 by GDMS

D3.2 Quantification of Sulphur in Copper and Copper Alloys by LA-ICP- MS

As mention before that LA-ICP-MS is a direct technique for elemental analysis. This section discusses about using the technique as routine analysis to quantify sulphur in copper samples. To establish traceability of the measurement results through the IDMS analysis as the reference values. The direct measurement was validated, estimated the measurement uncertainty and illustrated metrological traceability.

D3.2a Method Validation

The LA-ICP-MS method was validated by cross calibration among the calibrators with different calibration strategies and compared to the reference value and certified value. One CRM was used as a calibrator to quantify sulphur in another CRM which was used as sample, similar to the GDMS measurement (section D3.1). The different calibration strategies were validated. These include one-calibrator, two-calibrators (with cross-type) and mixed-calibrators as defined in Table 3-5. The mass fraction of sulphur in each sample was calculated based on equation 16. Figure D3-5 shows the comparison of different calibration strategies for sample BAM-M385 as an example. Calibration curves were plotted between the reference values versus $^{32}S/^{65}Cu$ with and without zero interception.

Table 3-5 Definition of the calibration strategy study

Calibration strategy	Assignment
1 calibrator by SRM 494	A
1 calibrator by BAM-M376	B
1 calibrator by BAM-228	C
1 calibrator by BAM-227	D
1 calibrator by SRM 494 including zero	E
1 calibrator by BAM-M376 including zero	F
1 calibrator by BAM-228 including zero	G
1 calibrator by BAM-227 including zero	H
2 calibrators by SRM 494 & BAM-M376	I
2 calibrators by SRM 494 & BAM-M376 including zero	J
2 calibrators by BAM-228 & BAM-227 including zero	K
4 calibrators by SRM 494, BAM-M376, BAM-228 & BAM-227 including zero	L

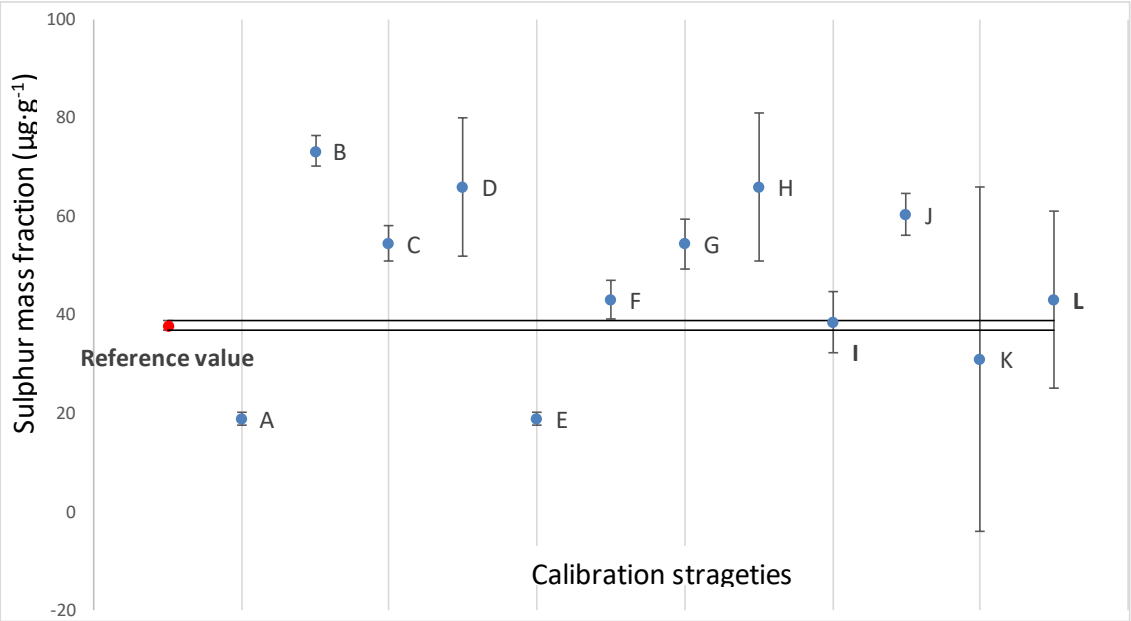

Figure D3-5 Comparison of the different calibration strategies of sample BAM-M385. For the definition please see Table 3-5.

One-point calibration in the LA-ICP-MS is quite critical. It must be noted that using one-point calibration inaccurate results are generated. Cross-type calibration generates results close to the reference values in all cases, but it also results is a large measurement uncertainty. The best results concerning trueness and measurement uncertainty have been obtained by two calibrators using the same matrix (calibration strategy I). Therefore, at least two calibrators were used for method validation and for determination of sulphur mass fraction in sample.

The two calibrators with the same type were selected to validate others, by comparing with reference values from the IDMS analysis as shown in Table D3-6. Compatibility between the reference value and measured value was observed by the E_n number and the results show that they are compatible in all cases. The measurement uncertainty varied from 6% to 56 % relative while % deviate from the reference value varied from 2 % to 19 %, but did not effects to compatibility due to the measurement uncertainty are wider.

Table D3-6 Method validation, E_n numbers by CRMs / RMs compare to reference value (Table D3-1)

RM/CRM name	Measured value ($\mu g \cdot g^{-1}$)	E_n	% diff.	Calibrator(s)*
NIST SRM494	(13.8 ± 7.9)	0.14	8 %	B & C
BAM-M385	(38.6 ± 6.2)	0.14	2 %	A & C
BAM-M376a	(129 ± 30)	0.15	4 %	A & B
BAM-228	(460 ± 100)	0.72	19 %	E
BAM-227	(1140 ± 260)	0.90	17 %	D

* A = NIST SRM494, B = BAM-M385, C = BAM-M376a, D = BAM-228 and E = BAM-227

D3.2b Quantification of Sulphur in Copper Metals and Its Alloys by LA-ICP-MS

According to the results from the method validation, the best calibration approach is the calibration by at least two calibrators. The three calibrators are used for sample analysis of pure copper, while the two calibrators are employed for analysis of alloys. To obtain the calibration curves the intensity ratios were plotted versus the sulphur mass fraction of the calibrators.

Table D3-7 Slope and linear least square of the calibration curves

Calibration strategy	Calibrator(s)	Type	Slope	R^2
3 calibrators	NIST SRM494	Pure copper	4.46×10^{-7}	0.9999
	BAM-M385			
	BAM-M376a			
2 calibrators	BAM-228 & BAM-227	Copper alloy	7.70×10^{-7}	0.9993

Sample no. SRM1034, Y001, 429, 422, and S26 were quantified by pure copper calibrators (SRM494, BAM-M385, BAM-M376a) whereas sample no. 826 and 367 were quantified by copper alloy calibrators (BAM-228 and BAM-227). The calculated results show in Table D3-8 with their measurement uncertainties. The resulting samples SRM1034 and Y001 show too low sulphur amounts for reliable

measurements by their U_{rel} are 670 % and 62 %, respectively. However, when the sulphur content is above 15 $\mu g \cdot g^{-1}$ the relative measurement uncertainties of the result are in the range of 12 % - 40 %.

Table D3-8 Sulphur mass fractions in copper materials as obtained by LA-ICP-MS and their individual uncertainty contributions.

List		**SRM1034**	**BAM-Y001**	**429**	**422**	**S26**	**BAM-367**	**826**
Measurement value and MU ($\mu g \cdot g^{-1}$), $k = 2$		(1.1 ± 7.7)	(7.4 ± 4.6)	(27.2 ± 7.5)	(139 ± 33)	(574 ± 60)	(206 ± 67)	(710 ± 130)
Relative measurement uncertainty (%)		670	62.2	27.6	23.7	10.5	32.5	18.3
Reference value*		(2.8 ± 0.2)	(5.4 ± 3.2)	20	154	466	(162 ± 9)	750
Uncertainty budget	**Type**	**% Contribution**						
Sulphur mass fraction of SRM494	B	7.3	18.3	4.6	0	1.8	-	-
Sulphur mass fraction of BAM-M385	B	0.5	1.3	0.4	0	0	-	-
Sulphur mass fraction of BAM-M376a	B	1.5	2.3	0	1.8	0	-	-
Sulphur mass fraction of BAM-228	B	-	-	-	-	-	2.6	0.3
Sulphur mass fraction of BAM-227	B	-	-	-	-	-	0.1	6.1
Observed $^{32}S/^{65}Cu$ of SRM494	A	15.8	39.5	9.9	0	3.8	-	-

List		SRM1034	BAM-Y001	429	422	S26	BAM-367	826
Observed $^{32}S/^{65}Cu$ of BAM-385	A	11.9	30.7	8.8	0	1.1	-	-
Observed $^{32}S/^{65}Cu$ of BAM-376a	A	0	0	0	0	12.5	-	-
Observed $^{32}S/^{65}Cu$ of BAM-228	A	-	-	-	-	-	2.0	0.3
Observed $^{32}S/^{65}Cu$ of BAM-227	A		-	-	-	-	2.4	91.1
Observed $^{32}S/^{65}Cu$ of sample	A	63.0	7.9	76.3	98.1	80.7	92.9	2.2

* see Table C3-1 (section C3)

D3.2c Measurement Uncertainty Budget

GUM workbench software was used to assess the measurement uncertainty of the results. The mathematical model is based on the external calibration strategy (equation 16) and the calibration curves (Table D3-7). The main factors contributing to the uncertainty budget are the $^{32}S/^{65}Cu$ intensity ratio of the sample and of the calibrators and the sulphur mass fraction of the used calibrator(s). The intensity ratio $^{32}S/^{65}Cu$ measured in the sample is by far the largest contribution to the uncertainty budget and makes up 85 % in all cases. Relative measurement uncertainties of the results are in the range of 12 % - 32 % when the sulphur content is above 15 $\mu g \cdot g^{-1}$. Figure D3-8 shows an example of the uncertainty budget for sample no. S26. The suitability of this analytical procedure with relatively high measurement uncertainties depend on the intended purpose of the analysis, e.g. for purity assessment of pure metals a measurement uncertainty of 30 % is perfectly suited.

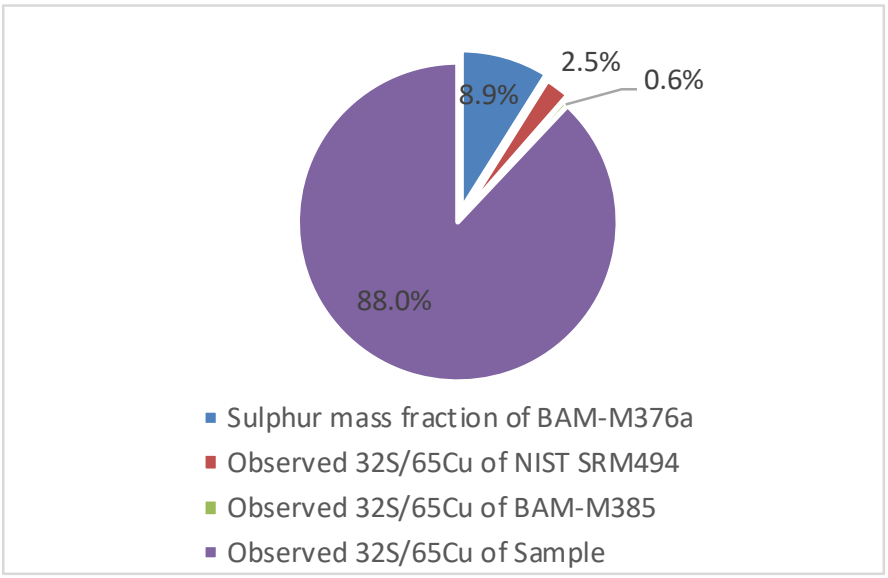

Figure D3-6 Measurement uncertainty budget of sample no. S26 from LA-ICP-MS

D3.2d Metrological Traceability

The unbroken chain of calibrations to the SI was established through IDMS analysis, thus the measurement result is considered reliable, acceptable and comparable. The metrological traceability chain is illustrated in Figure D3-7 of sample no 422 as an example.

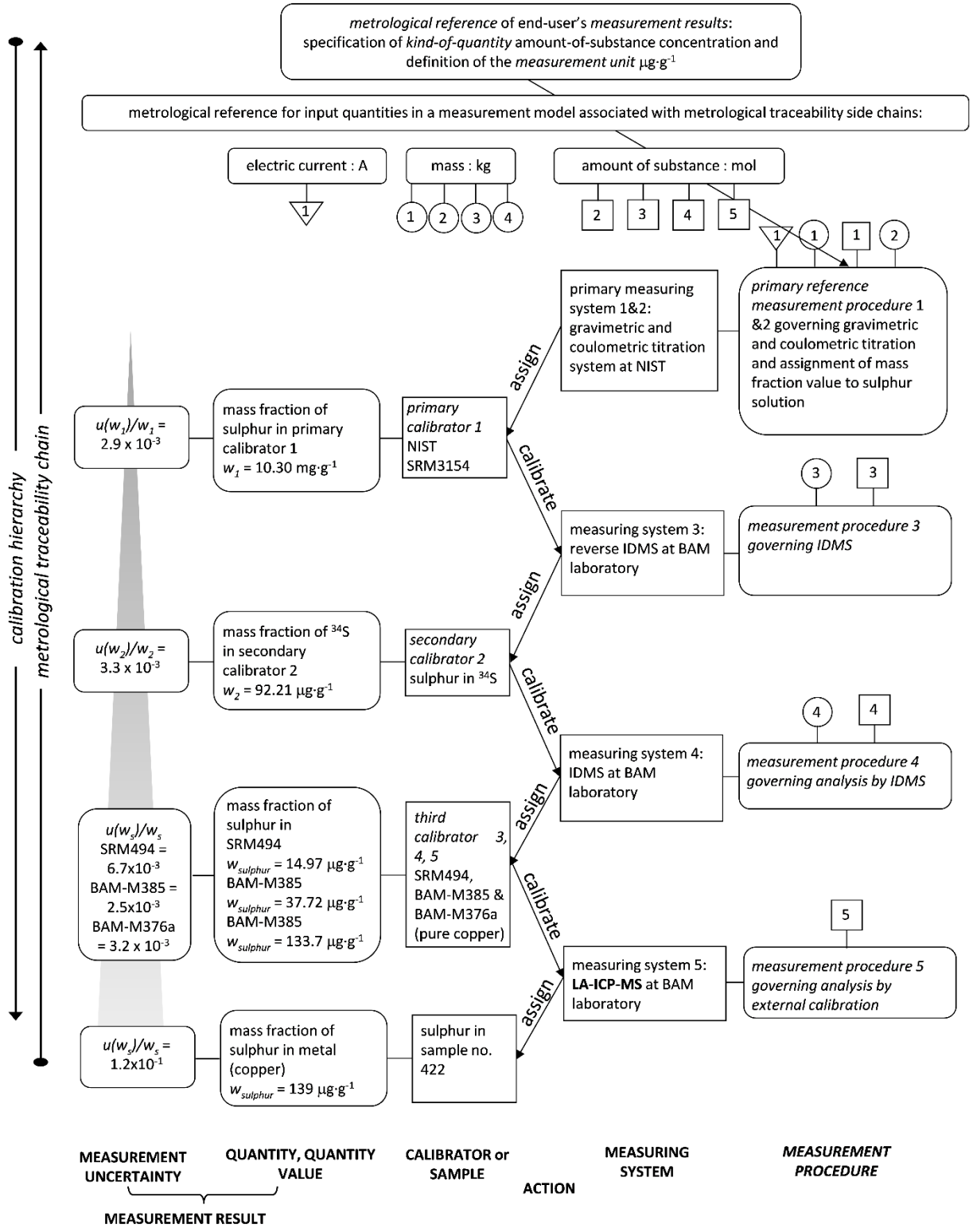

Figure D3-7 Metrological traceability chain of sample no. 422 by LA-ICP-MS

D3.3 Comparability and Compatibility of the Measurement Results by GDMS and LA-ICP-MS

Sulphur mass fraction of calibrators and sample from GDMS and LA-ICP-MS are comparable because there are traceable to the same reference which is SI units. Then, the two data series of measurement results are investigated the compatibility by employing degree of equivalence and E_n. The data from GDMS was used as reference value and the results show E_n below 1 in all cases except sample no. 429 which is low sulphur content. Figure D3-8 illustrates degree of equivalence and their expanded uncertainty of the samples.

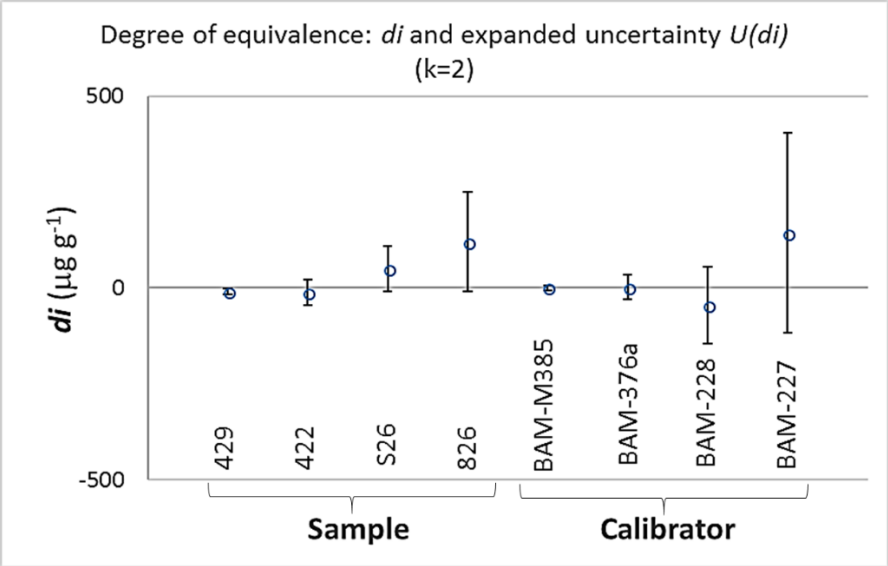

Figure D3-8 Degree of equivalence between GDMS and LA-ICP-MS in the same samples

This study focuses on some application of IDMS results which are used as reference values for the calibration of other analytical method such as GDMS and LA-ICP-MS. It is well known that GDMS and LA-ICP-MS are powerful technique for direct analysis of high purity solid metals, but they require reliable calibrators to generate reliable measurement results. A drawback of these techniques, the lack of appropriate certified reference materials for calibrating the instrument, was solved by applying IDMS analysis. The aim of this research to establish metrological traceability of the measurement results by GDMS and LA-ICP-MS to SI is described earlier.

D4. Method Development for the Quantification of Sulphur in Copper Samples Using LA-ICP-IDMS

This section explains the details of **using a PE frit for sample preparation** in LA-ICP-MS, including the crucial points and the quantification of sulphur in copper samples by LA-ICP-IDMS. Details on the method validation, the results and the measurement uncertainty are discussed. The metrological traceability chart is used to express the reliability of measurement results.

D4.1 Investigation of Using PE Frit for LA-ICP-MS

D4.1a Absorption Efficiency

The absorption efficiency of the PE frit was evaluated by an indirect method as described in the experimental section C4.3b. The result is illustrated in Table D4-1. The frit shows an excellent absorption behaviour concerning not only the absorption efficiency but also the reproducibility. The absorption efficiency of the frit was above 99.5 %. While loading sulphur amounts in the µg range the remaining sulphur, which is not adsorped, is in the ng range. The reproducibility of the frit's absorption was observed up to a level of 80 µg S. Although quantitative recovery is not essential in IDMS, a high recovery is generally considered a quality criterion and it makes the PE frit suitable for applying other calibration strategies such as external calibration.

Table D4-1 Absorption efficiency of the PE frit

Nominal S content (µg)	Doped S amount (µg) *	Remaining S (µg)	Absorption efficiency (%)
2	2.3444	0.0040	99.8304
5	5.3148	0.0316	99.4064
10	10.2546	0.0256	99.7504
20	20.1515	0.0511	99.7465
40	40.2878	0.1005	99.7504
80	80.9419	0.1570	99.8060

* gravimetric method

D4.1b External Calibration Strategy and Dynamic Range

An amount of sulphur ranging from 2 µg to 80 µg was loaded on the frits as mentioned before. Before the intensities were plotted against sulphur amount they were corrected for the frit blank. Linear regression was performed to obtain calibration curves. The corresponding determination coefficient (R^2) based on ^{32}S is 0.9987 for 0-40 µg

(Figure D4-1a). However, it is reduced to 0.9804 when including 80 µg in the calibration curve as shown in Table D4-2. Therefore, the dynamic range of the external calibration is reduced to the interval from 1 µg to 40 µg.

Dressler *et al.* published a calibration approach by using ^{13}C as an internal standard. The least square fit of their calibration curves was improved.[66] This approach was also applied in this work; however, the use of ^{13}C as an internal standard resulting is in the opposite: the R^2 slightly decreased to 0.996 as shown in Table D4-2 and Figure D4-1b. A reason for this is the variation of the ^{13}C intensity, which affected the $^{32}S/^{13}C$ ratio in a negative way. When considering the structure of the PE frit, it is obvious that the sequential arrangement of carbon free cavities and carbon containing walls are directly reflected in the stability of the measured ^{13}C intensity. Therefore, using ^{13}C which contains in the support material as internal standard is possible.

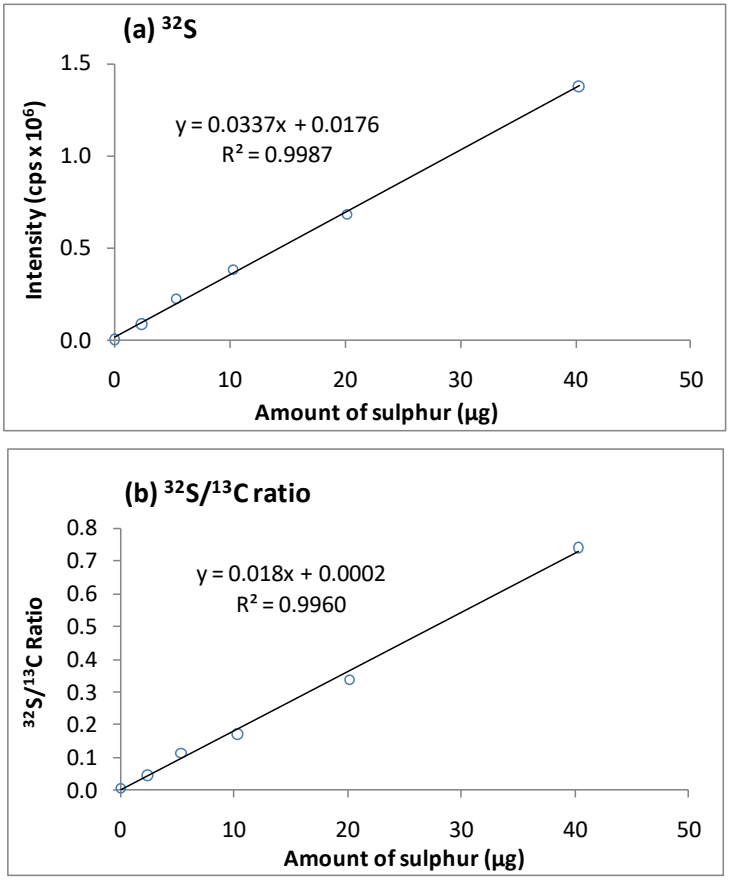

Figure D4-1 Calibration curves for (a) ^{32}S intensity and (b) $^{32}S/^{13}C$ ratio

Table D4-2 Sensitivity and corresponding determination coefficient of different external calibration strategies

Isotope / Isotope ratio	0 – 40 (µg S)		0 – 80 (µg S)	
	Sensitivity ($cps \cdot \mu gS^{-1}$)	R^2	Sensitivity ($cps \cdot \mu gS^{-1}$)	R^2
^{32}S	33,733	0.9987	45,682	0.9804
^{34}S	1,576	0.9986	2,143	0.9799
$^{32}S/^{13}C$	0.01804	0.9960	0.02719	0.9679
$^{34}S/^{13}C$	0.00085	0.9956	0.00128	0.9681

4.1c LOD, LOQ and Sensitivity Base on External Calibration Strategy

LOD and LOQ were evaluated for all applied procedures. LOD (blank + 3SD) and LOQ (blank + 10SD) of each calibration technique were 0.40 µg S and 0.47 µg S, respectively. The sensitivity at mass 32 of LA-ICP-MS was 3.4×10^4 $cps \cdot \mu gS^{-1}$ which is lower than those of conventional ICP-MS (solution form, measured by Element 2) about 200 times, since LA-ICP-MS requires small amount of the sulphur load to the instrument, which was about 0.012 µgS (calculated based on 2 µgS per frit, ablated area about 0.72 mm^2 per line scan). In comparison with ICP-MS loaded sulphur is about 0.48 µg S (calculated based on 2 $\mu g \cdot g^{-1}$, flow rate 100 $\mu L \cdot min^{-1}$). Some possibilities are the sample flow was diluted by He as carrier gas and sulphur was transported in gas phase which can occur fractionation by vapor condensation on the tubing walls, or different particle size.[67]

D4.1d Isotope Ratio vs. Sulphur Absorption Within and Between the Frits

The reproducibility of the sulphur absorption, which is relevant for IDMS analysis was investigated within and between frits. This was tested out by doping a sulphur standard solution on 3 frits and then measure the $^{32}S/^{34}S$ ratio to investigate the variation of the absorption. The variation of sulphur isotope ratio 'within' and 'between' the frits was below 2.5 % relative standard deviation as shown in Table D4-3. The data sets were tested by *T*-test statistic functions and found an insignificant difference. It should be noticed that the variation was without copper matrix.

Table D4-3 Isotope ratio vs. sulphur absorption within and between the frits

Frit no.	Line scan no.	$^{32}S/^{34}S$ ratio	average (within frit)	SD	% RSD
1	1	20.8706	21.2198	0.19	0.88 %
	2	21.1638			
	3	21.3088			
	4	21.3962			
	5	21.2857			
	6	21.2937			
2	1	19.7086	20.1957	0.42	2.09 %
	2	20.4257			
	3	20.4530			
3	1	20.8579	21.1615	0.30	1.44 %
	2	21.4656			
	3	21.1608			
average (between frit)		20.9492			
SD		0.52			
% RSD		2.49 %			

D4.1e Scanning Sulphur on Frits

Sample frit of back spike (sulphur standard), spiked solution, natural isotope and sample-spike blend of BAM-228 and BAM-227 were scanned to observe the dispersion of sulphur on the frits through the ^{32}S- and ^{34}S-intensities and the resulting isotope ratio $^{32}S/^{34}S$ over the time scale. The relative standard deviation of the intensities is between 4 % and 27 %, which reflects the alternating absorption behaviour of cavities and cell walls. The corresponding isotope ratio, scan line is significantly smoother and offers a considerably lower relative standard deviation between 9 % and 18 %, which is certainly due to the nature of isotope ratio measurements where a large part of fluctuations is compensated for. In summary the Figure. D4-2 shows the fluctuation of the sulphur intensities along the line scan, while the $^{32}S/^{34}S$ ratio is significantly less affected by this fluctuation caused by variations in sulphur and/or matrix concentration. Besides other previously described points, the here described PE frit approach is suitable for sulphur quantification by LA-ICP-IDMS.

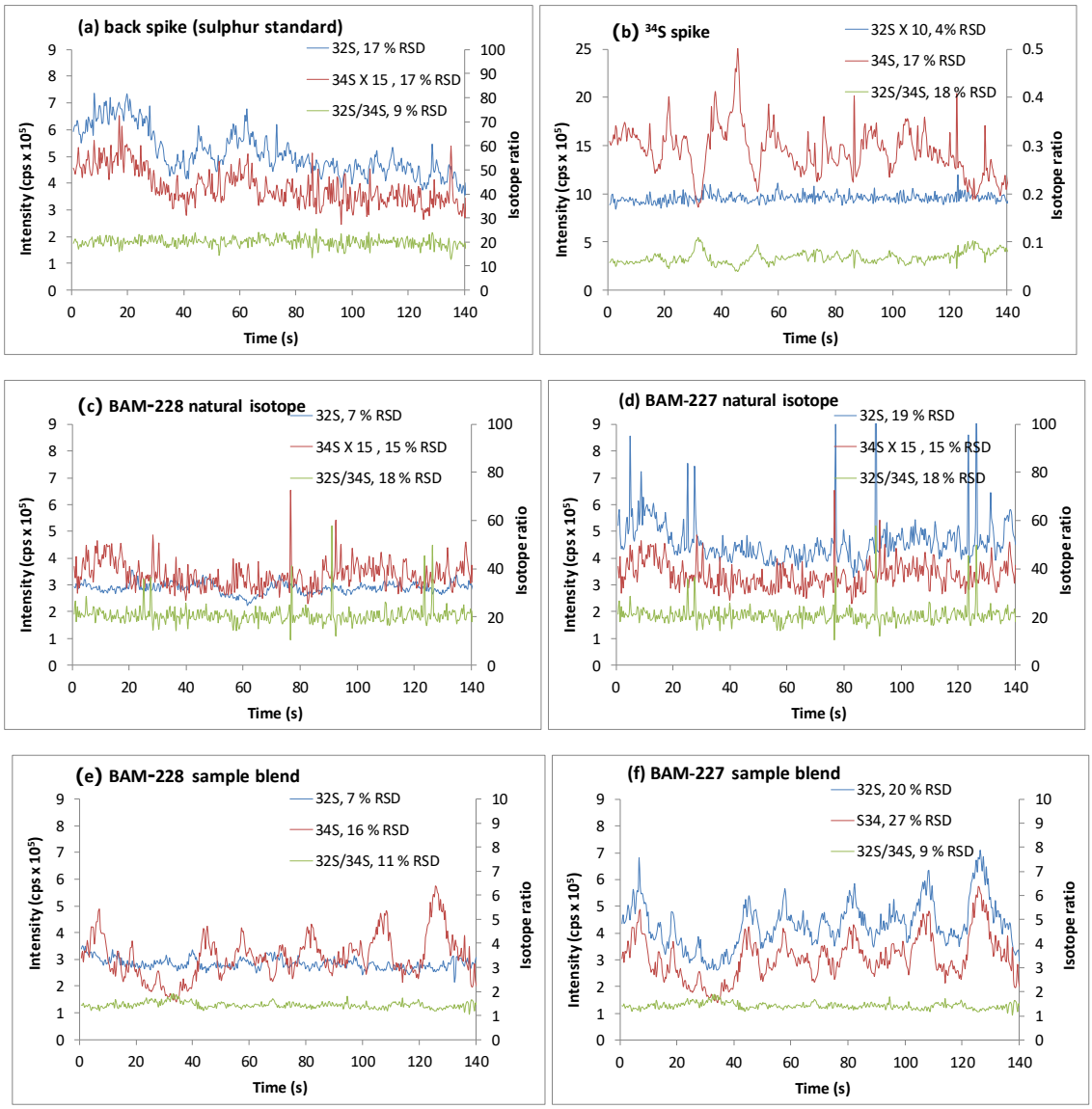

Figure D4-2 Scanning sulphur on frits (a) back spike, (b) ^{34}S spike, (c) BAM-228 natural isotope, (d) BAM-227 natural isotope, (e) BAM-228 sample blend, and (f) BAM-227 sample blend

D4.2 Quantification of Sulphur in Copper by LA-ICP-IDMS

The method was validated by employing three reference materials: BAM-M376a, BAM-228 and BAM-227. Then the measured values were compared with the reference values obtained by ICP-IDMS with sulphur-matrix separation (see section D1-3).[6] As mentioned before copper strongly affected sulphur measurement in general, therefore, the measurement results were corrected before evaluation. The effect of this correction is illustrated in Table D4-4 with their expanded measurement uncertainties (k=2), when

comparing the columns “matrix correction” (see section C2.3) and “without matrix correction”. The use of the matrix correction allows the results of BAM-228 and BAM-227 closer to the reference values. However, this matrix correction factor resulted in increasing the measurement uncertainty. This makes the result more reliable when all known corrections are included.

The measurement results were calculated based on equation 12 (see section B4). They were calculated for individual line scan of each frit. One reference material/sample was prepared for four sample frits and each frit was scanned three lines (n=12). Then results were reported as arithmetic mean.

Table D4-4 Sulphur mass fraction in copper samples and its uncertainty (k=2) by LA-ICP-IDMS

Sample no.	Mass fraction of sulphur in copper samples ($\mu g \cdot g^{-1}$)		
	Reference values*	LA-ICP-MS	
		without matrix correction	matrix correction
BAM-M376a	(133.7±0.9)	(178.0±47.1)	(184.0±47.5)
U_{rel} (%)	0.7	26.5	25.8
E_n	-	0.9	1.1
BAM-228	(385.5±2.4)	(434.0±44.2)	(426.0±43.9)
U_{rel} (%)	0.6	10.2	10.3
E_n	-	1.1	0.9
BAM-227	(1,376.6±6.2)	(1,356.0±210.4)	(1,374.0±218.7)
U_{rel} (%)	0.5	15.5	15.9
E_n	-	0.1	0.0

* IDMS with sulphur-matrix separation[6]

To avoid an overload of the frit by copper **matrix** the upper limit for copper loaded on one frit was set to 20 mg. By this means, BAM-M376a was found to certain sulphur by approximately 0.9 µg per frit (determined by external calibration) resulting in an analyte signal to procedural blank ratio of slightly less than 3. This of course directly affects the measurement accuracy in a negative way which is also expressed by the relative expanded measurement uncertainty (U_{rel}) up to 26 %.

D4.3 Uncertainty Budget

The associated measurement uncertainties were calculated as the mean of the individual measurement uncertainties (equation 20) plus the standard deviation of the mean of all individual results (equation 21). Variation of data in each line scan must be considered because homogeneity of sulphur dispersion on the frit shall not be ignored even though it was already proven by sulphur standard that the variation is insignificant. In order to avoid an under-estimation of the uncertainty, the sample is calculated on each line scan. For the measurement uncertainties of the results obtained without matrix correction, there are four major sources of uncertainty: 1) the measured isotope ratio of the sample-blends 2) the measured isotope ratio of the back spike 3) mass fraction of spike solution and 4) the measured isotope ratio of the natural sample. The detailed percentage of the four largest uncertainty contributions is depicted in Figure D4-3. Nevertheless, the other quantities do not contribute significantly (<2 %) including procedure blank.

$$\bar{u} = \sqrt{\frac{\sum u_i^2}{n}} \quad , \qquad \text{Equation 20}$$

$$u_c = \sqrt{\left(\frac{s}{\sqrt{n}}\right)^2 + \bar{u}^2} \quad , \qquad \text{Equation 21}$$

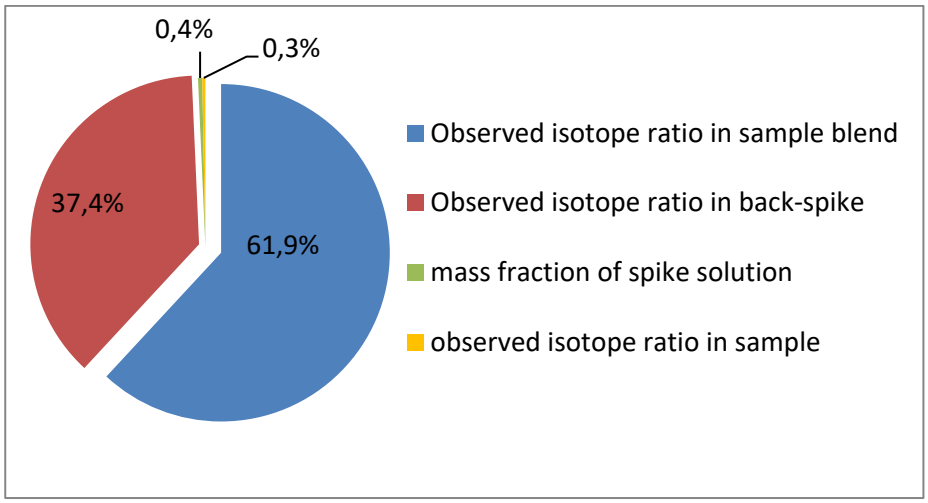

Figure D4-3 Uncertainty budget of sample no. 227

D4.4 Metrological Traceability

The metrological traceability to the SI for the determination of the sulphur mass fraction of sulphur, w_x, in copper metals by LA-ICP-IDMS is established by an unbroken

chain of comparisons, each accompanied by an uncertainty budget. This is visualized in Figure D4-4 showing the traceability from the kg down to the final mass fraction in the sample for the example of sample BAM-227.

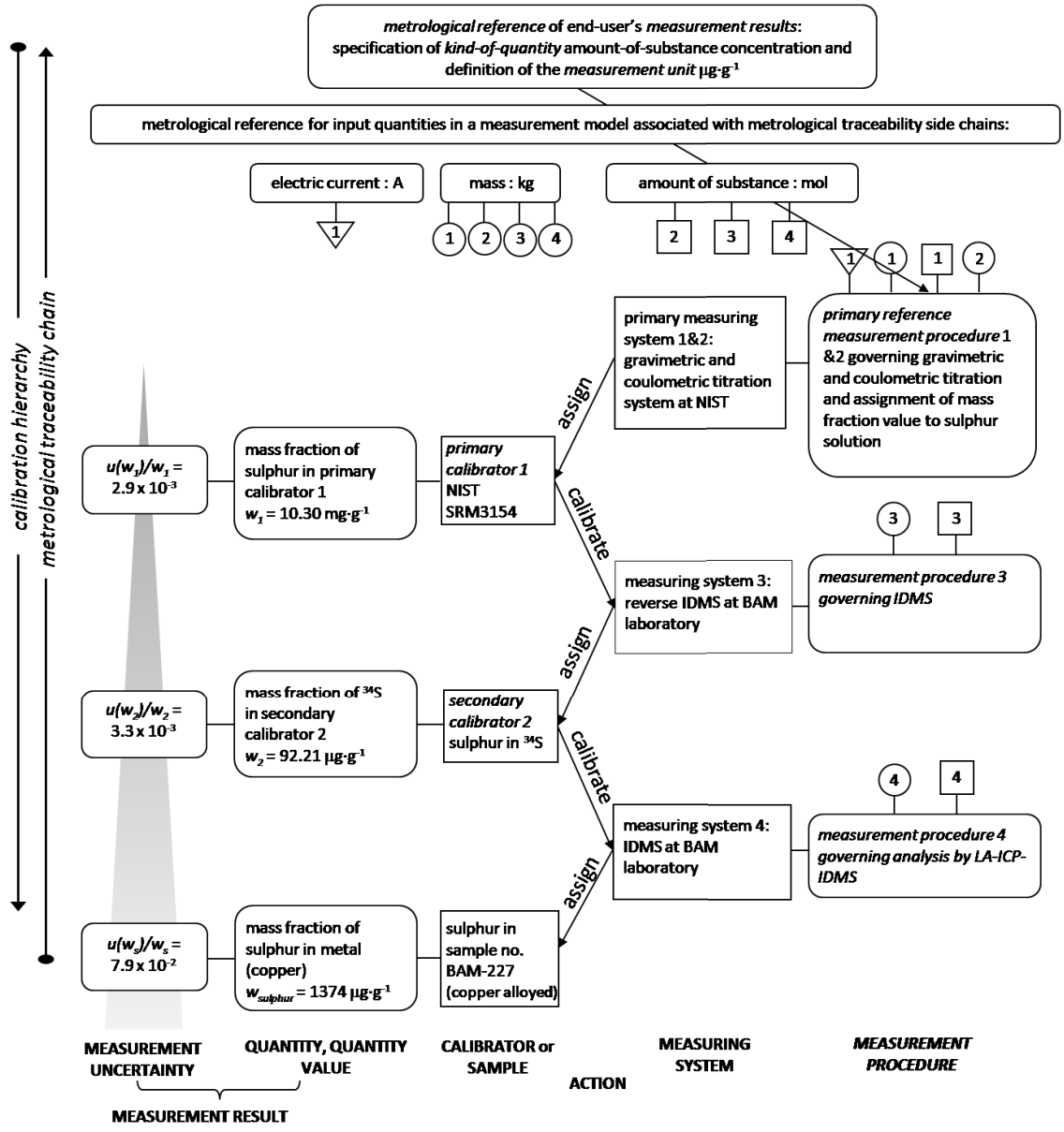

Figure D4-4 Metrological traceability chain of sample no. BAM-227

D4.5 Metrological Compatibility and Correlation Coefficient

D4.5a Metrological Compatibility

The E_n number is used to assess the comparability of the results between measured value and reference values. The agreement of the results is visualized in Figure D4-5, where the results are displayed together. For BAM-228 and BAM-227 the E_n number is below 1 whereas such a low sulphur content sample as BAM-M376a the E_n is 1.06 with U_{rel} 26 %. If expanding the uncertainty to 30 % (as the target measurement uncertainty) then the result is comparable to the reference value as shown in the Figure D4-5 on the right-hand side.

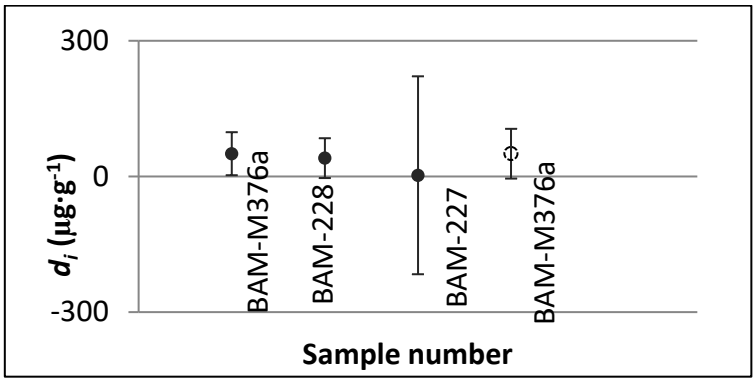

Figure D4-5 Degree of equivalence, d_i and expanded uncertainty $U(d_i)$ (k=2) in copper materials by LA-ICP-IDMS compared to reference value

D4.5b Correlation Coefficient (Pearson's Coefficient)

The correlation between the two techniques is a factor to show how well they are related. Pearson's correlation is regarded as one of the most useful parameters in statistic. Figure D4-6 shows the plot of mass fraction of sulphur in the same copper samples between ICP-IDMS vs. LA-ICP-MS and the Pearson's coefficient was 1. It was proved a strong relationship for the two techniques, so it can be concluded that measurement results from LA-ICP-IDMS were insignificantly different from ICP-IDMS.

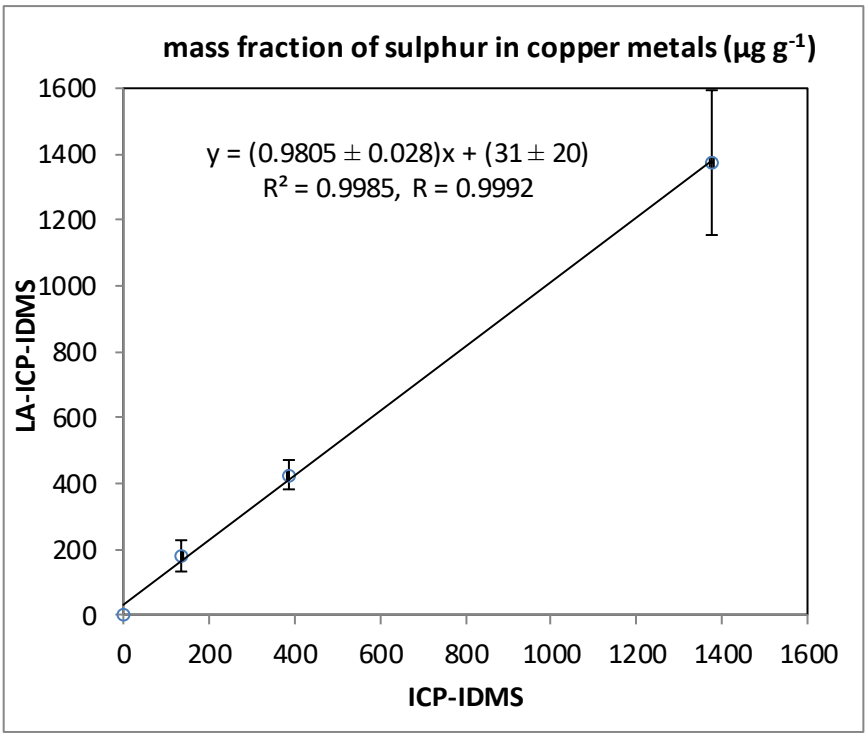

Figure D4-6 Correlations between ICP-IDMS vs. LA-ICP-IDMS

D4.6 Conclusion

The main properties of the newly developed LA-ICP-IDMS procedure, which is based on the use of a PE frit a support material, are listed in Table D4-5 and are compared to the properties of other sample preparation methods for LA-ICP-IDMS. According to table D4.5 the main benefits of the presented procedure here (LA-ICP-IDMS, PE frit) are as follows: 1) it is *more reliable* than most LA based routine analysis procedures, because the measurement results are traceable to the SI by applying the IDMS approach properly; 2) it is *less time consuming and cheaper* than conventional ICP-IDMS with sulphur-matrix separation and 3) it can be easily adopted to sulphur determination in any other metal sample, which is not possible for conventional ICP-IDMS; in the latter case the sulphur-matrix separation has to be developed specifically for the matrix material, which is highly laborious. The downside of the developed LA-ICP-IDMS procedure is the matrix introduction into the measurement system: A high content of a metal matrix negatively affects the sensitivity due to Cu deposition on the cones. These matrix effects, however, can be sufficiently controlled by applying the IDMS technique. Furthermore, analyte and matrix deposited on cones and sample holder can lead to memory effects, which requires flushing the system by He gas before each measurement. Another disadvantage is that the developed LA-ICP-IDMS method, requires sample preparation

which is not a direct analysis anymore. In summary, the major advantages (SI traceability, measurement uncertainty, reduced sample preparation) outbalance the disadvantages.

Table D4-5 Comparison between different sample preparation techniques (LA-ICP-IDMS)

Method / List	LA-ICP-IDMS			
	On-line spiking	Pellet (off-line)	Membrane	Frit
Type	published data	published data	published data	this work
Modification of sample introduction system	Yes	No	No	No
Direct method	Yes	No	No	No
Isotopic equilibration	No	Yes / No	Yes	Yes
Measurement uncertainty, U_{rel}	No, except for ref.[68] (15-27 %)	not established	not established	10-30 %
Metrological traceability	No, except for ref. [68]	not established	not established	Yes
Sample preparation time	< 1 day	≤ 1 day	≤ 1 day	1 day
Measurement time	No information	No information	No information	6-7
Cleanup step due to matrix	Yes / No	Yes / No	Yes / No	Yes

Part E Summary and Outlook

A reliable procedure was developed to quantify sulphur in pure copper and its alloys by ICP-IDMS with high efficiency of the sulphur-copper separation. The procedure was completely validated via an inter-laboratory comparison, a step-by-step validation while developing the procedure, and the setup of a complete uncertainty budget. Additionally, relative expanded measurement uncertainties were estimated to range below 1 %, while metrological traceability to the SI is clearly expressed. Therefore, the procedure is well-suited to provide reference values for the total sulphur mass fraction in copper materials. The feature of the developed procedure is summarized in Table E1 (see section D1 for detail).

Table E1 Feature of ICP-IDMS with sulphur-matrix separation

Feature of ICP-IDMS with sulphur-matrix separation
Accurate
Small measurement uncertainty < 1 % relative
Direct metrological traceable to SI
High matrix removal efficiency 99.999 %
High sulphur recovery above 80 %
Wide working range 15-1500 $\mu g \cdot g^{-1}$ (including standard addition)
Low LOD (0.20 $\mu g \cdot g^{-1}$) and LOQ (0.54 $\mu g \cdot g^{-1}$)
Low procedural blank (between 4 ng and 53 ng)
Reliable method with full validation method: CRM, Inter-laboratory comparison, step by step
Potential to be a reference method
Applicable to calibrate/validate GDMS and LA-ICP-MS method
Limitation of ICP-IDMS with sulphur-matrix separation
Time consuming
High cost due to employing ICP-MS, primary standard solution and enriched isotope
Skill needed

An application of IDMS results is used as reference values for the calibration of GDMS and LA-ICP-MS, which are powerful techniques for direct solid analysis. Both were used as routine analytical tools to quantify sulphur in copper samples by applying CRMs (produced by BAM) with exactly known sulphur content obtained by IDMS analysis. Both techniques were validated by CRMs and the results show a good agreement with the reference values. In case of GDMS, the measurement uncertainty is in the range of 3 % to 7%, while that for LA-ICP-MS is in the range of 10 % to 62 %. The measurement results from these methods are traceable to SI through IDMS results. This is clearly illustrated by the unbroken chain of calibration hierarchy in the metrological traceability scheme. The detail was discussed in section D3.

A newly LA-ICP-IDMS procedure, which is based on the use of a PE frit as a support material was developed to quantify sulphur in copper samples. The method is considered reliable, less time consuming and cheaper and user friendly. Actually, this is another application of ICP-IDMS results (with sulphur-matrix separation) which is used as reference method to validate a new approach.

Every measurement result is associated with measurement uncertainty estimated and clearly demonstrated metrological traceability unbroken chain to the comparability and traceability of the measurement results.

This research provides reliable measurement procedures which enable sufficiently low measurement uncertainties and SI traceability of the results. Therefore, these procedures are well suited for reference materials certification, reference values assignment and new developing procedure validation. In addition, the measurement results from ICP-IDMS (with separation procedure) can be regarded as reference values of the calibrator for routine analytical method. Applying such reference procedures to the quantification of sulphur in copper metals and its alloys, the results will be accepted worldwide in every technical and scientific section. Figure E1 expresses the applications of a reference procedure.

The challenge, quantification of sulphur in copper metal and its alloys by ICP-IDMS with sulphur-copper separation is completed. Not only the procedure was developed with full method validation, but some applications were also demonstrated Therefore, the outlook focuses on LA-ICP-IDMS procedure only. The authors suggest applying the procedure to other analytes and matrices such as nickel and zinc. To continue

and complete this work multi-elemental analysis by multi-spiking is recommended for wider applications. Additionally, variation of the material supporters are also of interest in examining, such as polypropylene, polystyrene, etc., which might improve the absorption efficiency and unique of the samples dispersion.

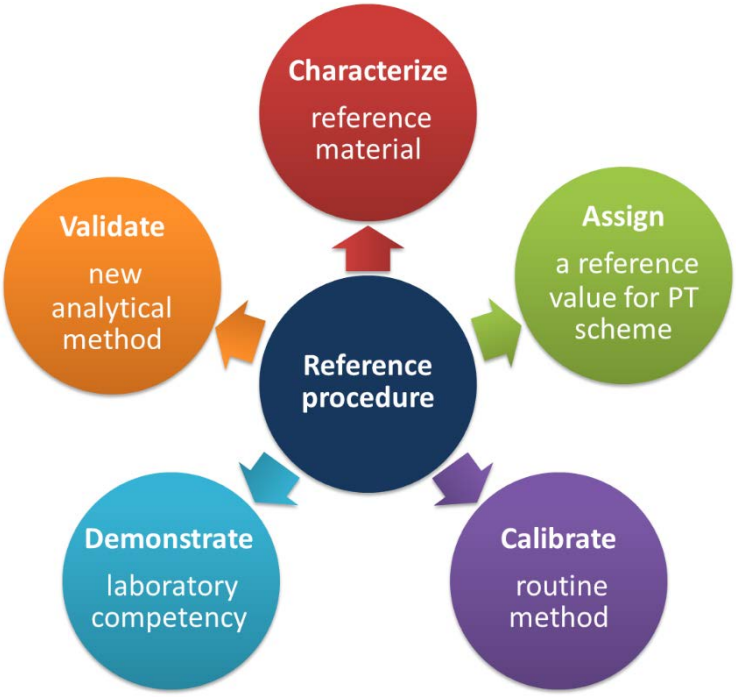

Figure E1 Application of a reference procedure.

Part F Appendix

Calculation of sample preparation for planning with sulphur-matrix separation

Table F1 Planning calculation for sample BAM-227

Sample name	BAM-227	ProcBalnk
Copper content ($g \cdot g^{-1}$)	~0.85	-
Sulphur content ($\mu g \cdot g^{-1}$)	1220	-
Sampling (g)	0.10	-
Amount of sulphur (μg)	122	-
Amount of ^{32}S (μg) in abundance	115.89	
Amount of ^{34}S in abundance	5.185	-
$^{32}S/^{34}S$ in abundance	22.35	-
Aimed $^{32}S/^{34}S$ ratio in sample blend	1	-
Stock spike solution (mL)*	1.201	0.43*
Amount of ^{34}S (μg) from stock	110.70	3.88
Total sulphur in sample blend (μg)	232.70	3.88
Add conc. HNO_3, 5 ml + H_2O_2, 1 ml digest by HPA-> rinse by Milli-Q water, 9 mL	15	15
Sampling sample blend solution (mL)	0.5	0.5
Amount of sulphur (μg)	7.76	-
Amount of copper (mg)	3.33	-
Add NH_3 excess (mL)	0.03	0.03
Final volume (dilute by 2 % HNO_3 (mL)	8	8
Add Amberlite resin excess (mL)	2	2
After separation dissolve by 2 % HNO3 (mL)	2	2
Conc. of sulphur in total ($\mu g \cdot mL^{-1}$)	3.88	1.94
Conc. of ^{32}S ($\mu g \cdot mL^{-1}$)	1.94	1.94

* sulphur mass fraction in spike solution (9.21 ± 0.31) $\mu g \cdot g^{-1}$

IDMS Equation from GUM Workbench

Model Equation:

{Calculation of sample mass fraction in µg S/g by using following equation:}
{$w_x = w_{yb} * K_{VV} * M_x * m_y * K_{my} * (R_y - R_{xy}) / (M_b * a_{xb} * m_x * K_{mx} * (R_{xy} - R_x))$*;}*

{Calculation of Buoyancy correction factors}
$K_{mx} = (1 - (\rho_a/\rho_w)) / (1 - (\rho_a/\rho_x))$;
$K_{my} = (1 - (\rho_a/\rho_w)) / (1 - (\rho_a/\rho_y))$;

{Calculation of correction factors for mass discrimination, K-factors}
{$K_{32} = R_{c32} / R_{co32}$*;}*

$K_{32} = R_{32/34\text{-}SRM3154} / R_{32/34obs\text{-}SRM3154}$;

{Correction of isotope ratio in sample blend}
$R_{xy11} = K_{32} * R_{xyo11}$;
$R_{xy12} = K_{32} * R_{xyo12}$;
$R_{xy21} = K_{32} * R_{xyo21}$;
$R_{xy22} = K_{32} * R_{xyo22}$;
$R_{xy31} = K_{32} * R_{xyo31}$;
$R_{xy32} = K_{32} * R_{xyo32}$;
$R_{xy41} = K_{32} * R_{xyo41}$;
$R_{xy42} = K_{32} * R_{xyo42}$;

$R_{y32} = K_{32} * R_{yo32}$;

{Calculation of isotope composition of the unspiked sample}
$R_{x32} = K_{32} * R_{xo32}$;
$R_{x33} = a_{33\text{-}IUPAC} / a_{34\text{-}IUPAC}$;
$R_{x36} = a_{36\text{-}IUPAC} / a_{34\text{-}IUPAC}$;
$SumR_x = R_{x32} + R_{x33} + R_{x34} + R_{x36}$;
$a_{x32} = R_{x32} / SumR_x$;
$a_{x33} = R_{x33} / SumR_x$;
$a_{x34} = R_{x34} / SumR_x$;
$a_{x36} = R_{x36} / SumR_x$;
$A_x = (a_{x32} * A_{32} + a_{x33} * A_{33} + a_{x34} * A_{34} + a_{x36} * A_{36})$;

{Calculation of molar massess from atomic weights}
$M_{34} = A_{34}$;
$M_x = A_x$;

$R_x = R_{x32}$;
$R_y = R_{y32}$;

{Calculation of mass fraction of sample in µg/g}

$T1 = w_{yb} * K_{vv} * M_x / (M_b * a_{x34})$; *{constant term}*

$w_{x11} = (T1 * (m_{y1} * K_{my} * (R_y - R_{xy11})) / (m_{x1} * K_{mx} * (R_{xy11} - R_x))) - (ProcBl / m_{x1})$;
$w_{x12} = (T1 * (m_{y1} * K_{my} * (R_y - R_{xy12})) / (m_{x1} * K_{mx} * (R_{xy12} - R_x))) - (ProcBl / m_{x1})$;
$w_{x1} = average\ (w_{x11}, w_{x12})$;

$w_{x21} = (T1 * (m_{y2} * K_{my} * (R_y - R_{xy21})) / (m_{x2} * K_{mx} * (R_{xy21} - R_x))) - (ProcBl / m_{x2})$;
$w_{x22} = (T1 * (m_{y2} * K_{my} * (R_y - R_{xy22})) / (m_{x2} * K_{mx} * (R_{xy22} - R_x))) - (ProcBl / m_{x2})$;
$w_{x2} = average\ (w_{x21}, w_{x22})$;

$w_{x31} = (T1 * (m_{y3} * K_{my} * (R_y - R_{xy31})) / (m_{x3} * K_{mx} * (R_{xy31} - R_x))) - (ProcBl / m_{x3})$;
$w_{x32} = (T1 * (m_{y3} * K_{my} * (R_y - R_{xy32})) / (m_{x3} * K_{mx} * (R_{xy32} - R_x))) - (ProcBl / m_{x3})$;
$w_{x3} = average\ (w_{x31}, w_{x32})$;

$w_{x41} = (T1 * (m_{y4} * K_{my} * (R_y - R_{xy41})) / (m_{x4} * K_{mx} * (R_{xy41} - R_x))) - (ProcBl / m_{x4})$;
$w_{x42} = (T1 * (m_{y4} * K_{my} * (R_y - R_{xy42})) / (m_{x4} * K_{mx} * (R_{xy42} - R_x))) - (ProcBl / m_{x4})$;
$w_{x4} = average\ (w_{x41}, w_{x42})$;

$$w_x = average\ (w_{x1}, w_{x2}, w_{x3}, w_{x4});$$

Table F2 Measurement uncertainty budget of sample no. BAM-M376a

Quantity	Names of quantities	Value	Standard Uncertainty	Uncertainty Contribution ($\mu g \cdot g^{-1}$)	% Contribution
A_{32}	Atomic weight of ^{32}S	31.972070730	150×10^{-9}	590×10^{-9}	0.0 %
A_{33}	Atomic weight of ^{33}S	32.971458540	150×10^{-9}	4.7×10^{-9}	0.0 %
$a_{33\text{-}IUPAC}$	Isotope abundance of ^{33}S (IUPAC)	7.4869×10^{-3}	30.0×10^{-6}	4.1×10^{-3}	0.0 %
A_{34}	Atomic weight of ^{34}S	33.967866870	140×10^{-9}	25×10^{-9}	0.0 %
$a_{34\text{-}IUPAC}$	Isotope abundance of ^{34}S (IUPAC)	0.04250	1.20×10^{-3}	-0.030	0.5 %
A_{36}	Atomic weight of ^{36}S	35.967080880	250×10^{-9}	100×10^{-12}	0.0 %
$a_{36\text{-}IUPAC}$	Isotope abundance of ^{36}S (IUPAC)	100.0×10^{-6}	50.0×10^{-6}	7.5×10^{-3}	0.0 %
A_x	Atomic weight of S in sample	32.064827 $g \cdot mol^{-1}$	707×10^{-6} $g \cdot mol^{-1}$		
a_{x32}	Isotope abundance of ^{32}S in sample (unspike)	0.949885	409×10^{-6}		
a_{x33}	Isotope abundance of ^{33}S in sample	7.491×10^{-3}	219×10^{-6}		
a_{x34}	Isotope abundance of ^{34}S in sample	0.042524	297×10^{-6}		
a_{x36}	Isotope abundance of ^{36}S in sample	100.1×10^{-6}	50.1×10^{-6}		
K_{32}	Correction factor for mass discrimination	0.95511	2.48×10^{-3}		
K_{mx}	Buoyancy correction factor for sample weighing	0.999984465	192×10^{-9}		
K_{my}	Buoyancy correction factor for spike weighing	1.00100878	2.31×10^{-6}		
K_{vv}	Correction factor for loss by evaporation of spike solution	1.003203504	0.0	0.0	0.0 %
M_b	Molar mass of spike element, ^{34}S (IUPAC)	33.967866870 $g \cdot mol^{-1}$	140×10^{-9} $g \cdot mol^{-1}$	-550×10^{-9}	0.0 %
M_x	Molar mass of S in sample (IUPAC)	32.064827 $g \cdot mol^{-1}$	707×10^{-6} $g \cdot mol^{-1}$		
m_{x1}	Mass of sample in sample blend 1	0.253880 g	100×10^{-6} g	-0.013	0.0 %
m_{x2}	Mass of sample in sample blend 2	0.254450 g	100×10^{-6} g	-0.013	0.0 %
m_{x3}	Mass of sample in sample blend 3	0.250600 g	100×10^{-6} g	-0.013	0.0 %
m_{x4}	Mass of sample in sample blend 4	0.251410 g	100×10^{-6} g	-0.013	0.0 %
m_{y1}	Mass of spike in sample blend 1	0.332570 g	100×10^{-6} g	0.010	0.0 %
m_{y2}	Mass of spike in sample blend 2	0.329450 g	100×10^{-6} g	0.010	0.0 %
m_{y3}	Mass of spike in sample blend 3	0.328920 g	100×10^{-6} g	0.010	0.0 %
m_{y4}	Mass of spike in sample blend 4	0.326350 g	100×10^{-6} g	0.010	0.0 %
ProcBl	Procedure blank	0.0126900 µg	65.0×10^{-6} µg	-260×10^{-6}	0.0 %
$R_{32/34obs\text{-}SRM\ 3154}$	Observed isotope ratio $^{32}S/^{34}S$	23.6152	0.0598	-0.32	55.6 %
$R_{32/34\text{-}SRM\ 3154}$	Isotope ratio $^{32}S/^{34}S$ by TIMS[8]	22.5550	0.0130	0.073	2.9 %
R_{x32}	Corrected isotope ratio $^{32}S/^{34}S$ in sample	22.337	0.164		
R_{x33}	Corrected isotope ratio $^{33}S/^{34}S$ in sample	0.17616	5.03×10^{-3}		
R_{x34}	Corrected isotope ratio $^{34}S/^{34}S$ in sample	1.0			
R_{x36}	Corrected isotope ratio $^{36}S/^{34}S$	2.35×10^{-3}	1.18×10^{-3}		

Quantity	Names of quantities	Value	Standard Uncertainty	Uncertainty Contribution ($\mu g \cdot g^{-1}$)	% Contribution
	calculated from IUPAC				
R_{xo32}	Observed isotope ratio $^{32}S/^{34}S$ in sample	23.387	0.161	-0.095	4.8 %
R_{xy11}	Corrected isotope ratio $^{32}S/^{34}S$ in sample bland 1.1	1.05786	3.46×10^{-3}		
R_{xy12}	Corrected isotope ratio $^{32}S/^{34}S$ in sample bland 1.2	1.05744	2.90×10^{-3}		
R_{xy21}	Corrected isotope ratio $^{32}S/^{34}S$ in sample bland 2.1	1.07381	3.79×10^{-3}		
R_{xy22}	Corrected isotope ratio $^{32}S/^{34}S$ in sample bland 2.2	1.07279	3.30×10^{-3}		
R_{xy31}	Corrected isotope ratio $^{32}S/^{34}S$ in sample bland 3.1	1.04986	4.37×10^{-3}		
R_{xy32}	Corrected isotope ratio $^{32}S/^{34}S$ in sample bland 3.2	1.04381	4.09×10^{-3}		
R_{xy41}	Corrected isotope ratio $^{32}S/^{34}S$ in sample bland 4.1	1.07044	3.94×10^{-3}		
R_{xy42}	Corrected isotope ratio $^{32}S/^{34}S$ in sample bland 4.2	1.07409	4.41×10^{-3}		
R_{xyo11}	Observed isotope ratio $^{32}S/^{34}S$ in sample bland 1.1	1.10758	2.21×10^{-3}	0.035	0.7 %
R_{xyo12}	Observed isotope ratio $^{32}S/^{34}S$ in sample bland 1.2	1.107140	987×10^{-6}	0.016	0.1 %
R_{xyo21}	Observed isotope ratio $^{32}S/^{34}S$ in sample bland 2.1	1.12428	2.68×10^{-3}	0.042	1.0 %
R_{xyo22}	Observed isotope ratio $^{32}S/^{34}S$ in sample bland 2.2	1.12321	1.85×10^{-3}	0.029	0.5 %
R_{xyo31}	Observed isotope ratio $^{32}S/^{34}S$ in sample bland 3.1	1.09921	3.57×10^{-3}	0.057	1.7 %
R_{xyo32}	Observed isotope ratio $^{32}S/^{34}S$ in sample bland 3.2	1.09287	3.21×10^{-3}	0.051	1.4 %
R_{xyo41}	Observed isotope ratio $^{32}S/^{34}S$ in sample bland 4.1	1.12075	2.93×10^{-3}	0.046	1.1 %
R_{xyo42}	Observed isotope ratio $^{32}S/^{34}S$ in sample bland 4.2	1.12458	3.57×10^{-3}	0.056	1.7 %
R_{y32}	Corrected isotope ratio $^{32}S/^{34}S$ in spike	873.0×10^{-6}	21.1×10^{-6}		
R_{yo32}	Observed isotope ratio $^{32}S/^{34}S$ in spike	914.0×10^{-6}	22.0×10^{-6}	-2.6×10^{-3}	0.0 %
$SumR_x$	Sum of all isotope ratio	23.516	0.164		
w_{x1}	S mass fraction in sample 1	133.672 $\mu g \cdot g^{-1}$	0.443 $\mu g \cdot g^{-1}$		
w_{x11}	S mass fraction in sample 1.1	133.700 $\mu g \cdot g^{-1}$	0.502 $\mu g \cdot g^{-1}$		
w_{x12}	S mass fraction in sample 1.2	133.644 $\mu g \cdot g^{-1}$	0.434 $\mu g \cdot g^{-1}$		
w_{x2}	S mass fraction in sample 2	134.177 $\mu g \cdot g^{-1}$	0.465 $\mu g \cdot g^{-1}$		
w_{x21}	S mass fraction in sample 2.1	134.244 $\mu g \cdot g^{-1}$	0.537 $\mu g \cdot g^{-1}$		
w_{x22}	S mass fraction in sample 2.2	134.110 $\mu g \cdot g^{-1}$	0.478 $\mu g \cdot g^{-1}$		
w_{x3}	S mass fraction in sample 3	132.497 $\mu g \cdot g^{-1}$	0.513 $\mu g \cdot g^{-1}$		
w_{x31}	S mass fraction in sample 3.1	132.900 $\mu g \cdot g^{-1}$	0.614 $\mu g \cdot g^{-1}$		
w_{x32}	S mass fraction in sample 3.2	132.095 $\mu g \cdot g^{-1}$	0.579 $\mu g \cdot g^{-1}$		
w_{x4}	S mass fraction in sample 4	134.385 $\mu g \cdot g^{-1}$	0.509 $\mu g \cdot g^{-1}$		
w_{x41}	S mass fraction in sample 4.1	134.144 $\mu g \cdot g^{-1}$	0.557 $\mu g \cdot g^{-1}$		

Quantity	Names of quantities	Value	Standard Uncertainty	Uncertainty Contribution ($\mu g \cdot g^{-1}$)	% Contribution
w_{x42}	S mass fraction in sample 4.2	134.626 $\mu g \cdot g^{-1}$	0.615 $\mu g \cdot g^{-1}$		
w_{yb}	S mass fraction in spike solution	92.210 $\mu g^{34}S \cdot g^{-1}$	0.155 $\mu g^{34}S \cdot g^{-1}$	0.22	27.3 %
ρa	Density of air	1.19320 $kg \cdot m^{-3}$	1.30 x 10^{-3} $kg \cdot m^{-3}$	150 x 10^{-6}	0.0 %
ρw	Density of balance weights	8000.00 $kg \cdot m^{-3}$	8.00 $kg \cdot m^{-3}$	0.0	0.0 %
ρx	Density of sample	8930.00 $kg \cdot m^{-3}$	8.00 $kg \cdot m^{-3}$	16 x 10^{-6}	0.0 %
ρy	Density of spike solution	1031.50 $kg \cdot m^{-3}$	1.80 $kg \cdot m^{-3}$	-270 x 10^{-6}	0.0 %
w_x	S mass fraction in sample	133.683 $\mu g \cdot g^{-1}$	0.430 $\mu g \cdot g^{-1}$		

References

1. Copper Development Assocoation (CDA) http://copperalliance.org.uk/industry/economy, Accessed 19 Feb, 2017.
2. E. I. Krupnikovaperlina, L. I. Sotnikova, S. A. Kuznetsova, V. A. Bliznyuk and V. G. Osintsev, *Met. Sci. Heat. Treat.*, 1985, 27, 223-225.
3. J. G. Martinez-Sierra, O. G. San Bias, J. M. M. Gayon and J. I. G. Alonso, *Spectrochim. Acta, Part B*, 2015, 108, 35-52.
4. R. Matschat, M. Czerwensky, M. Hamester, S. Pattberg, *Fresenius J. Anal. Chem*, 1997, 359, 418-423.
5. B. Lange, S. Recknagel, M. Czerwensky, R. Matschat, M. Michaelis, B. Peplinski and U. Panne, *Microchim. Acta.*, 2008, 160, 97-107.
6. P.Phukphatthanachai, N. Jakubowski, J. Vogl, U. Panne, *J. Anal. At. Spectrom.*, 2018, 33, 90-102
7. P. Phukphatthanachai, J. Vogl, H. Traub, N. Jakubowski and U. Panne, *J. Anal. At. Spectrom.*, 2018, 33, 12.
8. W. Pritzkow, J. Vogl, R. Koppen and A. Ostermann, *Int. J. Mass Spectrom.*, 2005, 242, 309-318.
9. R. M. C. Michael L. Gross, *The encyclopedia of mass spectrometry*, Elsevier Ltd., The Boulvard, Langford, Kidlington, Oxford. UK, Frist edn., 2010.
10. https://www.bipm.org/en/worldwide-metrology/, Accessed 6 Dec, 2017.
11. https://kcdb.bipm.org/, The BIPM key comparison database, Accessed May, 2018.
12. T. Kuroiwa, Y. Zhu, K. Inagaki, S. Long, S. Christopher, M. Puelles, M. Borinsky, N. Hatamleh, J. Murby, J. Merrick, I. White, D. Saxby, R. C. de Sena, M. D. de Almeida, J. Vogl, P. Phukphatthanachai, W. Fung, H. Yau, T. O. Okumu, J. N. Kangiri, J. A. Salas T´ellez, E. Z. Campos, E. C. Galv´an, N. Kaewkhomdee, S. Taebunpakul, U. Thiengmanee, C. Yafa, N. Tokman, M. Tunç and S. Z. Can, *Metrologia, 2017*, 54(Tech. Suppl.), 08008.
13. J. Vogl, H. Kipphardt, S. Richter, W. Bremser, M. R. A. Torres , J. V. L. Manzano, M. Buzoianu, S. Hill, P. Petrov, H. Goenaga-Infante, M. Sargent, P. Fisicaro, G. Labarraque, T. Zhou, G. C. Turk, M. Winchester, T. Miura, B. Methven, R. Sturgeon, R. Jährling, O. Rienitz, M. Mariassy, Z. Hankova, E. Sobina, A. I. Krylov, Y. A. Kustikov, V. V. Smirnov, *Metrologia*, 2018, 55.
14. S. Recknagel, *Report of the study CCQM-K64 Analysis of a copper alloy*, Bundesanstalt für Materialforschung und -prüfung (BAM), 2009.
15. JCGM200:2012, *JCGM: International Vocabulary of Metrology – Basic and General Concepts and Associated Terms*, 3rd edn., 2012, ch. 2008 version with minor corrections.
16. S. L. R. Ellison, M. Rosslein, A Williams, EURACHEM/CITAC guide: Quantifying Uncertainty in Analytical Measurement, Second edition, (2000) ISBN 0 948926 15 5, available from *www.eurachem.org*.
17. R. Thomas, *Practical Guide to ICP-MS a tutorial for beginners*, CRC Press Taylor & Francis Group, 2013.
18. S. M. Nelms, *ICP Mass Spectrometry Handbook*, Blackwell Publishing Ltd., 550 Swanton street, Carlton, Victoria 3053, Australia, 2005.
19. D. R. Lide, ed., CRC Handbook of Chemistry and Physics, Internet Version 2005, <http://www.hbcpnetbase.com>, CRC Press, Boca Raton, FL, 2005, p 10:178 - 10:180.
20. H. Niu and R. S. Houk, *Spectrochim. Acta, Part B*, 1996, 51, 779-815.

21. T. W. Burgoyne and G.M. Hieftje, *Mass Spectrom. Rev.*, 1996, 15, 19.
22. Thermo Frisher Scientific (Bremen) GmbH, *Thermo Sciencetific ELEMENT 2 & ELEMENT XR*, Evaluation100_08/29.1/03.
23. J. Vogl and W. Pritzkow, *Mapan-J. Metrol. Soc. I*, 2010, 25, 135-164.
24. J. Vogl, *J. Anal. At. Spectrom.*, 2007, 22, 18.
25. J. Pisonero, B. Fernandez and D. Gunther, *J. Anal. At. Spectrom.*, 2009, 24, 1145-1160.
26. J. S. Becker, C. Pickhardt and W. Pompe, *Int. J. Mass spectrom.*, 2004, 237, 13-17.
27. C. Pickhardt, A. V. Izmer, M. V. Zoriy, D. Schaumloffel and J. S. Becker, *Int. J. Mass spectrom.*, 2006, 248, 136-141.
28. C. K. Yang, P. H. Chi, Y. C. Lin, Y. C. Sun and M. H. Yang, *Talanta*, 2010, 80, 1222-1227.
29. B. Fernandez, P. Rodriguez-Gonzalez, J. I. Garcia Alonso, J. Malherbe, S. Garcia-Fonseca, R. Pereiro and A. Sanz-Medel, *Anal. Chim. Acta.*, 2014, 851, 64-71.
30. B. Fernandez, F. Claverie, C. Pecheyran, J. Alexis and O. F. X. Donard, *Anal. Chem.*, 2008, 80, 6981-6994.
31. H. Scholze, E. Hoffmann, C. Ludke and A. Platalla, *Fresenius J. Anal. Chem.*, 1996, 355, 892-894.
32. J. E. Reid, I. Horn, H. P. Longerich, L. Forsythe and G. A. Jenner, *Geostandard Newslett*, 1999, 23, 149-155.
33. M. Tibi and K. G. Heumann, *J. Anal. At. Spectrom.*, 2003, 18, 1076-1081.
34. S. F. Boulyga and K. G. Heumann, *J. Anal. At. Spectrom.*, 2004, 19, 1501-1503.
35. J. Malherbe, F. Claverie, A. Alvarez, B. Fernandez, R. Pereiro and J. L. Molloy, *Anal. Chim. Acta.*, 2013, 793, 72-78.
36. T. E. Corporation, Thermo Electron Corporation, 2005.
37. T. Gusarova, T. Hofmann, H. Kipphardt, C. Venzago, R. Matschat and U. Panne, *J. Anal. At. Spectrom.*, 2010, 25, 314-321.
38. F.L. King, J. Teng and R.E. Steiner, *J. Mass Spectrom.*, 1995, 30, 15.
39. Jianying Ahang, Tao Zhou, Yichuan Tang, Yanje Cui and J. Li, *J. Anal. At. Spectrom.*, 2016, 31, 10.
40. G. V. Hevesy and F. Paneth, *Z. Anorg. Chem*, 1913, 82, 323-328.
41. M. Srgent, P. Bedson, R. Harte and C. Harrington, The Royal Society of Chemistry, 2002.
42. M. Berglund and M. E. Wieser, *Pure. Appl. Chem.*, 2011, 83, 397-410.
43. G. Audi and A. H. Wapstra, *Nucl. Phys. A*, 1993, 565, 1-65.
44. T. W. May and R. H. Wiedmeyer, *At. Spectrosc.*, 1998, 19, 150-155.
45. J. Vogl, *Rapid Commun. Mass Spectrom.*, 2012, 26, 7.
46. IUPAC, *Gold Book: Compendium of Chemical Terminology*, Version 2.3.3, 2014.
47. P. J. Paulsen and W. R. Kelly, *Anal Chem*, 1984, 56, 708-713.
48. R. W. Burke, P. J. Paulsen, E. J. Maienthal and G. M. Lambert, *Talanta*, 1982, 29, 809-813.
49. A. Das, C-H. Chung, C-F. You and M.-L. Shen, *J. Anal. At. Spectrom.*, 2012, 27, 2088-2093.
50. P. R. Craddock, O. J. Rouxel, L. A. Ball and W. Bach, *Chem. Geol.*, 2008, 253, 102-113.
51. Bio-Rad Laboratories, Instruction Manual: AG50W and AG MP-50 Cation Exchange Resins
52. Bio-Rad Laboratories, Instruction Manual: Strong Anion Exchange Resin AG 1, AG MP-1 and AG 2.

53. D. M. McClenathan and G. M. Hieftje, *J. Anal. At. Spectrom.*, 2005, 20, 1326-1331.
54. R. K. Marcus and J. A. C. Broekaert, *Glow discharge plasmas in analytical spectroscopy*, J. Wiley, Chichester, England, 2003.
55. R. Matschat, J. Hinrichs and H. Kipphardt, *Anal. Bioanal. Chem.*, 2006, 386, 125-141.
56. H. Traub, M. Czerwensky, R. Matschat, H. Kipphardt and U. Panne, *J. Anal. At. Spectrom.*, 2010, 25, 690-696.
57. H. Traub, M. Walle, J. Koch, U. Panne, R. Matschat, H. Kipphardt and D. Gunther, *Anal. Bioanal. Chem.*, 2009, 395, 1471-1480.
58. Rohm and Haas Company, AMBERLITE™ CG50 (Type 1) Weak Acid Cation Exchange Resin Powder, 2007.
59. Bio-Rad Laboratories, Chelex® 100 and Chelex 20 Chelating Ion Exchange Resin Instruction Manual
60. GUM Workbench: user manual version 2.4, ISBN 978-3-00-032973-9, Germany, 2011.
61. M. B. Fricker, D. Kutscher, B. Aeschlimann, J. Frommer, R. Dietiker, J. Bettmer and D. Gunther, *Int. J. Mass Spectrom.*, 2011, 307, 39-45.
62. M. Pesavento and E. Baldini, *Anal. Chim. Acta.*, 1999, 389, 59-68.
63. R. Biesuz, M. Pesavento, G. Alberti and F. Dalla Riva, *Talanta*, 2001, 55, 541-550.
64. M. Pesavento, R. Biesuz, A. Profumo and T. Soldi, *Environ. Sci. Pollut. Res. Int.*, 2003, 10, 317-320.
65. C. Kramer, P. Ried S. Mahn , S. Richter , N. Langhammer and H. Kipphardt *Anal. Methods*, 2015, 7.
66. M. Voss, M. A. G. Nunes, G. Corazza, E. M. M. Flores, E. I. Muller and V. L. Dressler, *Talanta*, 2017, 170, 488-495.
67. R. E. Russo, X. L. Mao, H. C. Liu, J. Gonzalez and S. S. Mao, *Talanta*, 2002, 57, 425-451.
68. J. O. R. David N. Douglas, C. O'Cornnor, B. L. Sharp, H. Goenaga-Infante, *J. Anal. At. Spectrom.*, 2016, 31, 10.

Biography

PRANEE PHUKPHATTHANACHAI

Removed for online publication

PUBLICATIONS

1. New reference material for analysis of elements in glutinous rice produced at the National Institute of Metrology (Thailand), Accred Qual Assur (2010) 15:223–231

2. European Restriction of Hazardous Substances (RoHS) in Thai Electric and Electronic Industries: Economical Impact of Chemical Metrology

3. Final report on CCQM-K89: Trace and essential elements in Herba Ecliptae, CCQM-K89 Final Report, 2013

4. Key Comparison CCQM-K100 Analysis of Cu in Ethanol, Metrologia 5, 2014

5. Report of the key comparison CCQM-K108 determination of arsenic species, total arsenic and cadmium in brown rice flour

PUBLICATIONS RELATED TO THIS STUDY

Title, Authors, Reference	Status
1. Report of the CCQM-K123: trace elements in biodiesel fuel, T. Kuroiwa, Y. Zhu, K. Inagaki, S. Long, S. Christopher, M. Puelles, M. Borinsky, N. Hatamleh, J. Murby, J. Merrick, I. White, D. Saxby, R. C. de Sena, M. D. de Almeida, J. Vogl, **P. Phukphatthanachai**, W. Fung, H. Yau, T. O. Okumu, J. N. Kangiri, J. A. Salas T´ellez, E. Z. Campos, E. C. Galv´an, N. Kaewkhomdee, S. Taebunpakul, U. Thiengmanee, C. Yafa, N. Tokman, M. Tunç and S. Z. Can, *Metrologia, 2017*, 54(Tech. Suppl.), 08008.	Published
2. SI-traceable quantification of sulphur in copper metals and its alloys by ICP-IDMS, **P.Phukphatthanachai**, J. Vogl, N. Jakubowski, U. Panne, *J Anal Atom Spectrom*, 2018, 33, 90-102	Published
3. A new approach of using polyethylene frits for the quantification of sulphur in copper metals by isotope dilution LA-ICP-MS and comparison with conventional IDMS techniques, **P. Phukphatthanachai**, J. Vogl, H. Traub, N. Jakubowsi, U. Panne, *J Anal Atom Spectrom*, 2018, 33, 1506-1517	Published
4. SI-traceable quantification by GDMS and LA-ICP-MS as demonstrated for sulphur in copper and copper alloys, **P. Phukphatthanachai**, J. Vogl, H. Traub, N. Jakubowsi, U. Panne	Drafting manuscript

PRESENTATION RELATED TO THIS STUDY

No.	Conference/symposium	Type of the conference	Topic	Place	Date	Presentation
1	14th International Symposium on Biological and Environmental Reference Materials	International	Determination of total sulfur in a metal matrix by ICP-IDMS: Example Cu matrix	Gaylord National Resort & Convention Center National Harbor, Maryland, USA	11-15 October 2015	Poster
2	The Association of Thai Professionals in European Region (ATPER)	Thai National	Chemical metrology for Biodiesel industry: Example sulphur in biodiesel	Thon Hotel EU, Brussels, Belgium	10–11 September 2016	Oral
3	2018 Winter Conference on Plasma Spectrochemistry	International	An alternative approach of using pe frits for the quantification of sulfur in copper metals and its alloys by isotope dilution LA-ICP-MS.	Amelia Island, Florida, USA	8-13 January 2018	Oral
4	2018 Winter Conference on Plasma Spectrochemistry	International	Quantification of sulfur in copper metals and its alloys by ICP-IDMS	Amelia Island, Florida, USA	8-13 January 2018	Poster
5	European Symposium on Atomic Spectrometry Colloquium Analytische Atomspektroskopie Anwendertreffen Plasmaspektrometrie, ESAS & CANAS 2018	International / German	A new approach of using polyehtylene frits for the quantification of sulphur in copper metals by isotope dilution LA-ICP-MS	Bundesanstalt füf Materialforschung une-prüfung BAM, Berlin, Germany	20-23 March 2018	Poster
6	European Workshop on Laser Ablation	International	Quantification of sulphur in copper metals by isotope dilution LA-ICP-MS using polyethylene frits	Palais Beaumont, Pau, France	26-29 June 2018	Poster

No.	Conference/symposium	Type of the conference	Topic	Place	Date	Presentation
7	PhD Day 2018	International	Development and application of IDMS based procedure for total sulphur determination in copper metals and its alloy	Bundesanstalt füf Materialforschung une-prüfung, BAM, Berlin, Germany	31 May 2018	Poster
8	13.Symposium "Massenspektrometrische Verfahren der Elementspurenanalyse" zusammem wit dem 26. ICPMS-Anwendertreffen	German	How to quantify the exact amount of sulphur in organic and inorganic samples?	Bundesanstalt für Materialforschung une-prüfung, BAM, Berlin, Germany	3-6 September 2018	Poster
9	15th International Symposium on Biological and Environmental Reference Materials	International	How to quantify the exact amount of sulphur in organic and inorganic samples?	Humboldt-University, Berlin, Germany	24-26 September 2018	Poster